Université de Lille – UFR 3S

Faculté des Sciences Pharmaceutiques et Biologiques

INSERM U1008 – Unité « Advanced Drug Delivery Systems »

UMR 8207 CNRS – Unité Matériaux Et Transformations

Ecole Doctorale Biologie-Santé

In-situ forming implants for periodontitis treatment: Addressing the need for less toxic solvents

---

Implants se formant in-situ pour le traitement de la parodontite: réponse au besoin de solvants moins toxiques

Thèse de Doctorat

Soutenue le 15 mai 2024

Filipa do Nascimento Ramos

Dirigée par :

Pr. Florence Siepmann & Dr. Jean-François Willart

Jury

Pr. Juergen Siepmann	Université de Lille	Président du jury
Pr. Thomas Rades	Université de Copenhague	Rapporteur
Pr. Sevda Şenel	Université de Hacettepe	Rapporteur
Pr. Olivier Huck	Université de Strasbourg	Examinateur
Pr. Florence Siepmann	Université de Lille	Directeur de thèse
Dr. Jean-François Willart	Université de Lille	Co-directeur de thèse

Acknowledgements

After three years, I finally got to the end of my doctoral journey. As a consequence, it is now time to express my heartfelt gratitude to all of you who have supported, encouraged and guided me.

Firstly, I am truly thankful to ***Pr. Juergen Siepmann*** for the opportunity to work on his team. I would like to thank you for the trust you deposited in me, the mentorship and insightful feedback, which helped shaping the direction of my work.

Secondly, I am deeply grateful to my supervisors. ***Pr. Florence Siepmann***, I have to thank you for your guidance as well as your availability. Thank you for always finding five minutes so that I could have an answer to my questions; thank you for sharing your vast knowledge allowing me to progress further in my research and lastly, I could never forget your human skills that were highly appreciated throughout the last three years. ***Dr. Jean-François Willart***, I have always admired your enthusiasm and passion for research and teaching and I am so grateful that you shared a bit of it with me. Thank you for your patience, guidance, support and, thank you for all your scientific knowledge that I was lucky enough to be the recipient of.

Additionally, I would also like to express my gratitude to all jury members, namely ***Pr. Thomas Rades***, ***Pr. Sevda Şenel*** and ***Pr. Olivier Huck***, for their assessment of my thesis manuscript as well as their constructive feedback. The latter are deeply valued.

I wish to express my sincere appreciation to everyone who kindly contributed their time, expertise, and insights to this research project. Firstly, I have to mention ***Dr. Christel Neut***, who I had the privilege to meet and to witness her passion for her vast bacteria collection. It was always a joy to be around you and to observe your enthusiasm. Moreover, thank you ***Dr. Kévimy Agossa*** for all your expertise and practical insights, which gave me a more realistic idea of my research project application. Finally, thank you **Pr. Florence Danède**, **Isabelle Houcke** and **Séverine Mahieux**.

Although I was almost 2 000 km away from home, I was still lucky enough to find people who made the distance seem smaller. Thank you ***Yanis***, ***Fabiana***, ***Lise-Anne***, ***Charline*** and ***Nina*** for all the time spent together, for your support and advice. I cannot express how grateful I am for your welcoming nature since the moment I arrived. Lastly, I have to, evidently, thank you all for teaching me the French (and Italian, Belgium and Slovenian) way.

Additionally, I would like to thank the rest of the U1008 team, with whom I had the pleasure to share many pleasant moments, ***Laurence***, ***Dr. Suzanne Muschert***, ***Hugues Florin***, ***Jérémy Vérin***, ***Alexandra*** and ***Guillaume***.

I would also like to express my gratitude to the students who worked directly with me in my PhD project, ***Isabelle***, ***Alex*** and ***Eloise***. Thank you for all your hard work as well as the fun times we spent together.

Finally, I was lucky enough to be surround by people who encouraged me every step of the way. ***Mom*** and ***dad***, I am at a loss of words to express my gratitude towards you. Thank you for all the opportunities you have created for me. You always made sure to show me I could do whatever I desired because I would always have a safe place to come back to. Thank you for all your support, unwavering love and understanding. Lastly, I must thank my sister, ***Raquel***. You have shown me, time and time again, you are my biggest supporter. I hope you know that, as cliché as it may sound, you are one of my role models and I am so happy to follow into your footsteps.

Thank you all for making these three years possible!

List of abbreviations

AAP	American Academy of Periodontology
API	Active Pharmaceutical Ingredient
CAL	Clinical attachment loss
CAS	Chemical Abstracts Service
CFU	Colony Forming Units
CHX	Chlorhexidine
CHX DiHCL	Chlorhexidine dihydrochloride
COX	Cyclooxygenase
C_p	Specific heat capacity
CR	Cysteinated Ringer solution
DMSO	Dimethyl sulfoxide
DNELs	Derived no-effect levels
EC	European Community
EFP	European Federation of Periodontology
EMA	European Medicines Agency
EPA	Environmental Protection Agency
FDA	U.S. Food and Drug Administration
GCF	Gingival crevicular fluid
H_m	Enthalpy
HSP	Hansen solubility parameters
IBD	Inflammatory bowel disease
IBU	Ibuprofen
ISFI	In-situ forming implant
LDDS	Local drug delivery systems
mDSC	Modulated differential scanning calorimetry
MIC	Minimum inhibitory concentration
MMPs	Matrix metalloproteinases
M_w	Molecular Weight
NMP	N-methyl-2-pyrrolidone
NSAID	Nonsteroidal anti-inflammatory drug
OHRQoL	Oral health related quality of life
PB	Phosphate buffer

PBPs	Penicillin binding proteins
PD	Periodontal disease
PDL	Periodontal ligament
PEG 400	Polyethylene glycol
PGA	Polyglycolic acid
PGE2	Prostaglandin E2
PLA	Polylactic acid
PLA	Poly(dl-lactide)
PLA-PCL	Lactide/caprolactone copolymers
PLGA	Poly(lactic-co-glycolic acid)
RCS	Refrigerated cooling system
RED	Relative energy difference
SP	Solubility parameters
SRP	Scaling and root planning
T	Temperature
T_a	Annealing temperature
TAM	Thermal activity monitor
TEC	Triethyl citrate
T_{end}	Endpoint temperature
Tg	Glass transition temperature
TGA	Thermogravimetric analysis
T_m	Melting temperature
TPA	Texture profile analysis
WHO	World Health Organization
XRD	X-ray diffraction

Table of Contents

Chapter 1: Introduction 1

Periodontal diseases 3

1. General introduction 3

2. Aetiology 4

3. Classification of periodontitis 7

4. Treatment 10

4.1 Mechanical treatment: Scaling and root planning 10

4.2 Drug treatment 11

4.2.1 Infection control 11

Antibiotics 11

Antiseptics 14

4.2.2 Host modulation therapy 15

Nonsteroidal anti-inflammatory drugs 15

Matrix metalloproteinases inhibitors 16

4.3 Systemic vs local drug administration in periodontitis' treatment 17

4.3.1 LDDSs for periodontitis' treatment 18

Fibers 18

Strips, films or inserts 19

Microspheres 19

Nanosystems 19

Gels 20

4.4 *In-situ* forming implants 21

4.4.1 Composition of ISFIs based on the Atrigel® technology 22

Polymer 22

Solvent 25

N-methyl pyrrolidone 26
NMP: Toxicological studies 27
Dimethyl Sulfoxide 29
DMSO: Toxicological studies 29
Drug 32
5. Aim of the study 33
Chapter 2: Materials and Methods 35
Materials 37
1. Formulation of the in-situ forming implant 37
2. Microbiological tests 37
3. Analytical chemicals 37
Methods 38
1. Thermogravimetric analysis (TGA) 38
2. Modulated differential scanning calorimetry (mDSC) 39
3. X-ray diffraction (XRD) 40
4. Solubility of the APIs in PLGA 40
4.1. Cryo-milling 40
4.1.1. Mixer Mill MM400 41
4.1.2. CryoMill 42
4.1.3. Thermal activity monitor (TAM) 42
5. Solvent Screening 43
6. Preparation of the liquid formulations 44
7. *In-situ* implant formation 44
8. Drug release measurements 44
9. Dynamic mass changes in the implants' wet mass 45
10. Determination of the dynamic solubility of the APIs in the release medium 46
11. Mechanical tests 46
11.1. Syringeability 46

11.2. Texture profile analysis (TPA) 47
12. Microbiological tests (kill-time tests) 48
Chapter 3: Solubility of Ibuprofen and Chlorhexidine Dihydrochloride in PLGA 502H 49
1. General introduction 51
2. Physical characterization of the pure compounds 51
2.1. Poly(lactic-co-glycolic) acid 51
2.1.1. PLGA's characterization by TGA, XRD and DSC experiments 52
2.2. Ibuprofen 55
2.2.1. Ibuprofen's characterization by TGA, XRD and DSC experiments 56
2.3. Chlorhexidine dihydrochloride 58
2.3.1. CHX DiHCl's characterization by TGA, XRD and DSC experiments 59
3. Physical characterization of mixtures 61
3.1. General considerations on the solubility of the APIs within the polymer 61
3.1.1. Melting point depression 62
3.1.2. The annealing method 62
3.1.3. The recrystallization method/Demixing of the API in the polymer 63
3.2. Solubility of ibuprofen in PLGA 502H 65
3.3. Solubility of chlorhexidine dihydrochloride in PLGA 502H 74
4. Conclusion 77
Chapter 4: *In-situ* forming PLGA implants – Towards less toxic solvents 79
1. Solvent Screening through the application of the Hansen Solubility Parameters 81
1.1. General introduction 81
1.2. Solvent Screening 83
2. In-situ forming PLGA implants – Towards less toxic solvents 86
2.1. General introduction 86
2.2. Drug Release from the in-situ forming implants 87
2.2.1. Ibuprofen Release 87
2.2.2. Chlorhexidine Dihydrochloride's Release 93

2.2.3. Implants containing both ibuprofen and chlorhexidine 94
2.3. Mechanical tests 97
2.3.1. Syringeability 97
2.3.2. Texture Profile Analysis 99
2.4. Antimicrobial activity 103
3. Conclusion 106
Chapter 5: General conclusion and future perspectives 107
Supplementary Material 113
References 133
Résumé 157
Abstract 158

Chapter 1: Introduction

Periodontal diseases

1. General introduction

The periodontium is an intricate structure formed by four different tissues: the cementum, periodontal ligament (PDL), alveolar bone and lastly, the gingiva. Together, they work as a unit and are responsible for the tooth's anchorage as well as the protection of the underlying structures against the microflora present in the oral cavity . In particular, the cementum covers the root surface of the tooth and provides a strong connection to the alveolar bone through the PDL. The latter is a complex specialized tissue that allows the absorption of energy produced during mastication and the regulation of the same process due to the presence of nerve fibres (6–8). Finally, the gingiva serves as an initial "wall" protecting the periodontium's subepithelial components from the highly colonized oral cavity's bacteria (2,3,6,7). **Figure 1** depicts a schematic cross section of a tooth, highlighting its main components.

The healthy periodontium is characterized by the absence of any clinically detectable inflammatory periodontal disease (PD) and by the observation of a homeostasis state between the oral cavity's microflora and the host's immune response. This translates into a sharp edge pale pink gingiva tightly connect to the underlying structures, with no bleeding upon probing, and the lack of anchorage or bone loss (9–11). Any deviation from the previous description might indicate the presence of periodontal disease. The latter term refers to any disorder affecting the periodontium, which could originate from genetic, traumatic, inflammatory, neoplastic or metabolic syndromes. Nevertheless, the periodontal disease is most commonly associated with an inflammatory disorder, resulting from the interaction between the dental plaque's microbiome, the host immune response and environmental factors (12,13). Briefly, it includes gingivitis and periodontitis. The former consists in the mildest form of PD, represented by an inflamed gum. The underlying structures of the tooth are not affected and it is reversible upon appropriate oral hygiene. On the other hand, periodontitis, the irreversible form of PD, is verified when deeper periodontium tissues are implicated (12,14–16): it is observed bleeding upon probing, incremental decay of the PDL and alveolar bone, creating periodontal pockets (13,17–19). Ultimately, it might result in tooth loss (13,17,20–22).

Periodontitis is the 6th most prevalent disease globally. According to the "Global oral health status report" of the World Health Organization (WHO), 19% of the world's population suffered from severe periodontitis in 2019 (23). The prevalence of the disease's severe form increases with age and

it seems to similarly affect men and women (23). As expected, the disease is associated with a decrease in masticatory performance thus, reducing the oral health related quality of life (OHRQoL) (13,22,24).

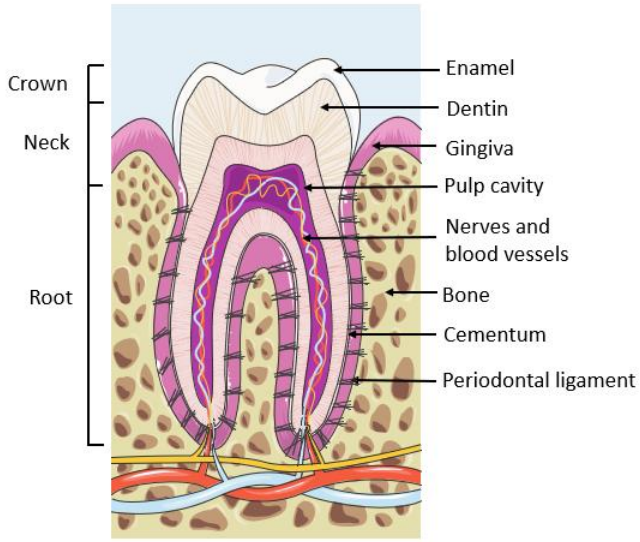


Figure 1: Schematic representation of a tooth's cross section, highlighting its major components. Obtained from smart.servier.com.

2. Aetiology

The human buccal cavity provides a habitat for roughly 700 bacterial species, forming the oral microbiome (25–27). The latter consists of a complex ecosystem of microorganisms that interact both metabolic and physically, leading to the formation of polymicrobial biofilms' niches structurally organized according to the bacteria's metabolic needs (28,29). The study of the spatial distribution of the healthy supragingival plaque was performed by Mark Welch et al. (30), who detected a "hedgehog-like" structure, radially arranged (**Figure 2**). According to this hypothesis, Corynebacterium filaments attach to prevailing colonizers, namely *Actinomyces* and *Streptococcus*. The distal tips of these filaments are surrounded by *Streptococcus*, *Porphyromonas*, *Haemophilus*/*Aggregatibacter* and *Neisseriaceae*. These species are located on the periphery due to its oxygen- and nutrient-rich environment. Moreover, the presence of oxidative species at this location produces an anoxic atmosphere abundant in carbon dioxide, lactate, acetate and peroxide at the centre of the biofilm. This area is then conducive to the proliferation of *Fusobacterium*, *Leptotrichia* and *Capnocytophaga*. Finally, the base of these hedgehog-like structure is mainly composed by *Corynebacterium* filaments (30). When this intricate ecosystem is disrupted, microbial dysbiosis is observed (27,31). The latter, combined with an immune dysregulation, inflammation processes and increased presence of periodontal pathogens, is a crucial key factor in the aetiology of periodontitis (26).

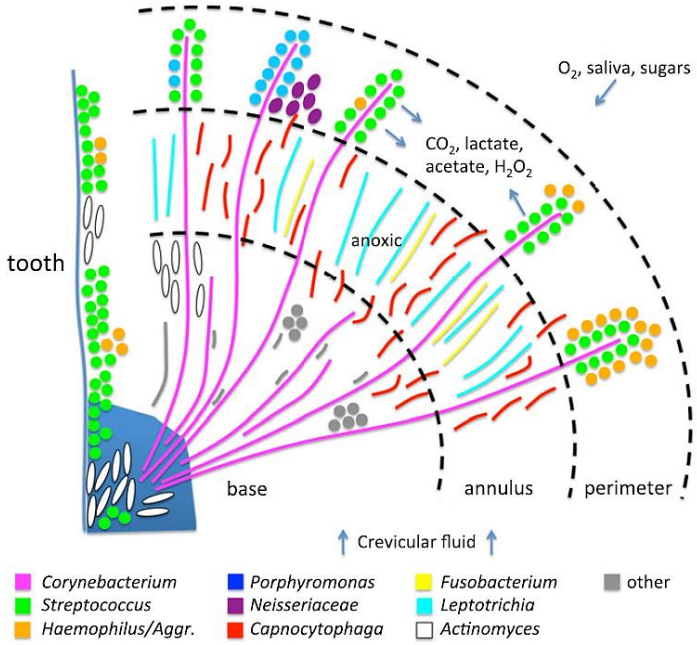


Figure 2: Spatial distribution of the healthy supragingival plaque, as defined by Mark Welch et al. (30). The base of this hedgehog-like structure is mainly composed by Corynebacterium filaments, which attach to prevailing colonizers (namely Actinomyces and Streptococcus). The distal tips of these filaments are surrounded by Streptococcus, Porphyromonas, Haemophilus/Aggregatibacter and Neisseriaceae. At the center of the structure, it is formed an anoxic environment, where Fusobacterium, Leptotrichia and Capnocytophaga proliferate. From Mark Welch et al. (30).

Many efforts have been employed in order to better understand the aetiology of periodontal disease. For instance, Socransky et al. (1998) categorised the periodontal bacterial communities as a colour-coded system, depending on cluster analysis, community ordination and associated disease severity (32). Furthermore, the same research defined the "red complex" as a combination of three bacterial species, namely *Porphyromonas gingivalis*, *Treponema denticola* and *Tannerella forsythia*, which were found as strongly associated with periodontal disease and its severity (27,28,32). However, as more research has been done, the number of species involved in the development of periodontitis has increased (26) to comprise, for example, *Filifactor alocis*, *Porphyromonas, Synergistetes*, *Peptostreptococcaceae* (33,34) and *Actinomyces actinomycetemcomitans*, being the latter associated with more advanced stages of periodontitis (35). Other models have been proposed, such as the synergistic interactions between core pathogenic species and commensals (36), the implication of the immune system in defining a healthy state or illness (37) and the polymicrobial synergy and dysbiosis model that combines characteristics of all the previously described hypothesis (27). The aforementioned showcases the complexity of the disease evolution, which is highly impacted by the role of synergistic microbial clusters, specific periodontal pathogens, and immune system dysregulation (26).

The increased knowledge of the pathogens involved in the progression of periodontitis clearly unveiled complex synergistic and antagonistic interconnections amongst the oral microbiome (26). In particular, it was demonstrated the positive correlation between most interspecies. Briefly, shifts in the prevalence of one species is frequently linked to corresponding shifts in others (38–41). In addition to the bacteria, also viruses have been found in the oral microbiome of both healthy and diseased states (42). Although it is not completely understood the significance of the oral virome in the development of periodontitis (26), the latter is able to initiate host immune responses thus, possibly explaining its implication on the disease progression (43). Such viruses include Epstein Barr virus, herpes simplex virus, and cytomegalovirus (44–47).

Although the molecular and cellular processes implicated in periodontitis' inflammation are not fully understood (48), it is well established the persistent accumulation of supra- and subgingival biofilms initiates a host immune response in the tooth surrounding tissues (31). The former induces the secretion of chemokine by epithelial cells and thus, recruits neutrophils to the junctional epithelium (49,50). As a consequence, it is observed a defensive proteolytic reaction, which disrupts the epithelial layer and stimulates the pathogens' invasion deeper into the periodontium, resulting in tissue breakdown and bone resorption (49). It is interesting to note that some periodontopathogens prosper under inflammatory processes, where the tissue destruction's by-products (namely, collagen breakdown products, amino acids, iron, heme), further facilitate the pathogens' growth (51,52). Moreover, when it is verified a disruption in the homeostatic communication between the oral flora and the host immune system, due to either microbial or inflammatory factors, dysbiosis is continued and the harmful effects of periodontitis is sustained in a cyclical manner. The tissue destruction verified in the periodontitis disease is a result of the TH17 cells proliferation in an interleukin (IL)-6 and IL-23 dependent manner as a consequence of a shift in the oral microbiome structure (53). Please note that as research continues to be developed, new alternative proposals have emerged in order to better understand the underlying mechanisms promoting the microbial dysbiosis and host inflammatory responses, leading to periodontal tissue destruction (26). For instance, it has been discussed that cell senescence may promote inflammation, having a role in periodontitis development (53,54). Briefly, albeit the involvement of a microbial challenge is necessary for the disease's development, the host inflammatory response is the key impetus for periodontium destruction (55,56).

Finally, periodontitis and its severity have also been associated with chronic inflammatory diseases, not confined in the oral cavity. Such pathologies which possibly promote the development of periodontal disease include cardiovascular diseases, rheumatoid arthritis, diabetes and inflammatory bowel disease (IBD) (57). Nevertheless, it seems that this is a reciprocal interaction, where the oral cavity dysbiosis may have an impact on the progression or severity of systemic pathologies (26). Lastly,

host environmental factors, namely poor diet, smoking and psychological stress, may contribute to periodontal disease due to the activation of the host inflammation processes (58–60).

3. Classification of periodontitis

It is important to rely on a classification system in order to better diagnose and treat periodontitis' patients. To this effect, the "*2017 Classification of Periodontal and Peri-Implant Diseases and Conditions"* was developed by the combined work of the American Academy of Periodontology (AAP) and the European Federation of Periodontology (EFP). This is currently the most commonly employed classification system and recognizes three forms of periodontitis, based on the knowledge of pathophysiology (15,16,61):

1. Necrotizing periodontitis
2. Periodontitis as a direct manifestation of systemic diseases
3. Periodontitis

The first type is marked by the occurrence of pain, lesion of the gingival margin, the presence of fibrin deposits and possibly, the observation of the alveolar bone. Posteriorly, periodontitis can be developed as a direct manifestation of a systemic disease which modifies the host immune response. Lastly, the remaining cases that do not exhibit the characteristics of the previous categories, are simply nominated as "periodontitis". However, the latter term should be further defined through a staging and grading scheme, adapted to each clinical case and allowing to have a universal and communicable understanding of the pathology's control, prognosis and oral and systemic health (15,16).

Periodontitis is divided into 4 stages (1 – 4) and their determination relies on the severity upon presentation, the intricacy management of the condition and its extension in the dentition. To this effect, several parameters are evaluated, namely the probing depth, clinical attachment loss (CAL), bone loss, tooth mobility and its loss (**Table 1**). On the other hand, the disease's grading provides valuable information regarding periodontitis' progression rate and the estimation of future risk to the patient's general health status. Periodontitis can be defined by three grades: i) grade A – low risk, ii) grade B – moderate risk and, iii) grade C – high risk of the condition progression (**Table 2**). As a consequence, the grading system takes into consideration individual patient factors, critical for periodontitis control (15,16,61).

Table 1: Stages of periodontitis, defined by the severity, complexity and extent of the disease. Adapted from *Papapanou et al. and Tonetti et al.* (15,16).

Periodontitis stage		**Stage I**	**Stage II**	**Stage III**	**Stage IV**
Severity	**Interdental CAL at site of greatest loss**	1 – 2 mm	3 – 4 mm	≥ 5 mm	≥ 5 mm
	Radiographic bone loss	Coronal third (< 15%)	Coronal third (15% - 33%)	Extending to mid-third of root and beyond	Extending to mid-third of root and beyond
	Tooth loss	No tooth loss due to periodontitis		Tooth loss due to periodontitis of ≤ 4 teeth	Tooth loss due to periodontitis of ≥ 5 teeth
Complexity	**Local**	Maximum probing depth ≤ 4 mm Mostly horizontal bone loss	Maximum probing depth ≤ 5 mm Mostly horizontal bone loss	**In addition to stage II:** Probing depth ≥ 6 mm Vertical bone loss ≥ 3 mm Furcation involvement Moderate ridge defect	**In addition to stage III:** Need for complex rehabilitation due to: 1. Masticatory dysfunction 2. Secondary occlusal trauma (tooth mobility degree ≥2) 3. Severe ridge defect 4. Bite collapse, drifting, flaring 5. Less than 20 remaining teeth (10 opposing pairs)
Extent and distribution	Add to stage as descriptor	1. Localized (<30% of teeth involved) 2. Generalized 3. Molar/incisor pattern			

CAL: clinical attachment loss

Table 2: Grades of periodontitis. Adapted from *Papapanou et al. and Tonetti et al.* (15,16).

Periodontitis grade			**Grade A: Slow rate of progression**	**Grade B: Moderate rate of progression**	**Grade C: Rapid rate of progression**
Primary criteria	**Direct evidence of progression**	**Longitudinal data (radiographic bone loss or CAL)**	Evidence of no loss over 5 years	< 2 mm over 5 years	≥ 2 mm over 5 years
	Indirect evidence of progression	**% bone loss/age**	< 0.25	0.25 – 1.0	> 1.0
		Case phenotype	Heavy biofilm deposits with low levels of destruction	Destruction commensurate with biofilm deposits	Destruction exceeds expectation given biofilm deposits; specific clinical patterns suggestive of periods of rapid progression and/or early onset disease (e.g., molar/incisor pattern; lack of expected response to standard bacterial control therapies)
Grade modifiers	**Risk factors**	**Smoking**	Non-smoker	Smoker < 10 cigarettes / day	Smoker ≥ 10 cigarettes / day
		Diabetes	Normoglycemic /no diagnosis of diabetes	HbA1c < 7.0 % in patients with diabetes	HbA1c ≥ 7.0 % in patients with diabetes

CAL: clinical attachment loss; HbA1c: glycated haemoglobin.

Please be aware that the grade of periodontitis should be determined recurring to direct evidence. The indirect data should only be used when the latter information is missing. Moreover, it is initially assumed a grade B pathology that can alter to A or B, based on evidence. Finally, periodontitis grade is also affected by the occurrence of risk factors.

4. Treatment

The treatment of periodontal diseases strives to regain periodontal health, avoid the disease's progression and its reappearance and lastly, preserve the dentition in a healthy state, well-being, and function (12,62). Furthermore, being periodontitis characterized by a bacterial dysbiosis and inflammation, it is of utmost importance to manage and control these parameters (20–22,62,63). To this extent, both surgical and non-surgical methods are available (12). Furthermore, it is relevant to note that the periodontitis' patient plays a key role in the disease's treatment: compliance and thorough oral hygiene leads to a more successful treatment with lower risks of reoccurrence. On the contrary, non-compliance results in unpredictable consequences (63,64).

4.1 Mechanical treatment: Scaling and root planning

Periodontitis' first line of treatment is typically scaling and root planning (SRP) (12,63,65). This procedure is defined by the mechanical removal of the pathogenic biofilm and calculus (both supra- and sub-gingival), delaying the recolonization of the affected periodontal pockets (66,67). As a consequence, it is observed a decrease of the inflammation and pocket probing depth and an improvement of the clinical periodontal attachment (12,63,65,66).

Although the efficacy of SRP is well established, the procedure is still considered as challenging and time-consuming, requiring the clinician's experience, skill and patience (63,65,68). Moreover, the success of the treatment is also dependent on several parameters namely, the limited access to deep and complex lesions, the pocket geometry (65,66), the ability to perceive the calculus in the root surface (69), the pockets' probing depth (70) and, the presence of specific pathogens (71,72). As a result of the aforementioned, combined with a highly colonized oral cavity, it is not possible to attain the complete eradication of the bacterial biofilm (63,65,67,73). In fact, numerous studies have demonstrated that a substantial number of teeth will display residual biofilm and calculus, after SRP (17,65,74). This highlights the need for frequent removal of the pathogenic bacteria and maintenance therapy (65).

When the SRP treatment goals are not accomplished in patients presenting an advanced form of the disease, several types of periodontal surgery can be considered in order to i) decrease the pockets' depth, ii) get a better access for the debridement of remaining bacterial plaque and, iii) attempt to regenerate the lost periodontal support (12,63,75).

4.2 Drug treatment

Due to periodontitis' microbial foundation, the use of antimicrobial therapy has been considered as an adjunct to SRP (62,66,76), particularly in more advanced stages of the disease (67,77). The use of antimicrobials promotes the reduction of bacterial load both at subgingival areas as well as at extra-pocket sites, which are insufficiently treated by SRP (78). Moreover, host modulation therapy can be applied. The latter concept refers to the alteration of the host's status or function in order to treat the pathology. In the particular case of periodontitis, where an inflammatory process is well established, the host modulation therapy mostly targets the decrease of the host inflammatory response (22,48). The current section highlights some of the numerous molecules that can be effective as an adjunctive therapy to SRP in the treatment of periodontitis.

4.2.1 Infection control

The antimicrobial selection takes into consideration the aetiology of the periodontal disease. Briefly, these drugs are generally divided into antibiotic and antiseptic agents. It is relevant to mention that numerous agents have been considered yet, only a limited number has been employed in drug delivery systems (62).

Antibiotics

Several antibiotics have been suggested for the treatment of periodontitis. Amongst them, amoxicillin and metronidazole, either in monotherapy or in combination, are the most commonly employed antimicrobials (78). Additionally, macrolides have been proposed, namely azithromycin and clindamycin. Lastly, it is relevant to note tetracyclines used to be extensively applied in the treatment of the disease's advanced stages nevertheless, they are no longer recommended due to their adverse effects and the increased risk of developing bacterial resistances. Briefly, the administration of systemic antibiotics alone does not eradicate periodontitis however, it may ameliorate the clinical outcomes of the mechanical plaque removal, particularly, in the advanced stages of the pathology (77). **Table 3** depicts the main features of the most commonly employed systemic antibiotics.

Table 3: Main characteristics of antibiotics agents employed in the treatment of periodontitis.

Antibiotic	Mechanism of Action	Advantages	Disadvantages
Metronidazole	Inhibition of DNA synthesis (62,73,79)	Active against gram-positive and gram-negative anaerobic bacteria (73,78–80), including periodontopathogens	Ineffective against *A. actinomycetemcomitans* (*in-vitro)* (62,79)
Amoxicillin (β-lactam)	Inhibition of bacterial cell wall synthesis by binding to penicillin binding proteins (PBPs)	Activity against gram-negative and gram-positive bacteria Well absorbed after oral administration (79)	Highly susceptible to β-lactamases[1], inhibiting amoxicillin activity (79)
		Augmentin®: amoxicillin + clavulanic acid[2] (β-lactamase inhibitor) Amoxicillin resistance bacteria may be susceptible to the combination of these compounds (79)	---
Azithromycin (Macrolide)	Inhibition of bacterial protein synthesis by connection to and interfering with the assembly of the50S large ribosomal subunit (81)	Broad-spectrum antimicrobial (81) *In-vitro* activity against numerous gram-negative periodontopathogens, including *P. gingivalis* (82) and *A. actinomycetemcomitans* (83) Relatively nontoxic (79,81)	Unclear efficacy in the treatment of periodontitis (84)
Clindamycin	Inhibition of the bacterial protein synthesis by binding to the 50S ribosomal subunit (79)	Broad-spectrum antibiotic: Aerobic, anaerobic, and β-lactamase producing pathogens (85) High oral absorption, significant tissue penetration, and stimulatory effects on the host immune system (85)	Limited number of studies (62) Ineffective against *E. corrodens*[3] and *A. actinomycetemcomitans* (*in-vitro*) (79) Reported recurrence of the disease (62)

[1] β-lactamases are common in periodontal pockets, being linked to the periodontal pocket depth (79)

[2] Clavulanic acid has no antimicrobial activity however, it presents an unprotected β-lactam ring, for which several b-lactamase enzymes of oral origin have a greater affinity (79)

[3] Eikenella corrodens is commonly found in the periodontal flora and it is suspected be a periodontopathogen (86)

Table 3 (cont.): Main characteristics of antibiotics agents employed in the treatment of periodontitis.

Antibiotic	Mechanism of Action	Advantages	Disadvantages
Tetracycline	Inhibition of protein synthesis by connecting to the 30S ribosomal subunit (79) Inhibition tissue collagenase activity (62)	Broad-spectrum antimicrobial (Gram-positive and gram-negative) (62,73) Antiproteolytic properties thus, preventing tissue destruction Inhibition of matrix metalloproteinases, avoiding tissue destruction and alveolar bone loss (67) High substantivity[4] in the oral cavity (62)	Widespread development of bacteria resistant to tetracyclines: no longer recommended (73,79) Inactive against *P. aeruginosa* (73)
		Doxycycline and minocycline(62): greater oral absorption, more prolonged half-lives and enhanced lipid solubility, when compared to tetracycline (62)	Development of bacteria resistant to tetracyclines
Ciprofloxacin (Fluoroquinolone)	Inhibition of bacterial DNA topoisomerase II, affecting its replication (79,87)	Activity against a wide range of gram-negative aerobic and facultative bacteria (79,87) Good activity against gram-positive bacteria (79) Inhibition of most strains of *A. actinomycetemcomitans* at an MIC of approximately 0.01 µg/ml (87) Relatively well tolerated (79)	Little activity against obligate gram-negative anaerobes (79)
Ofloxacin (Fluoroquinolone)	Inhibition of bacterial DNA topoisomerase II, affecting its replication	Active against gram-positive bacteria and anaerobes Marked antibacterial activity against periodontopathogens (including *Bacteroides* and *Fusobacterium* species, and *A. actinomycetemcomitans*) High chemical stability Relatively safe (62)	Limited number of studies

MIC: minimum inhibitory concentration

[4] Ability of a compound to adhere to oral surfaces

Antiseptics

It is relevant to note the European Federation of Periodontology does not suggest the use of systemic antibiotics when treating stages I to III periodontitis due to the potential development of antibiotic resistances, affecting both the patient and public health (88,89). As a consequence, antiseptics can be employed as an alternative to the previous drug class. Chlorhexidine (CHX) belongs to such category, being largely used since the 1950s (67), and it will be described in more detail in the present section. Other examples of antiseptics include povidone-iodine (79,90,91), cetylpyridinium chloride (92), sanguinarine (62), and hydrogen peroxide (93). Please be aware that antiseptics in periodontology are mostly employed locally, in the form of mouthwashes and subgingival irrigation solutions during professional debridement (94).

Chlorhexidine is a broad-spectrum antimicrobial, commonly employed in dentistry (62,79,95). It has been locally used for the control of the dental biofilm and it has also shown to be effective in the treatment of PD (62,96). CHX's antibacterial properties derive from its cationic nature (73). As a consequence, it presents a high affinity to negatively charged ions and molecules, including salivary proteins and the microorganisms' cell wall. CHX prevents the formation of pellicles, thin layers of saliva proteins, through the connection to salivary glycoproteins. It also binds to salivary bacteria, preventing the latter's adsorption onto the tooth surface. Additionally, this antiseptic modifies the cell's osmotic balance, resulting in the bacterial cell lysis or important function limitation (62,73). In fact, this antimicrobial agent holds bacteriostatic and bactericidal activity, depending on its concentration (95). Moreover, chlorhexidine exhibits high substantivity (62,79) thus, remaining in the oral cavity for a prolonged period of time, after application (62,73). It is relevant to note the antiseptic agent maintains its properties in a basic environment, which is verified in the periodontal pockets (73).

Finally, this substance has been identified in the WHO's Model List of Essential Medicines (97) due to its safety profile, extensive availability, and versatility. The latter list compiles the medications considered as essential to attend the fundamental requirements of an effective health care system (96).

Several studies have been performed so as to evaluate the impact of CHX mouthrinses in the control of plaque and gingival inflammation in gingivitis' patients. A systematic review demonstrated that combining the use of CHX and mechanical oral hygiene has a positive effect on the control of microbial biofilm and gingivitis. In fact, it was revealed that the combination of the two techniques allowed the reduction of the biofilm and gingivitis, by 33% and 26%, respectively, when compared to the mechanical oral hygiene alone (98).

4.2.2 Host modulation therapy

As previously discussed, periodontitis is characterized by deleterious inflammatory processes which culminate in the destruction of the periodontium. As a consequence, host modulation therapy can be here employed to alter the host's immune response in order to avoid, or improve, tissue impairment (67,99). Ultimately, the host modulation therapy should result in an equilibrium between proinflammatory and anti-inflammatory mediators, halt the disease's progression and promote the resolution of inflammation as well as the tissues' repairment (99). This section will mainly focus on nonsteroidal anti-inflammatory drugs (NSAIDs) and matrix metalloproteinases inhibitors however, other approaches will be briefly discussed.

Nonsteroidal anti-inflammatory drugs

Nonsteroidal anti-inflammatory drugs (NSAIDs) have been assessed as an adjunctive therapy for the treatment of periodontitis (48,100). NSAIDs are amongst the most prescribed molecules worldwide and are, in their majority, weak organic acids able to hinder the cyclooxygenase (COX) pathway of arachidonic acid metabolism. This can be performed either in a non-selective or selective manner, if the NSAID inhibits both COX isoforms (COX-1 and COX-2) or only COX-2, respectively (100,101). As a result of COX inhibition, the production of prostaglandins, namely prostaglandin E2 (PGE2), is ceased (99,102). Please note PGE2 is generated by several resident (such as fibroblasts) and recruited (e.g., macrophages and neutrophils) cell types in the tooth supporting tissues as a response to lipopolysaccharide or proinflammatory cytokines (48,99). PGE2 is a vasodilator which facilitates both vascular permeability and up-regulates osteoclastic bone resorption in periodontitis (48,103,104).

Several studies have been conducted to better understand the role of NSAIDs in the treatment of periodontal diseases. For instance, reports have shown that patients taking NSAIDs for extended periods of time displayed a reduction in the gingival inflammation as well as probing depths when compared to the control group (105). Furthermore, animal studies and longitudinal clinical trials where the patients received daily administration of oral NSAIDs for a prolonged period of time (up to several years) showed a reduction in the alveolar bone loss (31,48,99,106,107). However, this form of treatment (oral administration for extensive periods of time) display some drawbacks. For instance, i) side effects are frequently observed (31,48), ii) it is highly dependent on patient compliance for numerous years until it is observed the advantageous impact on bone resorption (48) and, iii) the positive results decay when the treatment is interrupted (100,108,109). In summary, limited clinical benefits have been associated with serious side effects, precluding this systemic therapy for periodontitis' treatment (48).

Matrix metalloproteinases inhibitors

Matrix metalloproteinases (MMPs) are enzymes secreted by several infiltrating cell types in the periodontium, namely by the neutrophils which are recruited to the inflamed site. MMPs promote tissue destruction and bone resorption due to the degradation of numerous extracellular matrix proteins, such as collagen (67,110).

It has already been established that tetracyclines (particularly, doxycycline) can function as MMPs inhibitors, regardless of their antimicrobial activity. Moreover, the combination of SRP with the employment of sub-antimicrobial doses of doxycycline results in statistically significant benefit, when compared to SRP alone (100). The same meta-analysis study, showed a clinical attachment level gain larger (0.3 – 0.4 mm) than the one obtained with SRP alone (110). These outcomes are comparable to the ones obtained when local administration of antimicrobials is applied (111). Sub-antimicrobial doses of doxycycline (20 mg, twice daily for 3 months) were, in fact, the first host response modulation treatment marketed for periodontitis' treatment (112). Nevertheless, some studies did not show the same doxycycline's positive impact as it was observed in a large-scale clinical trial (48).

Lastly, other adjunctive treatment approaches have been analysed:

1. *Biological therapy*: it is mostly employed based on the pathogenesis similarity between periodontitis and rheumatoid arthritis, including numerous anti-cytokine agents. Animal studies using an anti-tumour necrosis factor-alpha therapy have shown the reduction of the inflammatory cell infiltrate in rats (113) as well as the decrease in alveolar bone loss in primates (114). However, up to date, only small clinical studies have analysed the potential efficacy of anti-cytokine treatment in humans, showcasing the rather unpredictable outcomes. For instance, one study, where infliximab was intravenously administered to rheumatoid arthritis' patients, revealed an increase in gingival inflammation and no impact on the periodontal pockets depth (115). On the contrary, another analysis using the same intravenous drug resulted in the reduced bleeding upon probing and lower probing depth when compared to the control group (rheumatoid arthritis' patients without infliximab therapy) (116). It is relevant to note that the immunosuppressant action of this type of therapy may result in important side effects (48).
2. *Bisphosphonates*: this drug's class is able to bind to the surfaces of the teeth, avoiding bone resorption. Clinical studies starring bisphosphonates have been reported however, the drugs' efficacy revealed to be limited. Moreover, bisphosphonates administration

might lead to osteonecrosis of the jaw, precluding the use of this type of drug for the treatment of periodontitis (100).

3. *Pro-resolving lipid mediators*: these molecules correspond to natural resolution agonists, secreted endogenously as a routine response to inflammation. As a consequence, the development and employment of this treatment seems to be more beneficial when compared to solely inflammation inhibitors, which play a role in the host immune response (117). However, more research is required to better characterise the effects of pro-resolving lipid mediators in periodontitis (48).

In summary, the previous sections reflect some of the numerous molecules that can be employed for the treatment of periodontitis. These can be selected according to the disease's aetiology and severity and the patient's associated systemic diseases and risk factors (e.g., smoking, diet, physiological stress). Finally, the treatment's success is dependent on several factors, namely, oral home care, continuous effort to manage the risk factors, maintenance therapy and follow-up after active treatment.

4.3 Systemic vs local drug administration in periodontitis' treatment

Although there are numerous molecules that can potentially be used as adjunctive therapy in the treatment of periodontitis, the latter is still considered as vastly challenging. This can be explained by the relatively low drug partitioning into the periodontal pockets as well as the large flow rate of gingival crevicular fluid (GCF) that rapidly removes the drug from the target site (17,118). For instance, it has been predicted that the GCF is replaced approximately 40 times per hour in a 5 mm deep periodontal pocket. Additionally, the expected half-life of an API (active pharmaceutical ingredient) in the gingival crevice is roughly 1 minute. Cleary, the observed high clearance rate represents one of the major drawbacks in keeping an effective drug concentration within the periodontal pocket (119). Accordingly, the use of conventional administration routes (including oral, intramuscular, intravenous, and subcutaneous) entails large systemic API levels whereas the drug concentration at the intended site of action is minimal. Hence, this can result in i) severe side effects associated with limited or even subtherapeutic drug efficacy, ii) recurrent drug administration in order to maintain therapeutic drug concentration thus, potentially decreasing the patient's compliance and, iii) bacterial resistances upon antimicrobial systemic administration (17,22,95,118,119). As a consequence, the employment of

advanced local drug delivery systems (LDDSs) has been proposed so as to overcome the previous shortcomings, releasing the API in a controlled manner at the target site (17,22,118,119).

4.3.1 LDDSs for periodontitis' treatment

A LDDS for the treatment of periodontitis is characterized by a drug reservoir and a limiting component which controls the API release rate. To this extent, it is possible to keep effective drug concentrations in the periodontal pocket for prolonged periods of time, independently of the drug loss promoted by the high GCF clearance (119). Up to date, several local controlled drug delivery systems have been developed, encompassing a large range of materials (non-resorbable and bioabsorbable matrices) as well as presenting different forms (e.g., solid, semi-solid). This section will focus on these existing systems.

Fibers

Fibers consist of a reservoir-type delivery system that are circumferentially placed into the target site and kept in position through the employment of a cyanoacrylate adhesive or a periodontal dressing (120,121). Cellulose acetate hollow fibers containing tetracycline were produced with the aim of hindering the periodontal microflora (122). This study evidently shows the reduction of the necessary drug amount when compared to systemic delivery systems (1/1000). However, it was not able to provide a controlled drug delivery. In fact, roughly 95% of tetracycline was released in the first 2 h after application (122). In order to overcome the burst release, it has been suggested to fabricate drug-impregnated fibers, employing several polymers namely, poly(ε-caprolactone), polyurethane, polypropylene, cellulose acetate propionate and ethyl vinyl acetate (120,121).

Actisite® is a U.S. Food and Drug Administration (FDA)-approved ethylene vinyl acetate-inert fiber containing tetracycline. This system was employed for the treatment of periodontitis and showed to sustain the effective drug release for up to 10 days at the lesion site (123). Nevertheless, it was discontinued due to its non-biodegradability. Albeit having showed positive outcomes when treating the periodontal disease, the placement of the Actisite® device required the dentist's consummate skills and led to the patient's discomfort. Moreover, being it non-biodegradable, it was necessary to remove the system after treatment, which frequently resulted in gingival inflammation (120,121,124).

Strips, films or inserts

Strips, films or inserts are polymeric thin bands where the API is dispersed within the polymer. These systems present some advantageous in comparison with the previously described fibers. For instance, their size and shape can be tailored in order to better fit into the periodontal pocket hence, avoiding their placement discomfort (121). Initially, these systems were formulated using non-biodegradable materials however, they would soften in the presence of GCF becoming challenging to remove and resulting in inflammation (125). Consequently, several biodegradable polymers have been tested for tetracycline's delivery. These include poly-hydroxybutyric acid, poly lactic-co-glycolic acid (PLGA), atelocollagen, gelatin and chitosan (121,126,127).

Periochip® is a FDA-approved insert, composed of chlorhexidine gluconate in a biodegradable matrix of hydrolyzed gelatin/glutaraldehyde. This system reveals a controlled chlorhexidine release for 7 days nevertheless, it is possible to observe a significant burst effect (128).

Microspheres

Microspheres are solid spherical polymeric structures, presenting a diameter between 1 and 1000 μm. These systems, where the API is dispersed within the polymeric matrix, are able to provide controlled drug delivery at the periodontal pocket. Up to date, both biodegradable and non-biodegradable materials have been employed, including natural and synthetic polymers. The final formulation can be directly injected into the target site. Microparticles present a variety of advantages. Amongst them, it is possible to highlight the ease of administration, the stability of the employed APIs, the ability to provide controlled drug delivery and increased bioavailability. However, they are also associated with some downsides, including i) their complex and costly production (when compared to preformed implants), ii) their demanding administration with possible syringe clogging leading to an incomplete dose and, iii) the low retention time in the periodontal pocket (120,121,129).

Arestin® corresponds to FDA-approved microspheres, loaded with minocycline hydrochloride, which displays an effective drug concentration up until 14 days (130).

Nanosystems

Nanosystems (such as micelles, metallic and polymeric nanoparticles and liposomes) have been largely used in dentistry and are able to precisely deliver the API to difficult access-lesion sites due to the reduced size of the particles. This drug delivery system present several advantages, namely, improvement of the drug loading capability, larger surface-volume rate, decreased dosing frequency

and good biocompatibility (131). It is relevant to note metallic nanoparticles (such as silver, gold, and titanium dioxide) possess antibacterial properties, being commonly employed in dentistry (132). However, they are cytotoxic and non-degradable, limiting their use (120). As a consequence, polymeric nanoparticles (containing, for instance, chitosan (133) and PLGA) have been tested for the treatment of periodontal diseases. Additional, liposomes have also gained attention due to their ability to improve solubility, change drug pharmacokinetics and biodistribution, control the drug release, site-specific targeting and tissue permeability (134).

Finally, albeit several APIs are promising and could be used in nanosystems, there are no marketed products. This might be explained by their complex and costly production as well as the lack of stability of the final formulations (120,121).

Gels

Gels are becoming one of the most promising therapeutic approaches in the dentistry field due to i) their ease of production and administration avoiding patient's discomfort, ii) biocompatibility, iii) biodegradability and, iv) stability (121). However, gels are also associated with possibly early, accidental removal from the site of action due to mechanical stress (either, mastication or tooth brushing). Hence, the drug exposure to the target site in unreliable (135). Moreover, it is frequently observed a moderately rapid release of the dissolved/dispersed API at initial time points. Finally, gels can be produced with numerous polymers, including carbopol, carboxy methyl cellulose and chitosan (121).

Several gels are already on the market. Amongst them, it is possible to identify Elyzol® (metronidazole benzoate in a glycerine-oleate and sesame oil basis), Parocline® (based on Eudragit RS, hydroxyl ethylcellulose, triacetin, glycerol and magnesium chloride, that releases minocycline hydrochloride) and Chlo-site® (both chlorhexidine digluconate and dihydrochloride are present in a xanthan gum vehicle) (135).

Table 4 summarises the marketed LDDSs employed in the treatment of periodontitis. It is relevant to note the majority of the marketed products, as well as the formulations being currently developed and described in literature, use antibiotics as a mean of managing the periodontal disease. Nevertheless, it is well established that the application of low doses of the latter drug class during extended periods of time may result in the spread of bacterial resistances. This is largely unwanted once the emerging bacterial resistances is leading to the increasing number of ineffective antibiotics

against severe pathologies. As a consequence, antibiotics should be replaced by other drug categories, such as antiseptics (135).

In addition to this limitation, other criteria should be met in order to formulate the ideal LDDS for periodontitis' treatment. For instance, it should be biocompatible and biodegradable, easily formulated with a limited production cost, effortlessly placed into the periodontal pocket with minimal patient's discomfort, bioadhesive presenting an appropriate retention time, and should provide reliable controlled effective drug release. The previously discussed LDDSs only meet some of these requirements. As a consequence, i*n-situ* forming implants (ISFIs) are an interesting alternative, which can be tailored to meet the aforementioned criteria (135).

4.4 *In-situ* forming implants

ISFIs are liquid drug release formulations that form solid or semi-solid depots after subcutaneous injection (136). After more than 30 years of research, ISFIs are still considered an attractive parenteral drug delivery system due to its well-established benefits. Amongst them, it is possible to cite the less invasive and painful administration, through small size needles directly into the periodontal pocket, the site-specific action, higher retention time, controlled drug delivery for an extended period of time (ranging from some days to numerous months), decrease in side effects occurrence, and enhanced patient comfort and compliance (129,136,137). When looked at from a manufacturing perspective, ISFIs are produced by relatively simple processes, translating in costs' reduction (136,138). Moreover, the desired drug release kinetics can be obtained by tailoring the formulation's compounds (polymers, solvents and additives) (129,138). To this extend, it seems obvious that ISFIs have gained large popularity in numerous fields, including periodontitis (20,21), cancer (139,140), opioid use disorder (141), and schizophrenia (142).

In-situ forming implants can be categorized based on their mechanism of implant formation into: i) *in-situ* cross-linked polymer systems, ii) *in-situ* solidifying organogels, and iii) *in-situ* phase separation systems (129). The latter group can be induced by abrupt changes in environmental temperature or pH and, solvent exchange (129). The current work will solely focus on the ISFIs formed by solvent exchange. This delivery system was first introduced by Dunn et al. (143) in 1990, and it is better known as the Atrigel® technology. To this extent, a water-immiscible biocompatible and biodegradable polymer is dissolved in a water miscible organic solvent (usually, N-methyl pyrrolidone (NMP)). The selected drug is posteriorly added, forming an injectable solution or dispersion. After subcutaneous injection in the site of action, the water-miscible solvent dissipates into the surrounding tissues as the

aqueous fluids penetrate into the injected formulation. As a result, the polymer, which is insoluble in water, precipitates entrapping the API and forming a solid implant. The drug is ultimately released through diffusion or erosion. The final solid form acquires the lesion shape with appropriate adhesive and retention time in the administration site (22,129).

Up until this moment, only four ISFIs are available in the market (Atridox®, Eligard®, Sublocade® and Perseris®) (138). It is relevant to note all of them are based on the Atrigel® technology (129). These systems correspond to viscous polymeric solutions hence, the Atrigel®-based products are generally commercialized as prefilled syringes. In addition, the API and polymeric solutions are kept in different syringes in order to avoid their degradation (138): one contains the biodegradable and biocompatible polymer dissolved in the organic solvent whereas the second syringe is composed by the API. **Table 5** illustrated the marketed in-situ forming implants based on solvent exchange.

4.4.1 Composition of ISFIs based on the Atrigel® technology

Polymer

A key parameter in the formulation of ISFIs based on solvent exchange is the polymer. The ideal polymer employed in this type of system is biocompatible, biodegradable and it is non-miscible in aqueous media while presenting an adequate solubility in the water-miscible organic solvent. The latter is a requirement so that the polymer's precipitation can occur and form a solid implant, when in contact with an aqueous solution (129,138,144). Moreover, the polymer's physicochemical properties (e.g., glass transition temperature (Tg), crystallinity, molecular weight and intrinsic viscosity) have an important impact in the formation of the system and thus, the drug release kinetics. In particular, crystalline polymers possess a larger degree of hydrogen bonding hence, facilitating the API release. On the other hand, amorphous polymers undergo faster degradation. Low molecular weight polymers (approximately 18 kDa) better dissolve in organic solvents when compared to higher molecular weights compounds. As a result, the former leads to a larger swell associated with a slower solidification (144). Finally, the polymer concentration in ISFIs can range between 10 wt% and 80 wt%. The latter parameter as well as the polymer viscosity affect the syringeability of the final dosage forms and thus, the drug release kinetics (129).

Table 4: Marketed local drug delivery systems for the treatment of periodontitis. The *in-situ* forming implants will be described in the following section. Adapted from Agossa K. (145).

Form	**Composition**			**Release kinetics**		**Biodegradability**	**Commercial name**
	API	**Dose (w/w)**	**Vehicle**	**In vitro release at 24h**	**Release duration**		
Fibers	Tetracycline HCl	25%	Ethylene vinyl acetate	---	9 days	No	Actisite® (Alza Corporation, Palo Alto, CA, USA)
Inserts	Chlorhexidine gluconate	34%	Hydrolyzed gelatin (cross-linked with glutaraldehyde)	40%	7 – 10 days	Yes	Periochip® (Dexcel Pharma, Northampton, UK)
Microparticles	Minocycline HCl	2%	---	---	14 days	Yes	Arestin® (OraPharma, Horsham, PA, USA)
Gels	Metronidazole benzoate	25%	Glycerilmono-oleate + sesame oil	---	----	Yes	Elyzol® (Dumex-Alpharma, Copenhagen, Denmark)
	Minocycline HCl	2%	HEC + aminoalkyl methacrylate copolymer + triacetine + MgCl2 + glycerine	---	---	Yes	Dentomycin® (Blackwell -Supplies, Kent, UK)
							Parocline® (Sunstar, Levallois-Perret, France)
							Periocline® (Sunstar, Osaka, Japan)
	Chlorhexidine digluconate + chlorhexidine dihydrochloride	1.5%	xanthan gum	---	---	Yes	Chlo-site® (Ghimas, Casalecchio di Reno, Italy)

HCl: hyclate; HEC: hydroxyethylcellulose; MgCl2: magnesium chloride

Table 5: Marketed *in-situ* forming implants, based on the Atrigel® technology.

Product	Powder Syringe (API)	Liquid Syringe	Needle (Gauge)	Duration	Application
Atridox® *1988*	Doxycycline hyclate	PLA in NMP	23 (blunt cannula)	7 days	Chronic periodontitis
Eligard® *2002* Variable dosing regimens	Leuprolide acetate	PLGA in NMP	20 or 18	1 – 6 months	Advanced prostate cancer
Sublocade® *2017*	---	Bruprenorphine PLGA (L/G 50:50) in NMP	19	1 month	Opioid use disorder
Perseris® *2018*	Risperidone	PLGA (L/G 80:20) in NMP	18	1 month	Schizophrenia

PLA: poly(dl-lactide); PLGA: poly(lactic-co-glycolic acid); (L/G): lactic/glycolic acid ratio; NMP: N-methyl pyrrolidone

Numerous polymers can be employed in the formation of ISFIs. Amongst them, it is possible to mention polyorthoesters, polycaprolactone, polyhydroxyacids and, polyanhydrides (129,138,144). However, poly(dl-lactide) (PLA), poly(lactic-co-glycolic acid) (PLGA), and lactide/caprolactone copolymers (PLA-PCL) are preferable due to their FDA approval and long records of clinical use (129,138).

The current project employs PLGA as the FDA-approved biodegradable and biocompatible polymer for the preparation of *in-situ* forming implants. PLGA is a copolymer of lactic (PLA) and glycolic acid (PGA), existing in several compositions of the latter monomers. PLA and PGA are naturally occurring compounds and thus, they are metabolized through normal metabolic pathways, rendering PLGA biodegradable. These monomers differ in their properties therefore, being possible to tailor the final formulation by modifying the PLGA structure. For instance, a higher ratio of PLA renders PLGA hydrophobic, due to the presence of a methyl group. As a consequence, it is verified a lower water uptake and a slower degradation. The contrary occurs when it is used a larger content of PGA. Additionally, the ratio between these monomers also contribute to the establishment of either a crystalline or amorphous polymer (144). It is relevant to note PGA is a highly crystalline polymer (45-55% crystallinity) thus, showcases large tensile strength (146). Briefly, the PLA:PGA ratio selection as well as its distribution within the polymer allows to tailor the PLGA so as to attain the desired ISFIs' drug release kinetics (144).

Solvent

Considerable amounts of solvent are employed in the production of *in-situ* forming implants. As a result, the solvent presents a crucial role in the development of this type of formulations. In fact, it is implicated in the matrix phase inversion as well as the initial burst release (147). The ideal solvent must meet some criteria including, the ability to dissolve the selected biodegradable polymer, appropriate water affinity, suitable viscosity to facilitate the injection and lastly, it should be non-toxic and biocompatible so as to guarantee the safety of the treatment at the same time as it does not cause any adverse effect or tissue irritation at the administration site (138,147–150).

Numerous solvents have been described for the development of PLGA-based ISFIs. Briefly, they can be divided into two groups: i) highly water-miscible solvents and ii) non-miscible ones. The first category includes N-methyl pyrrolidone (NMP), dimethyl sulfoxide (DMSO), acetone, propyleneglycol, tetrahydrofuran, glycofurol, 2-pyrrolidone and benzylalcohol (138,148,150–152). These are described as strong solvents, leading to the formation of homogeneous solutions characterised by low viscosity and thus, ease of administration. Additionally, they promote a fast phase inversion, producing the solid

implant in a few seconds to minutes (147). However, they are also associated with an evident burst release. On the contrary, hydrophobic solvents (such as, benzyl benzoate, ethyl acetate, triacetin and triethyl citrate) are defined as weak solvents (150,152), which lead to slow phase inversion systems, where the final implant can take weeks to months to fully solidify (147). Moreover, the use of hydrophobic solvents results in the presence of large viscosities hence, postponing the aqueous media penetration into the drug release system and reducing the burst release as well as the polymer degradation (153). However, the high viscosity is linked to a challenging ISFI's injection into the administration site (154).

The possible solvent toxicity seems to be one of the major drawbacks concerning the development of ISFIs due to the lack of sufficient toxicological data regarding the employment of organic solvents in parenteral use (150).

Up until this moment, NMP and DMSO are pointed out as the most favourable solvents, not only because of their pharmaceutical precedence in approved parenteral products but also due to their large solvating ability, allowing to dissolve an extensive variety of polymers (138,148–151,155).

N-methyl pyrrolidone

NMP (C_5H_9NO) is an aprotic, highly polar organic solvent, identified by the European Community (EC) number 212-828-1 and by the Chemical Abstracts Service (CAS) registry number 872-50-4 (156). It is widely employed in several fields, including chemical, electrical, petrochemical and surface treatment (156–158). Additionally, its low acute toxicity, lack of carcinogenic effects, low volatility, low flammability and large solvating ability led to NMP's FDA approval and introduction into the pharmaceutical industry (157), where it can assume several functions, including act as i) a pharmaceutical intermediate, ii) an important solvent for drug's extraction, purification and, crystallization and, iii) an excipient in drug delivery systems (such as in the case of the already marketed *in-situ* forming implants) (157,158).

It should be noted that, as an excipient, NMP should ensure the safety of the treatment, both during and after the drug release system's administration (157). However, NMP has demonstrated to potentially lead to important side effects, including i) reproductive toxicity (damage to the unborn child), ii) serious eye irritation, iii) skin irritation, iv) dermatitis with blistering, oedema, and erythema when the individual is exposed to prolonged or repeated contact, v) respiratory irritation and, vi) neurological toxicity when inhaled in high concentrations (156,158–160).

NMP: Toxicological studies

Skin irritation

Three workers repeatedly employed NMP 99% as a cleaning agent for a few minutes, in a period of 3 days (with their unprotected hands). This led to the development of acute painful swelling, excessive wrinkling of their skin and burning sensation. These observations, verified after repeated exposure to the solvent, were ascribe to the important hygroscopic effect of NMP on the stratum corneum (161). The same results were observed in a different industry, where numerous employees displayed skin irritation after several days of dermal exposure to NMP (158).

Mucous membrane irritation

To investigate the acute effects of NMP, six human male volunteers were exposed to this chemical by inhalation (in concentrations of 0, 10, 25, and 50 mg NMP/m^3) for eight hours on four different days. Posteriorly, analysis of the individuals' plasma and urine, during and after exposure, were performed as well as changes in nasal volume were determined. The results revealed no distress to the eyes or respiratory tract upon the eight-hour exposure period, and the volunteers' nasal volume remained unaltered. The authors noted that NMP was absorbed through the respiratory tract and rapidly removed from the human organism. Finally, although no eye or respiratory irritation was noted, it was still discussed that exceptionally large peak exposures or warm NMP vapours may be capable of condensation leading to the formation of an aerosol vapour that might be an eye irritant. Therefore, this solvent is considered as a mild irritant (162).

Furthermore, several employees of a semiconductor company developed serious eye irritation and headaches, when subjected to levels as low as 0.7 ppm of NMP vapours. In fact, concentrations of the latter varying between 15 to 17 ppm were reported as "immediately uncomfortable", while levels of 49 to 83 ppm were described as "unbearable". Importantly, it should be noted this study demonstrated some limitations due to the methods employed to evaluate NMP exposure (which included informal interviews and subjective judgements) (158,159).

Development or Reproductive Toxicity

Numerous animal studies attempted to evaluate the reproductive toxicity of NMP. For instance, single NMP doses of 166 mg/kg were administered intraperitoneally to mice on different days of

gestation. After 7 days, 23% of the implanted foetuses deceased whereas, the same concentration on day 9 led to a large rate of foetal malformations (159).

Another research team administered NMP dermally to pregnant rats, in concentrations of 75, 237, and 750 mg/kg/day, on days 6 to 15 days of gestation. The higher dose (750 mg/kg) led to maternal toxicity, which was translated into a lower body weight gain during pregnancy. Moreover, foetal toxicity was also observed at the same dose, indicated by the decreased number of live foetuses per dam, a greater percentage of resorption sites, lower foetal's bodyweight and an apparent delay in skeletal development. Importantly, no toxicity, either maternal or foetal, was determined at the lower doses (159).

The possible teratogenic effect of NMP was assessed. To this extend, pregnant CD rats inhaled either 0.1 or 0.36 mg/L of NMP, for 6 hours daily, on days 6 to 15 of gestation. Numerous dams exhibited occasional lethargy and irregular breathing during the first three days of exposure. However, NMP did not produce any considerable teratogenic effects (159).

Interestingly, there is limited information of the NMP's impact on the male reproductive system. Nevertheless, it has been demonstrated that NMP is able to impair spermatogenesis, hence possibly causing infertility in male rats (157).

The previous observations should encourage the pharmaceutical industry to reconsider the use of NMP as an excipient as well as prompt all fields to better inform and protect their employees (157). In fact, i) the European Union identified these hazardous and instituted a harmonised classification and labelling system (156), ii) the Environmental Protection Agency and European Union has acknowledged NMP as a developmental toxicant and, iii) the FDA enlisted NMP in class 2 of residual solvents which should be limited in pharmaceutical products owing to its inherent toxicity (151,163).

Consequently, the European Commission limited the use of NMP. Briefly, it cannot be marketed on its own or in mixtures at concentrations of 0.3% (w/w) or larger, unless the suppliers conduct a chemical safety assessment employing the mandatory Derived No-Effect Levels (DNELs)[1] for employee exposure of 14.4 mg/m³ for inhalation and 4.8 mg/kg/day for dermal exposure (156).

[1]Derived No-Effect Levels (DNELs): the level of chemical exposure above which humans should not be exposed.

Dimethyl Sulfoxide

DMSO (C_2H_6OS) is a polar aprotic solvent (164) identified by the EC number 200-828-1 and by the CAS registry number 67-68-5. It is widely employed as a cryoprotective agent in the preservation of cells and tissues (164,165). Additionally, it has been reported to act as a free radical scavenger and a penetration enhancer in topical formulations (for instance, it is used in topical solutions of diclofenac sodium and ioxuridine to treat osteoarthritis and herpes zoster, respectively) (164,166). Moreover, it has been described that DMSO may possess anti-inflammatory, antioxidant, anaesthetic and analgesic properties (164,167).

However, this solvent can lead to numerous side effects, such as skin and eye irritation (165,168). In fact, DMSO is able to produce erythema and pruritis immediately after dermal exposure to the undiluted solvent (168). CNS depression (168), nausea, abdominal cramps, neurological effects (167), arrhythmia and hepatotoxic effects (165) are also described in literature. Lastly, it is recognised to disrupt phospholipid bilayers and to interact with ion channels and sodium–potassium ATPases (164).

DMSO: Toxicological studies

Oral toxicity

Acute

In order to assess the solvent's acute oral toxicity, single doses of DMSO of 10, 20 and 40 g/kg were administered to groups of 5 females and 5 males Carworth CFN rats. After treatment, the animals were kept under observation for 14 days. The results showed that all deceases occurred in a 24h-window following administration, with only one exception. It should be noted that the fatal doses produced ataxia, muscle weakness, reduced motor activity and bradypnea. The oral LD50 of DMSO in Carworth CFN rats was determined to be 28.5 mg/kg, when employing this test conditions (169).

Chronic

Pure-bred Pembrokeshire Corgis (ages ranging from 4 to 5 months) were divided into groups of 5 males and 5 females each and received an oral dose of a 50% of an aqueous solution of DMSO (once per day, 5 days a week) for 2 years. 9, 3, or 1 ml/kg/day were administered to the different groups while the control group received 1 ml distilled water/kg/day. The main results are listed (169):

1. Occasional vomiting (when administering a dose of 9 ml/kg/day) as well as transitory "head shaking" on weeks 11 and 13 (3 ml/kg/day and 9 ml/kg/day) were observed
2. Ocular abnormalities were displayed, independently of the dose taken
3. Increase in haemoglobin levels and total red cell count when employing the highest dose
4. Persistence diuresis in dogs submitted to DMSO concentrations of 3 or 9 ml/kg/day.

Inhalation toxicity

Acute

A study revealed that there was no significant impact of DMSO in rats after inhaling 200 mg/m^3 (62.8 ppm) for 30 days (168).

Chronic

The prolonged (13 weeks) inhalation toxicity of DMSO was also tested. Three groups of the Crl:CD®BR rats (composed of 10 females and 10 males each) were subjected to an atmosphere of 100% DMSO, during 6 h a day, every day. The control group was solely exposed to air. Interestingly, the results obtained only denoted the exposure to a mildly irritant environment. In fact, it was not observed any treatment-related effects in clinical, histopathological, haematological, urinalysis, or reproductive toxicity findings (169).

Dermal toxicity

Acute

The acute dermal toxicity of the same compound was determined. To do so, groups composed of 4 to 14 unshaved rats (with a bodyweight comprised between 108-182 g) were immersed in a DMSO solution (40, 60, 80 or 100%). Posteriorly, they were retreated, enabling to drain off the excess solution. The subjects were kept under analysis for 24h. Although no significant observations were done immediately the start of the test, 13 out of the 14 rats submitted to the 100% DMSO solution died in the following 24h. None of the other concentrations led to any death. This specific test concluded that the dermal DL50 of DMSO in Sprague Dawley rats is of approximately 40000 mg/kg (169).

Chronic

4 sets of rhesus monkeys were submitted to dermal daily doses of 0, 1, 3, or 9 ml/kg bodyweight of a 90% aqueous DMSO, everyday day for 1.5 years. Fascinatingly, i) all monkeys developed skin scaling and flaking upon DMSO exposure, in the initial phase of the analysis, ii) numerous animals displayed erythema, independently of the applied dose, and iii) in fact, DMSO did not produce any other behavioural or physical signs, haematological or biochemical alterations, organ weights and histological changes when compared to the control group (169).

Nevertheless, it is important to note that, up until this moment, no standard carcinogenicity analysis has been conducted with this compound. Thus, according to the ICH Guidance for Industry Q3C, DMSO is classified as a Class 3 solvent and more studies need to be performed to better understand its carcinogenic impact (151,155,163).

Lastly, it should be noted that the production of in-situ forming implants replacing NMP or DMSO for innocuous solvents is in accordance with sustainability in drug release and green chemistry. The latter term was introduced by the Environmental Protection Agency (EPA), and it translates into the development of chemical products and processes that minimizes or even prevents the use and production of harmful substances to human health and environment. It is applied throughout the entire lifecycle of a given product, from its design to disposal (170,171). To this extend, 12 principles were created, aiming to accomplish safe and sustainable development so as to guarantee the needs of the present without compromising the needs of the upcoming generations (170). These principles include:

i. **Principle 4**: design of safer chemicals and products, assuring that the final product is effective and non-toxic (170,171)
ii. **Principle 5**: employment of safer solvents and auxiliaries. These are frequently employed in large volumes and numerous of them are considered as quite toxic, not only to the environment but to the people exposed to them (researchers, employees at chemical manufacturing companies, and end users). Hence, a key step towards green chemistry is to reduce, remove or replace the solvents and auxiliaries for innocuous ones (170,172,173)
iii. **Principle 10**: design chemicals and products to degrade into harmless substances after use, avoiding their accumulation in the environment (171,173).

Drug

As expected, the API's properties (e.g., solubility, molecular weight, particle size) play a major role in the drug release kinetics. Consequently, their study is essential to better understand the behaviour of the final formulation. For instance, hydrophilic APIs are associated with a faster release rate when compared to hydrophobic ones. In fact, the diffusion of the latter prevents the water uptake by the polymeric matrix hence, reducing the drug release rate (144). Furthermore, other drug properties should be considered namely, the drug's pH, loading, solubility and stability (147). Importantly, the API can either be dissolved or dispersed in the final formulation, leading to the formation of a homogeneous or heterogeneous system, respectively. Evidently, this can result in different release profiles (147).

ISFIs are compatible with a wide range of active pharmaceutical ingredients thus, allowing the incorporation of numerous drugs in the same device (138). Clearly, the APIs selection is dependent on the ISFI application. In the specific case of periodontitis' treatment, and given its marked microbial dysbiosis and inflammation, the employment of both an antiseptic as well as an anti-inflammatory could be useful. In the present project, ibuprofen, a NSAID, and chlorhexidine dihydrochloride, an antiseptic, were selected to integrate the ISFI systems.

5. Aim of the study

The development of *in-situ* forming implants present an interesting potential for the treatment of periodontitis. However, up until this moment, most of the formulated systems include NMP or DMSO in their composition. Albeit they are FDA-approved, these solvents have been included in the ICH Guidance for Industry Q3C, promoting their restricted use in pharmaceutical products, owing to their potential toxicity. Additionally, NMP and DMSO are highly miscible in aqueous media. As a consequence, they produce fast phase inversion systems, where the solid implant is formed within seconds or minutes, leading to a high burst release.

To this extend, the main aim of the current work is to identify a less toxic solvent to replace the previously stated ones, and which can lead to the formation of ISFI. Notably, it is not required to use only a single solvent to dissolve the selected biodegradable and biocompatible polymer (PLGA). On the contrary, blends of numerous solvents might be employed. As a result, the properties of the final solvent mixture can be fairly easily adjusted by merely varying the amounts of the single solvents.

To do so, Hansen Solubility Parameters (HSP) are employed as a prediction tool, in order to determine the solvents able to dissolve PLGA. After promising non-toxic solvents (and blends of) are found, their ratio is varied, and their macroscopic properties are screened. Finally, and since i) periodontal inflammation is initiated and perpetuated due to the oral microbiome dysbiosis and ii) the periodontium destruction results from the host inflammatory response, two APIs (ibuprofen and chlorhexidine dihydrochloride) are incorporated in the systems and the drug release of the final formulations is evaluated. Lastly, the mechanical and microbiological properties of the systems are analysed.

Briefly, the main aims of this work can be summarized as follows:

1. Replacement of previously employed solvents (NMP and DMSO) by non-toxic ones,
2. Better understanding of the interaction between the employed APIs (ibuprofen and chlorhexidine dihydrochloride) and the biodegradable and biocompatible polymer (PLGA),
3. Preparation of *in*-situ forming implants and evaluation of the drug release kinetics, and
4. Assessment of the mechanical and microbiological properties of the final formulations.

Chapter 2: Materials and Methods

Materials

1. Formulation of the in-situ forming implant

Poly (D,L-lactic-co-glycolic acid) (PLGA, 50:50 lactic acid: glycolic acid, acid end groups, Resomer RG 502H; Evonik, Darmstadt, Germany); ibuprofen (BASF, Ludwigshafen, Germany); chlorhexidine dihydrochloride (micronized) (Evonik, Darmstadt, Germany); polyethylene glycol (PEG 400) (Fisher Scientific, Loughborough, UK); triethyl citrate (Thermo scientific, Kandel, Germany); ethanol (absolute anhydrous; Carlo Erba Reagents, Val de Reuil, France); Chlo-site (1 % chlorhexidine dihydrochloride; 0.5 % chlorhexidine digluconate, xanthan gum; Ghimas, Casalecchio di Reno, Italy).

2. Microbiological tests

Columbia blood agar base (Oxoid, Basingstoke, United Kingdom); alpha-D(+)-Glucose (Acros Organic, Geel, Belgium); L-cysteine hydrochloride hydrate (Sigma Aldrich, St Louis, USA); Bacto™ Agar (BD, Le Pont de Claix, France); horse blood defibrinated (Thermo Fisher Diagnostics, Landsmeer, The Netherlands); ringer tablets (Merck, Darmstadt, Germany); pancreatic digest of casein (Life Technologies Corporation, Detroit, USA); pancreatic digest of gelatin (BD, Le Pont de Claix, France); yeast extract (Oxoid, Basingstoke, United Kingdom); L(+)-arginine hydrochloride (Acros Organics, Geel, Belgium); pyruvic acid, sodium salt (Acros Organics, Geel, Belgium); sodium bicarbonate (Sigma Chemical, St Louis, USA); Tween® 80 (AppliChem, Darmstadt, Germany); hemin (Sigma-Aldrich, St. Louis, USA); menadion (Merck, Darmstadt, Germany); acid fuchsin (Acros Organics, Geel, Belgium).

3. Analytical chemicals

Acetonitrile and orthophosphoric acid (Fisher Scientific, Loughborough, UK); potassium dihydrogen phosphate (Thermo scientific, Kandel, Germany); sodium hydroxide (Sigma Aldrich, St. Louis, USA); triethylamine (Acros Organic, Geel, Belgium); ultra-pure water Veolia (Veolia, Vendin le Vieil, France), N-methyl-2-pyrrolidone (NMP) (Fisher Scientific, Loughborough, UK).

Methods

1. Thermogravimetric analysis (TGA)

TGA was conducted to determine the thermal degradation of the polymer and APIs employed in the current study. To do so, a thermogravimetric analyser Q500 (TA instruments, Guyancourt, France) was used. 5 to 8 mg samples were placed in an aluminium pan and on a weighing scale (sensibility 0.1 µg, precision 0.01 %). This system was kept under a dry atmosphere using a constant flow rate (50 mL/min) of highly pure nitrogen gas (99.999 %). The temperature reading was calibrated with the measurements of the Curie points of alumel and of nickel (TA instruments). The mass reading was calibrated using certified calibration weights (TA instruments). All measurements were performed at a heating rate of 5 °C/min. Both ibuprofen and chlorhexidine hydrochloride measurements were completed from room temperature to 300 °C whereas PLGA was analysed until 550 °C.

Finally, the weight loss as a function of time curves were investigated with the Universal analysis software (TA instruments, Guyancourt, France).



Figure 3: Thermogravimetric analysis Q500 (TA instruments, France).

2. Modulated differential scanning calorimetry (mDSC)

A Q200 mDSC (TA instruments, France) was used in order to analyse the thermal behaviour of PLGA, ibuprofen, chlorhexidine dihydrochloride and blends of these compounds. Temperature-modulated DSC was selected in order to better distinguish between reversible (e.g., glass transition) and non-reversible (e.g., water loss) events. The apparatus is equipped with a refrigerated cooling system (RCS 90), allowing for a temperature range between -90 °C and 550 °C. The temperature and enthalpy measurements were calibrated with indium and sapphire standards, at the same scan rates as the ones employed in the experiments.

The experiments were performed as follows: samples of 1 – 10 mg were accurately weighed into aluminium DSC pans (the latter were selected depending on the size of the samples, their properties upon heating and the events in study); the temperature scans (heating and cooling) were carried out at a heating rate of 5 °C/min combined with a modulation amplitude of 0.663 °C and a period of 50 s, under a continuous dry nitrogen flow of 50 mL/min, to improve the heat transfers and the temperature homogeneity. The glass transition was defined as the inflection point of the specific heat capacity (Cp) jump.

The final thermograms were investigated with the Universal Analysis Software (TA instruments, France).

a) **b)**



Figure 4: a) mDSC Q200 (TA instruments, France); b) DSC's thermostatic oven.

3. X-ray diffraction (XRD)

X-ray diffraction measurements were conducted recurring to a PanAlytical X'PERT PRO MPD diffractometer (Almelo, The Netherlands) (λCuKα = 1.5418 Å for combined Kα1 and Kα2), equipped with an X'celerator detector (Almelo, The Netherlands).

Powder samples of PLGA, ibuprofen and chlorhexidine dihydrochloride were placed into Lindeman glass capillaries, fitted in a rotating sample holder to avoid artefacts due to crystallites' preferential orientation. The diffraction patterns were obtained from 2θ = 3 to 35° for the polymer and 2θ = 3 to 60° for both APIs, all of them with a scan step of 0.0167 °/s.

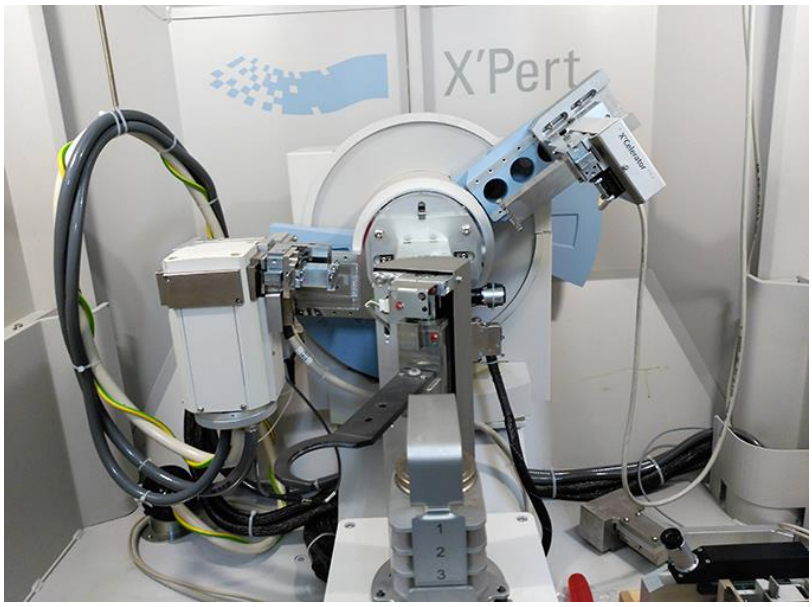


Figure 5: PanAlytical X'PERT PRO MPD (Almelo, The Netherlands).

4. Solubility of the APIs in PLGA

4.1. Cryo-milling

In the present study, cryo-milling was performed using two different apparatus: a Mixer Mill MM400 and an oscillatory CryoMill (both from Retsch GmBH, Haan, Germany).

4.1.1. Mixer Mill MM400

The Mixer Mill MM400 is composed of two vibrating arms, each of them containing a grinding jar with an internal volume of 10 mL. The latter can carry samples with a size of up to 600 mg. The milling is then performed by a milling ball with a diameter of 10 mm. Both milling jar and ball were made of zirconium oxide. The Mixer Mill arms vibrate in an arc shape with a vibration speed that can be adjusted between 3 Hz and 30 Hz (180 min^{-1} and 1800 min^{-1}).

Blends of each API individually and PLGA 502H in different ratios were accurately weighed (sample sizes between 500 and 700 mg) and placed into the 10 mL grinding jars containing a 10 mm ball. These were then immersed in a liquid nitrogen bath (T = 77 K) for approximately 5 minutes. After, the samples were placed on the equipment where the vibration frequency was set to 30 Hz. The effective grinding period (5 min) was alternated with 5 min pause periods so as to avoid the sample's heating due to the collisions throughout the process. The samples were milled for a range of effective milling times from 10 minutes to 15 minutes.

a) **b)**



Figure 6: a) Mixer Mill MM400 (Retsch GmBH, Haan, Germany) and b) 10 mL grinding jar containing a milling ball of 10 mm diameter.

4.1.2. CryoMill

Like the Mixer Mill, the CryoMill (Retsch GmBH, Haan, Germany) is also composed of two vibrating arms. However, only one of them carries a grinding jar with an internal volume of 50 mL; the other contains a counterweight. The grinding jar is placed into a cavity where the liquid nitrogen flows during the process. Consequently, the milling is conducted at temperatures of approximately -196 °C (77 K).

Blends of each API individually and PLGA 502H in different ratios were accurately weighed (final mass of 1 g) and placed into the 50 mL grinding jar with a 15 mm diameter zirconium oxide grinding ball. The samples were precooled for 30 s at 5 Hz, cryo-milled for 15 min at 30 Hz and intermediately cooled for 5 min to avoid heating of the system. The samples were milled for an effective grinding time of 60 mins.



Figure 7: CryoMill (Retsch GmBH, Haan, Germany).

4.1.3. Thermal activity monitor (TAM)

A thermal activity monitor III (TA instruments, Guyancourt, France) was used to determine the solubility of ibuprofen in PLGA. To do so, the cryo-milled samples were placed into disposable ampoules. The latter were sealed, placed in the TAM (stabilized at the starting temperature for 48 h), equilibrated and lowered into the measurement position. To minimize the temperature disturbance

due to the introduction of the samples, the latter were loaded into the machine in two steps, being followed by an equilibration stage of 30 min.

The thermograms were carried out at a heating rate of 1 °C/h, from room temperature to approximately 85 °C. Finally, the dissolution endpoint T_{end} was calculated from the heat flow signal as the intersection of the falling edge of the dissolution endotherm and the post dissolution baseline.



Figure 8: Thermal activity monitor III (TA instruments, Guyancourt, France).

5. Solvent Screening

Hansen Solubility Parameters were used as a preliminary test in order to select non-toxic FDA-approved for parenteral use solvents (and blends of), able to dissolve the selected polymer, PLGA 502H. To do so, these parameters were calculated, listed and represented as a 3D-graph, employing OriginLab 2022.

After this analysis, the most promising mixtures (RED $\leq$ 1.05) were evaluated, in practice. To do so, the solvent blend (70%) was added to 30 % PLGA 502H (*100% = solvent mixture + polymer*) and incubated overnight at 37 °C and 80 rpm, in order to accelerate the dissolution process. At predetermined timepoints within the next 24h, the blends were evaluated in order to assess the dissolution of PLGA. Clear, homogenous, and liquid solutions at room temperature were selected to test implant formation and other macroscopic properties were observed, such as elasticity and brittleness.

6. Preparation of the liquid formulations

PLGA, ibuprofen and/or chlorhexidine dihydrochloride were dissolved/dispersed in the investigated solvent mixtures in glass vials under magnetic stirring (Thermo Scientific, Loughborough, UK) at room temperature. The polymer and ibuprofen were completely dissolved, whereas chlorhexidine dihydrochloride was dispersed in the form of tiny particles. The vials were subsequently kept at rest for 3 h at room temperature to remove air bubbles. The composition of the liquids was varied as indicated in the following chapters.

7. *In-situ* implant formation

One hundred µL of the liquid formulation were placed at the bottom of a 1.5 mL Eppendorf vial using a standard syringe. One mL preheated (37 °C) phosphate buffer pH 6.8 (50 mM KH2PO4 and 22.4 mM NaOH) was carefully added using a pipette, initiating solvent exchange and implant formation. The vials were horizontally shaken at 80 rpm and kept at 37 °C (GFL 3033; Gesellschaft fuer Labortechnik, Burgwedel, Germany).

8. Drug release measurements

At predetermined time points, the release medium was completely replaced with fresh phosphate buffer pH 6.8. The withdrawn samples were filtered using: (i) 0.45 µm PVDF syringe filters (Agilent technologies, Santa Clara, USA) *for formulations containing only ibuprofen*, or (ii) 5 µm Blunt Fill Needles (Becton Dickinson, New Jersey, USA) *for formulations containing chlorhexidine dihydrochloride*. The drug contents in the samples were determined by HPLC-UV analysis using a Thermo Fisher Scientific Ultimate 3000 Series apparatus, equipped with a LPG 3400 SD/RS pump, an auto sampler (WPS-3000 SL) and a UV–Vis detector (VWD-3400RS) (Thermo Fisher Scientific, Waltham, USA). Ten µL samples were injected into a reversed phase column C18 (Gemini 5 µm; 110 A◦; 150 × 4.6 mm; Phenomenex, Le Pecq, France). The flow rate was set to 1 mL/min. The mobile phase was a blend of an aqueous solution of 115 mM H_3PO_4 containing 0.5% triethylamine (v/v) (Eluent A) and acetonitrile (Eluent B). For chlorhexidine, a 70:30 blend of Eluent A:Eluent B (v/v) was used and the detection wavelength was 239 nm (the retention time was about 4.8 min). For ibuprofen, a 38.5:61.5 blend of Eluent A:Eluent B (v/v) was used and the detection wavelength was 225 nm (the retention time was

about 5.6 min). The calibration curves were linear (R2 > 0.999) in the range of 0.5 to 10 µg/mL for chlorhexidine dihydrochloride and 0.5 to 200 µg/mL for ibuprofen. Furthermore, the pH of the release medium was measured at each sampling time point using a pH meter (InoLab pH Level 1; WTW, Weilheim, Germany).

All experiments were conducted in triplicate. Mean values +/- standard deviations are reported.

In addition, optical macroscopy pictures were taken at pre-determined time points, using a Samsung Galaxy A30s smart phone (Altice, Lisbon, Portugal), equipped a 25 MP, f/1.7, 27mm (wide) PDAF camera.

For a selected system [30 % PLGA (*100 % = PLGA + drug + solvents*), 2 % chlorhexidine dihydrochloride (*100 % = PLGA + drug*), 85 % PEG 400/10 % TEC/5 % ethanol (*100 % = total solvent system*)], drug release was measured as described above, but the experiments were optionally terminated after 7 d. The bulk fluid was removed and water pockets within the implants were opened with a 20 G syringe needle. The contents of 9 pockets were pooled. The pH of the liquid was measured using pH indicator paper (Macherey-Nagel, Hoerdt, France), and their chlorhexidine concentrations was determined as described above. The experiment was conducted in triplicate. Mean values +/- standard deviations are reported.

9. Dynamic mass changes in the implants' wet mass

Implants were formed *in-situ* and drug release was measured as described in section 8. At pre-determined time points, the bulk fluids were withdrawn, and excess water on the surface of the implants was carefully blotted with precision wipes (Kimberly-Clark, Rouen, France). The implants were accurately weighed [*wet mass (t)*]. The *change in wet mass (%)* at time *t* was calculated as follows:

$$wet\ mass\ change, \%\ (t) = \frac{mass\ (t) - mass\ (t=0)}{mass\ (t=0)} \text{ x } 100\ \% \quad (1)$$

where mass (t = 0) is the weight of the liquid formulation used for implant preparation. Each experiment was conducted in triplicate. Mean values +/- standard deviations are reported.

10. Determination of the dynamic solubility of the APIs in the release medium

The solubility limit of both ibuprofen and chlorhexidine dihydrochloride was determined, employing the shake-flask method. To do so, an excess of the solid drug was added to 30 mL of ultra-pure water in amber flasks. The latter were horizontally shaken (GFL 3033; Gesellschaft fuer Labortechnik, Burgwedel, Germany) at 37 °C and 80 rpm for 21 days. At predetermined timepoints, 500 µL were sampled using a 1 mL syringe, and filtered (PVDF syringe filter 0.45 µm *for ibuprofen* and Blunt Fill Needle with Filter 5 µm, *for chlorhexidine dihydrochloride*). The samples were then diluted and analysed through HPLC-UV. Each experiment was performed in triplicate. Mean values +/- standard deviations are reported.

11. Mechanical tests

11.1. Syringeability

The work required to expulse the investigated liquid formulations from a 2 mL syringe (Injekt; B. Braun, Melsungen, Germany) coupled with a 19G needle, was determined using a texture analyzer (load cell: 50 kg, TA.HD PlusC; Stable Micro Systems, Surrey, UK). The syringe was filled with 1 mL formulation and fixed in a universal syringe rig. A syringe plunger clamp was used to drive the piston of the syringe downward at a constant speed of 1 mm/s. Force-distance profiles were recorded at room temperature. All experiments were conducted in triplicate. Mean values +/- standard deviations are reported.

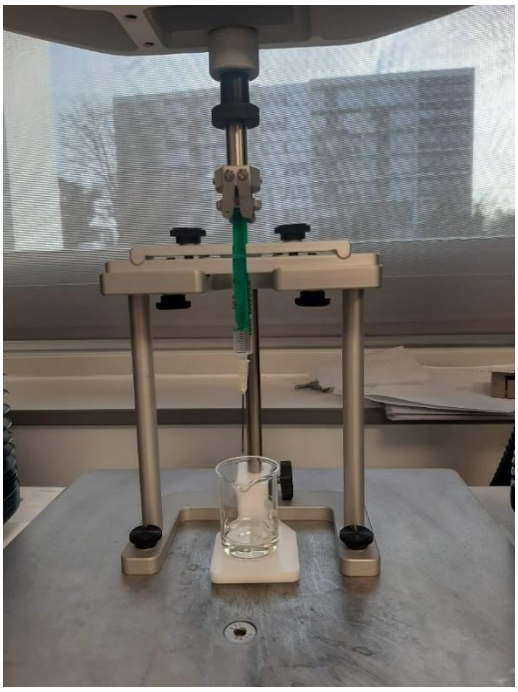


Figure 9: Syringeability's test set-up.

11.2. Texture profile analysis (TPA)

The solid *in-situ* forming implants' texture profile was investigated using a texture analyser (TA.HD Plus C, loadcell: 5 kg). Briefly, agarose was dissolved in phosphate buffer pH 6.8 (0.6% w/v), under constant magnetic stirring, at a temperature of approximately 150 °C. 70 mL of the resulting solution was placed into a Petri dish. Upon cooling and gel formation, 6 mm cylindrical holes were pierced and filled with 200 µL liquid formulation. The Petri plates were then horizontally shaken (GFL 3033; Gesellschaft fuer Labortechnik, Burgwedel, Germany).at 80 rpm and 37 °C, until implant formation.

Finally, a "double compression test" was conducted. To do so, two compression-traction cycles were performed: a 5 mm spherical probe was driven downwards (at a constant test speed of 2 mm/s). When in contact with the solid implant, the exerted force and probe movement was plotted as a function of time. When approximately half of the sample depth was reached, the probe was driven upwards until the same height it had first been in contact with the formulation. This position was held for 15 s before a new compression-traction cycle (similar to the first one) was again completed. These measurements allowed for the calculation of the implants' hardness, springiness, resilience and adhesion.

All tests were conducted in triplicate at room temperature. Mean values +/- standard deviations are reported.

12. Microbiological tests (kill-time tests)

To evaluate the antimicrobial activity of the *in-situ* forming implants, kill-time tests were performed with a *Streptococcus parasanguinis* strain (from the collection of the Laboratory of Bacteriology at the College of Pharmacy, University of Lille, France). The strain was cultured in Wilkins-West liquid medium (WWL). Dilutions were made in cysteinated Ringer solution. The bacterial strain was grown on Columbia agar plates, supplemented with cysteine chlorhydrate (0.3 g/L) as reducing agent and blood for the growth of strict anaerobes.

The bacteria suspension was exposed to the ISFIs for different time periods and the surviving bacteria populations were counted. One mL liquid formulation was placed into a 15 mL Falcon tube (Fisher Scientific, Waltham, MA, USA). Nine mL WilkinsWest liquid medium (WWL medium) were added, and the tube was incubated for 24 h at 37 °C in a horizontal shaker (80 rpm, Mini Orbital Shaker S05; Stuart Scientific, Staffordshire, UK). Upon solvent exchange, the solid implant formed. The bulk fluid was completely removed, and 8 mL fresh WWL medium was added, as well as 1 mL bacterial inoculum, followed by incubation at 37 °C under anaerobic conditions. At pre-determined time points, 100 µL samples were withdrawn and several times 10-fold diluted (1 + 9) with cysteinated Ringer solution (number of dilutions as required). One hundred µL of each dilution were plated on Columbia agar in Petri dishes, which were incubated for 48 h at 37 °C under anaerobic conditions. Colonies were counted, the results are expressed as log CFU/mL (CFU = Colony Forming Units).

For reasons of comparison, the antimicrobial activity of the solvents was evaluated as follows: 1 mL solvent (or solvent mixture) was exposed to 8 mL fresh WWL medium and 1 mL bacterial inoculum, followed by incubation at 37 °C under anaerobic conditions. At pre-determined time points, 100 µL samples were withdrawn and treated as described above.

Chapter 3: Solubility of Ibuprofen and Chlorhexidine Dihydrochloride in PLGA 502H

1. General introduction

ISFIs formed through solvent exchange are an interesting approach for the treatment of periodontitis. These correspond to advanced local drug delivery systems, mainly composed of three components: a biodegradable and biocompatible water-immiscible *polymer* is dissolved, or dispersed, in a water-miscible organic *solvent*; posteriorly, the *APIs* are added. It has been previously discussed that the physicochemical properties of all of the latter compounds present an important impact on tailoring the final formulation and hence, the drug release kinetics.

As a consequence, the present chapter attempts to physically characterize the amorphous polymer (PLGA 502H) as well as both crystalline drugs (ibuprofen and chlorhexidine dihydrochloride) by TGA, XRD and DSC. Additionally, the APIs solubilities within the polymer are analysed.

2. Physical characterization of the pure compounds

2.1. Poly(lactic-co-glycolic) acid

Poly(lactic-co-glycolic) acid consists in a widely employed FDA and EMA (European Medicines Agency)-approved biodegradable and biocompatible polymer. In fact, it is a copolymer of polyglycolic acid (PGA) and polylactic acid (PLA), generally synthetized through a ring opening copolymerization (**Figure 10**) (174–176).

PLGA has been largely employed in the formulation of controlled drug delivery systems mainly because its properties can be tailored according to the desired final dosage form. Amongst the techniques used to do so, it is possible to mention the variation of PLGA's molecular mass, ratio between PLA and PGA and esterification of the carboxylic-end groups. These modifications enable the adjustment of the final PLGA behaviour in order to obtain the sought-after release and degradation kinetics. Interestingly, PLGA copolymers acquire the features of their individual monomers, playing an important role on the size, degradation profile, hydrophilicity, crystallinity and mechanical strength of the final molecule (174–176).

PLGA grade 502H was selected for the present study and its main properties are described in **Table 6**. This is composed of a 50:50 ratio of PLA and PGA, with a carboxylic acid end group. As an amorphous form, it is characterized by a glass transition temperature, where the material goes from a glassy state to a rubbery one. Remarkably, this temperature seems to be greater than 37 °C for most

PLGA forms, indicating that the molecule is in a glassy state at a physiological temperature and the PLGA is primarily immobile.

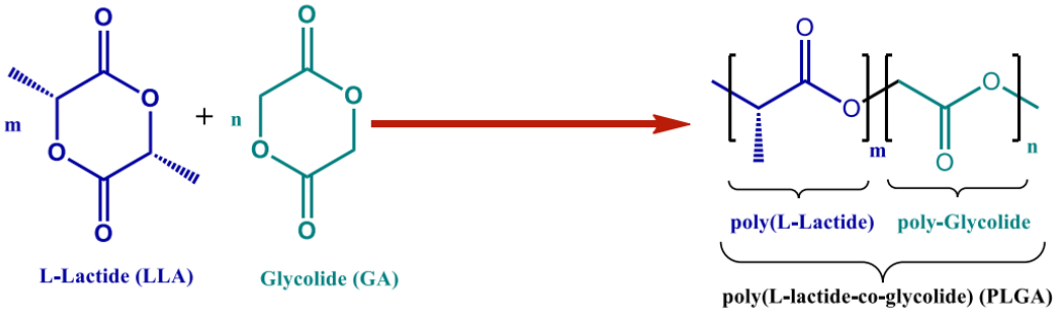


Figure 10: Poly(lactide-co-glycolide) synthesis (m = number of lactide units; n = number of glycolide units). Adapted from Butreddy et al. (177).

Table 6: PLGA 502H physicochemical properties (https://www.sigmaaldrich.com/).

PLGA 502H	
Form	Amorphous
Feed Ration Lactide: glycolide	50 : 50
End group	Acid
Molecular Weight (M_w)	7 000 – 17 000 g/mol
Degradation timeframe	< 3 months
Glass transition temperature	42 – 46 °C

2.1.1. PLGA's characterization by TGA, XRD and DSC experiments

PLGA 502H's thermogravimetric analysis was performed at 5 °C/min, up to 550 °C (**Figure 11**). A strong loss of mass (close to 100%) was observed between 180 °C and 320 °C revealing the thermal degradation of the polymer.

Figure 12 shows the polymer's X-ray diffraction diagram, recorded at room temperature, in a capillary, between 3° and 35° in 2θ. It was possible to observe the lack of Bragg peaks, indicating PLGA's amorphous state.

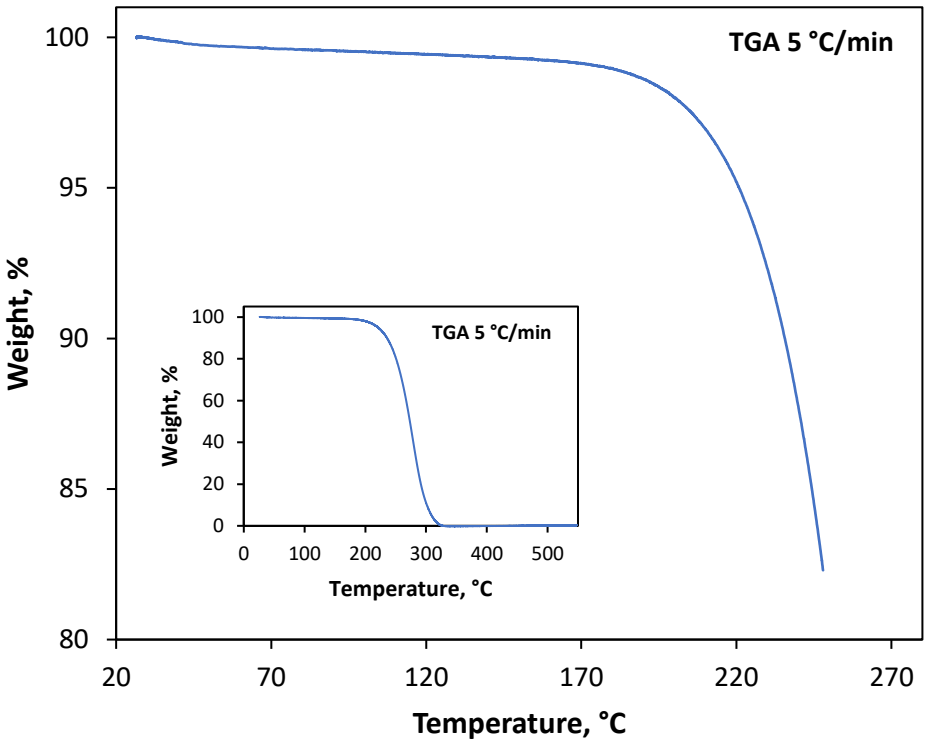


Figure 11: TGA scan (5 °C/min) of PLGA 502H.

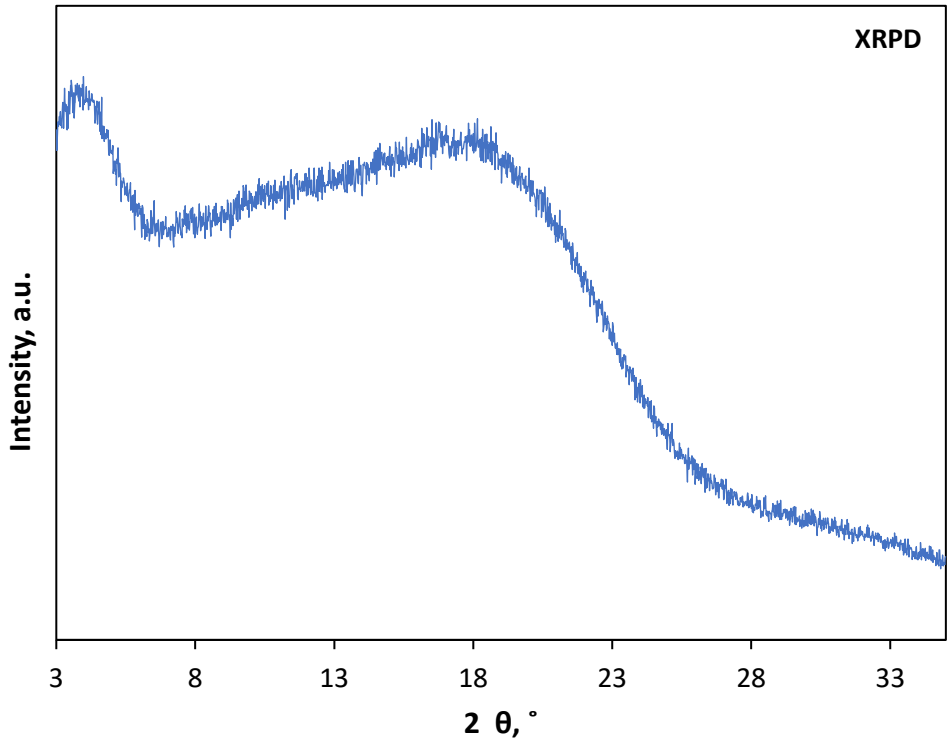


Figure 12: XRD patterns of commercial PLGA 502H, recorded at room temperature.

The amorphous nature of PLGA 502H should be noted. It is well known that amorphous polymers generally present higher degradation rates when compared to their crystalline form. Consequently, it may be observed a faster degradation of the polymeric matrix, promoting the drug release. In addition, this amorphous nature may result in a better distribution of the API within the polymer, foreseeing more consistent (therefore, predictable) drug release kinetics.

Lastly, **Figure 13** depicts the mDSC thermograms of PLGA 502H in a closed T0 aluminium pan, performed at a heating rate of 5 °C/min, between 20 °C and 120 °C. The mDSC allows to distinguish reversible (e.g., glass transition temperature) from non-reversible (e.g., water loss) events.

On the left-hand side, where the *total heat flow* is represented as a function of the temperature, Run 1 (full blue curve) corresponds to the sample's first heating cycle. It clearly displays an endothermic peak superimposing a specific heat capacity's jump characteristic of a glass transition. As observed above, PLGA 502H is presented in its amorphous form, which is characterized by a lack of long range order, being considered intrinsically unstable (178). As a consequence, and following the first law of thermodynamics, the amorphous material (as well as all systems) has the tendency to convert into a lower energetic state. For that reason, it can be expected for PLGA to undergo structural relaxation processes, during storage at room temperature (below the Tg), resulting in the reduction of the enthalpy. This finally gives rise to the endothermic peak represented in Run 1 (full blue line) which corresponds to the recovery of the enthalpy lost during the storage below the glass transition temperature. The lack of the endotherm in Run 2 (full black curve) confirms this hypothesis.

In order to reduce the influence of the overlapping endothermic peak previously discussed, the results are now depicted as the *reversing heat flow* as a function of the temperature, on the right-hand side of **Figure 13**. Run 1 (dash blue line) corresponds to PLGA's first heating cycle and it is evidently displayed a jump on the specific heat capacity (ΔC_p = 0.42 J /(g °C), typical of the glass transition of PLGA at approximately Tg = 42.0 °C. It is relevant to note this polymer's glass transition temperature is described in literature to be between 42 °C and 46 °C (**Table 6**). Run 2 (dash black curve) represents the sample's second heating scan. This time, it is observed a slight decrease in the polymer's Tg (Tg = 37.5 °C; ΔC_p = 0.5 J /(g °C)). As stated earlier, it is observed an enthalpy relaxation during storage. This leads to the development of some local order of the molecules, reducing the system energy. As a result, there is a decrease in the molecular mobility which can be translated into a slightly higher Tg in Run 1, when compared to Run2.

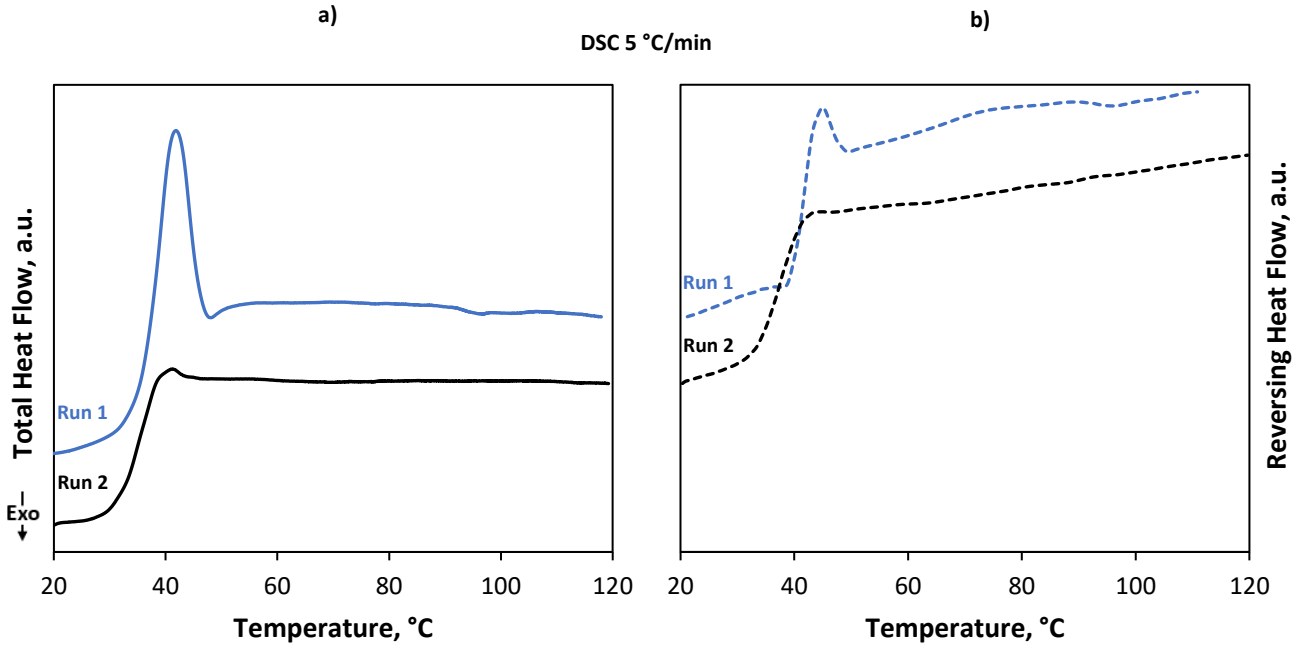


Figure 13: PLGA 502H mDSC thermograms, recorded at a heating rate of 5 °C/min. Run 1: first heating scan of the polymer. Run 2: PLGA's second heating scan. Both the total (a) as well as the reversing heat flow (b) are represented as function of the temperature.

2.2. Ibuprofen

Ibuprofen (IBU), 2-(4-isobutylphenyl) propionic acid, is a NSAID. It is extensively used for its anti-inflammatory, analgesic and antipyretic properties. Ibuprofen presents a chiral carbon, responsible for the presence of two enantiomers: S(+)-ibuprofen, the pharmacologically active form, and R(-)-ibuprofen. Generally, the commercial API is depicted as the racemic mixture, containing a 50:50 blend of both enantiomers (179). Briefly, both forms are included in the marketed products due to a typically more cost-effective manufacturing process, avoiding the additional financial and time resources to separate both enantiomers. After administration, approximately 50 to 65% of the R-enantiomeric is converted into the active form (180). **Table 7** shows some of ibuprofen's physicochemical properties (179,181).

Table 7: Physicochemical properties of Ibuprofen (Pubchem).

Ibuprofen	
Molecular Formula	$C_{13}H_{18}O_2$
Molecular Weight (M_w)	206.28 g/mol
Form	Crystalline
Melting Point	75 – 77.5 °C
Glass transition temperature	-46 °C

2.2.1. Ibuprofen's characterization by TGA, XRD and DSC experiments

The TGA scan of ibuprofen is represented in **Figure 14**. The analysis was performed at 5 °C/min, up to 300 °C. The thermogravimetric study revealed that ibuprofen is thermally stable up to approximately 110 °C, where it is observed a pronounced mass loss indicating either sublimation or thermal degradation. As a result, DSC scans containing this drug did not exceed 110 °C.

Figure 15 shows ibuprofen's XRD pattern, recorded at room temperature in a capillary, between 3° and 60° in 2θ. Clear Bragg peaks were observed, demonstrating ibuprofen's crystallinity (182).

Finally, **Figure 16** depicts ibuprofen's DSC thermograms in a hermetic aluminium pan, performed at a heating rate of 5 °C/min, between -85 °C and 100 °C. Run 1 (dark green line) corresponds to the first heating (5 °C/min) of the crystalline sample and shows an endothermic peak ranging from 70.7 °C to 83.0 °C, representative of the ibuprofen's melting (179). The corresponding melting temperature (T_m) and enthalpy of melting (ΔH_m) are respectively 77.2°C and 135.4 J/g. The melt was then cooled to -85 °C and re-heated, at a heating rate of 5 °C/min. The corresponding thermogram is represented in **Figure 16** by Run 2 (light green curve). This displayed a specific heat jump (ΔC_p = 0.44 J/(g °C)), characteristic of a glass transition at Tg = -43.6 °C (179). Briefly, this demonstrates the quench of the melt leads to the formation of the API's glassy form. Additionally, it was not detected any exothermic peak due to recrystallization above the Tg, confirming that the ibuprofen's amorphous form obtained after the liquid quench acquires an apparent "stability" when heated to such temperatures.

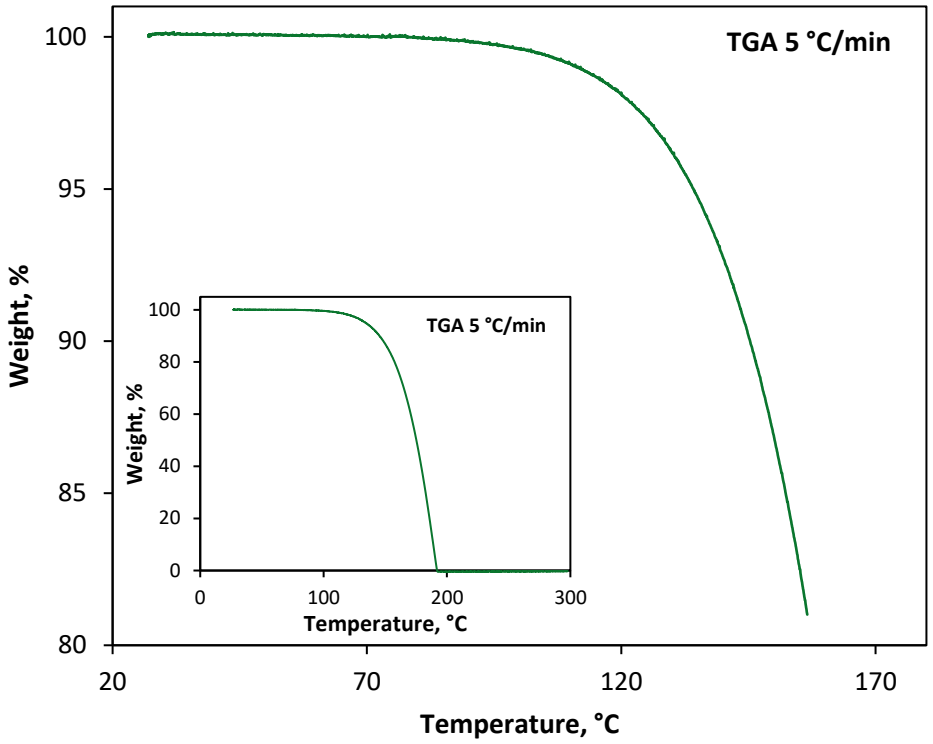


Figure 14: TGA scan (5 °C/min) of ibuprofen.

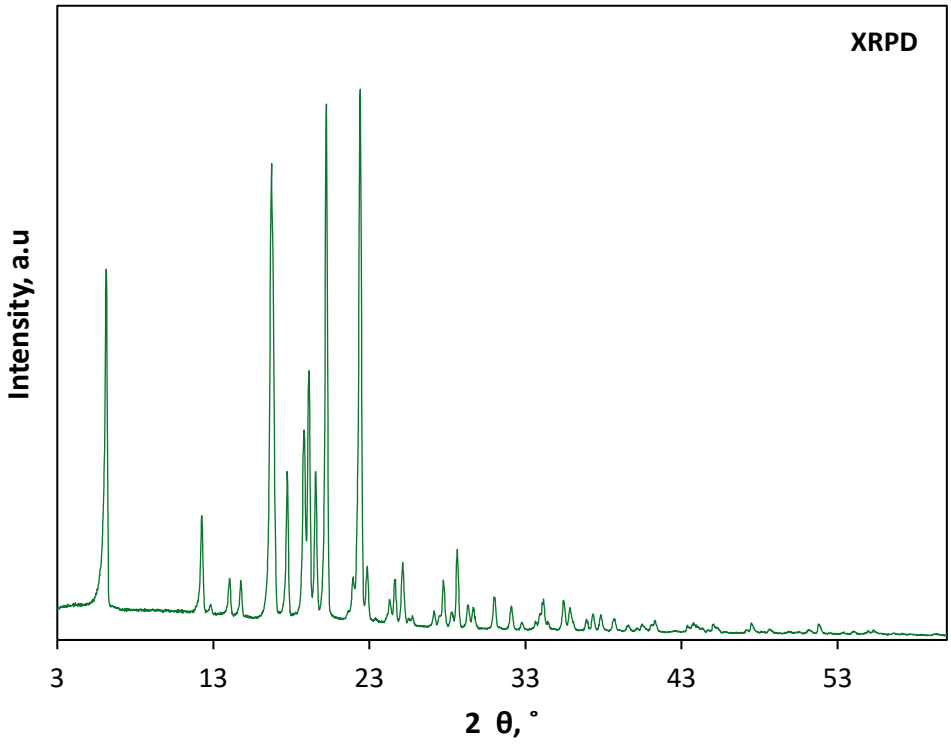


Figure 15: XRD patterns of ibuprofen, recorded at room temperature.

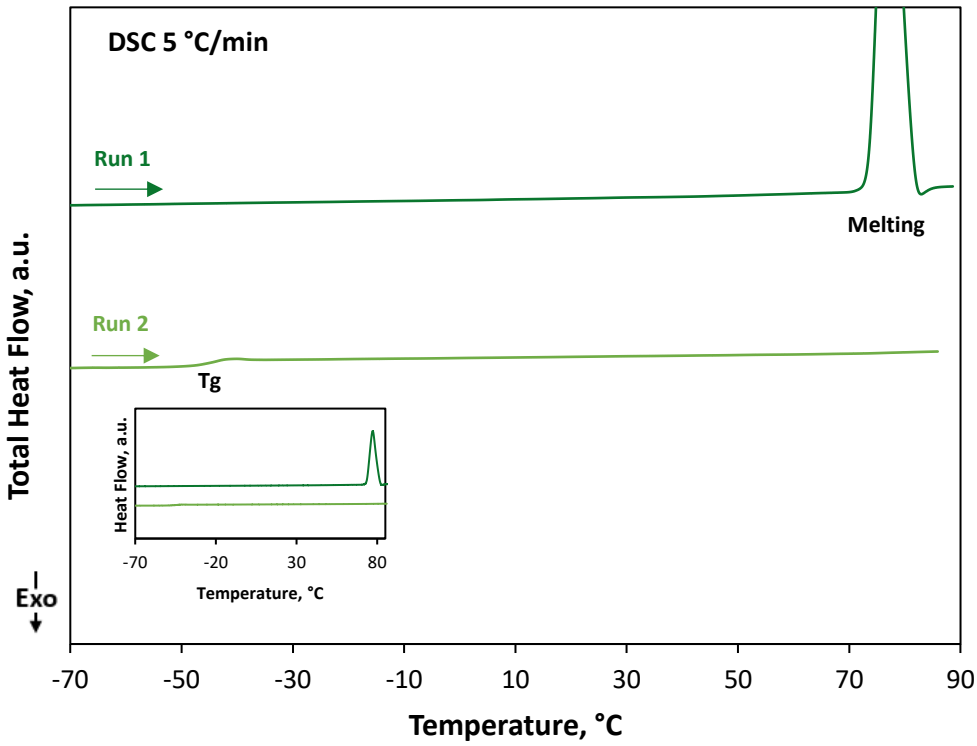


Figure 16: Ibuprofen's DSC thermograms, recorded at a heating rate of 5 °C/min. Run 1: first heating scan of the drug. Run 2: ibuprofen's second heating scan. Both ibuprofen's melting and glass transition temperature are identified.

2.3. Chlorhexidine dihydrochloride

Chlorhexidine is a broad-spectrum antimicrobial biguanide, largely used due to its activity against a wide variety of pathogens. It is employed as both an antiseptic as well as for the treatment of inflammatory dental conditions, such as periodontitis (183,184). Chlorhexidine is presented as several chemical salts, including free-base, diacetate, digluconate and dihydrochloride (CHX DiHCl). The latter was selected as the API in the current study. **Table 8** shows some of chlorhexidine dihydrochloride's physicochemical properties.

Table 8: Physicochemical properties of chlorhexidine dihydrochloride.

Chlorhexidine Dihydrochloride	
Molecular Formula	$C_{22}H_{30}Cl_2N_{10} \cdot 2HCl$
Molecular Weight (M_w)	578.37 g/mol
Form	Crystalline
Melting Point	≈ 267 °C

2.3.1. CHX DiHCl's characterization by TGA, XRD and DSC experiments

Figure 17 shows the TGA scan of chlorhexidine dihydrochloride, recorded upon heating (5 °C/min), between 25 °C and 300 °C. It shows a significant and abrupt mass loss starting at approximately 230 °C, indicating thermal degradation.

Chlorhexidine dihydrochloride's X-ray diffraction diagram is depicted in **Figure 18**. This analysis was completed in a capillary at room temperature, between 3° and 60° in 2θ. Clear Bragg peaks were observed, indicating the crystalline nature of the drug in study, particularly identifying its Form I (185).

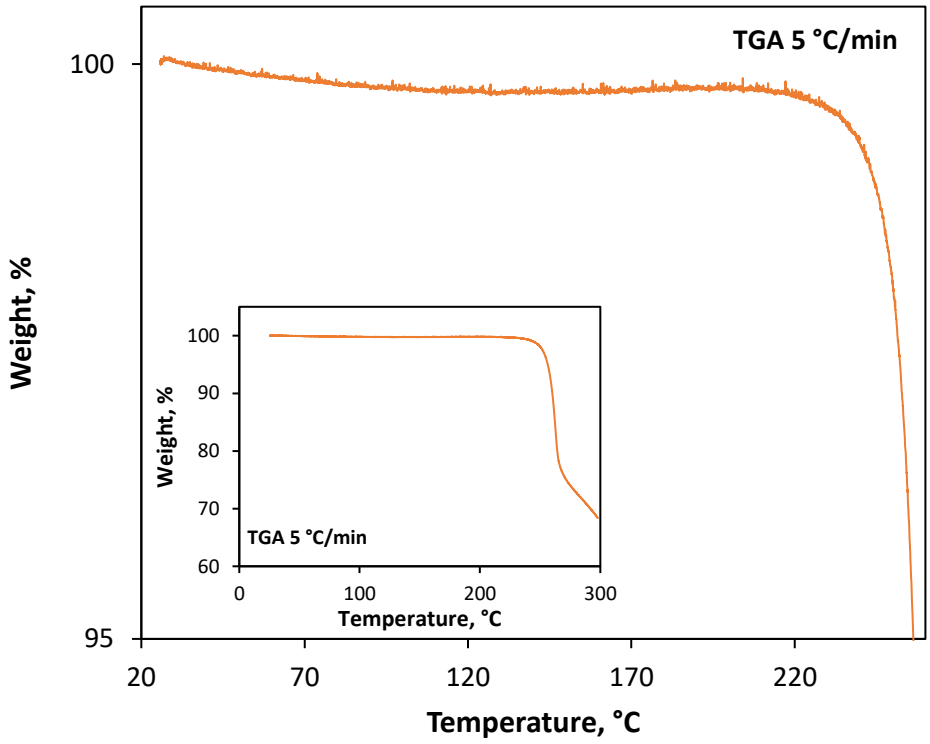


Figure 17: TGA scan (5 °C/min) of chlorhexidine dihydrochloride.

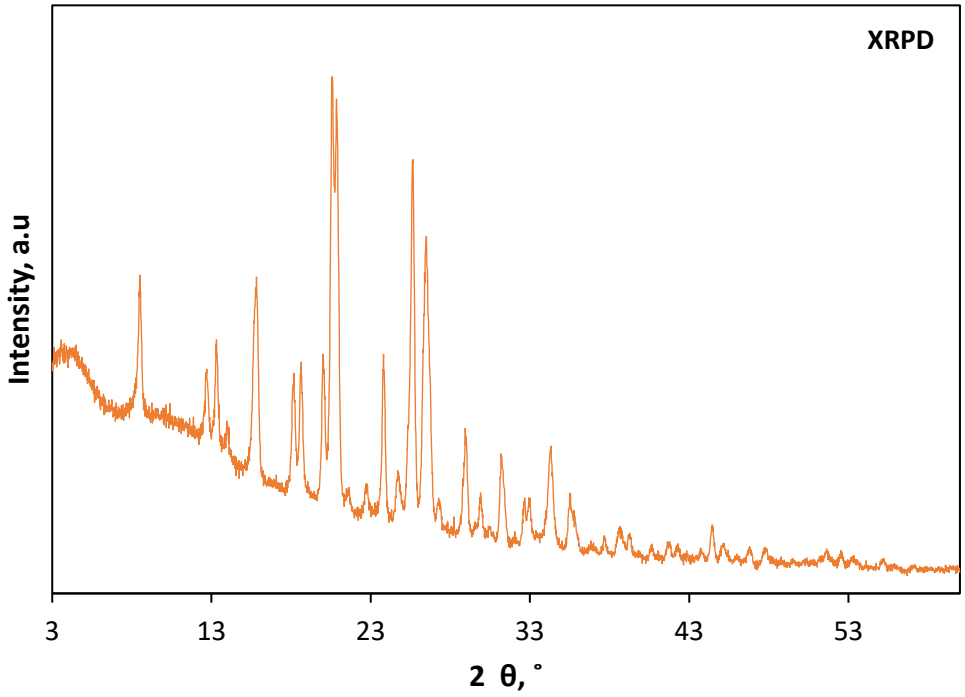


Figure 18: XRD patterns of chlorhexidine dihydrochloride, recorded at room temperature.

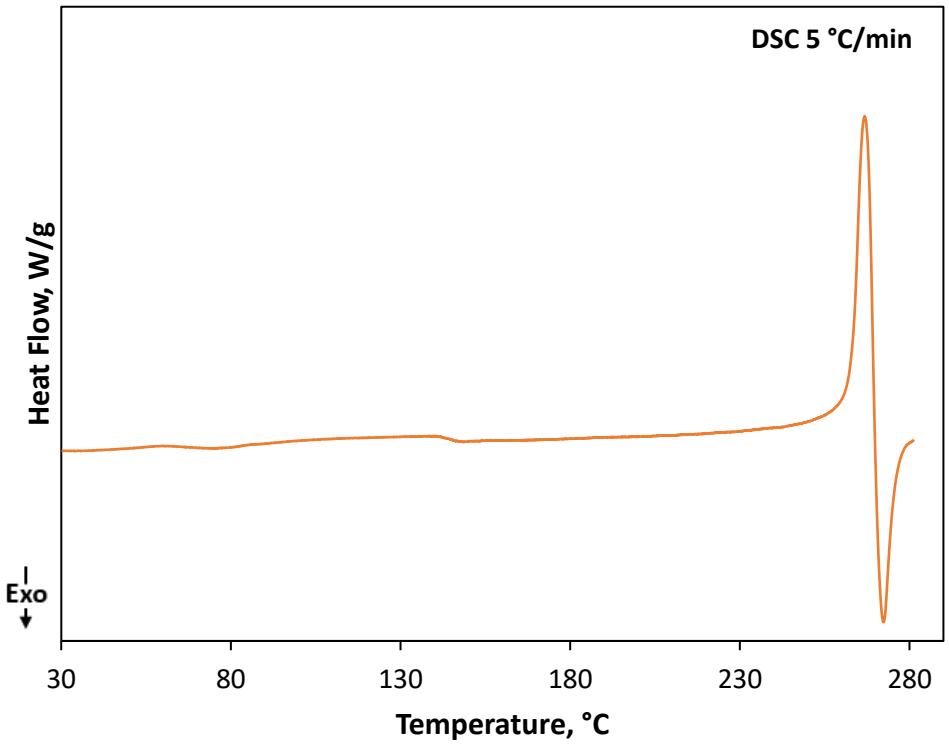


Figure 19: Chlorhexidine dihydrochloride's DSC thermograms, recorded at a heating rate of 5 °C/min.

Figure 19 depicts the DSC scan of chlorhexidine performed at 5 °C/min between 20 °C and 280 °C, in a hermetic aluminium pan. It is detected an endothermic peak owing to the melting of the crystalline material. However, this endotherm overlaps with a strong exotherm which occurs exactly in the temperature range where the TGA scan showed a strong mass loss (**Figure 17**). Therefore, the latter peak must be attributed to the material's chemical degradation. This degradation prevents the direct accurate determination of the API's melting temperature and enthalpy. Finally, it also prevents the safe undercooling of the melt and thus, the characterisation of the glass transition. However, this Tg was characterized by Elisei et al. (185). In latter analysis, the amorphous form of chlorhexidine dihydrochloride was obtained directly in the solid state (i.e., without any heating processes) by mechanical milling of the commercially available Form 1. As a result, the study found that the glass transition temperature of chlorhexidine is Tg = 93 °C and the Cp jump amplitude at Tg is ΔC_p = 0.41 J/(g°C) (185).

3. Physical characterization of mixtures

3.1. General considerations on the solubility of the APIs within the polymer

The solubility of active pharmaceutical ingredients within a polymeric matrix is of keen interest in the development of new dosage forms in the amorphous state, indicating the maximum amount of drug which can be molecularly dispersed into a polymer matrix without the risk of recrystallization. Additionally, the glass transition temperature of the mixture is also of prime interest as it provides information on the molecular mobility and thus, on the recrystallization rate of the drug fraction exceeding the solubility limit. In the particular case of *in-situ* forming implants, the solubility and the glass transition temperature provide a strong indication on the fractions of drug which can be trapped in the matrix at the molecular level or in the form of crystallites. This structural composition of the implant is then expected to play a major role on the ISFI's drug release kinetics (186).

Nevertheless, determining the drug-polymer solubility is a challenging task due to the general high viscosity of the polymeric matrix at room temperature. As a result, the system is characterized by low molecular mobility, slowing down the dissolution of the API in the polymer and, ultimately, making it demanding and extremely time-consuming to reach the equilibrium saturated state (187–192).

Consequently, the existing methods are based on the equilibrium thermodynamics at high temperature followed by the extrapolation of the acquired data to room temperature (187,189).

Although there is no standard method to determine the solubility of the API within the polymer, several approaches have been described (187,188,191,192). Amongst these approaches, it is relevant to point out the following methods.

3.1.1. Melting point depression

Briefly, a physical blend of an amorphous polymer and a crystalline drug is heated in a DSC device until the achievement of the solubility equilibrium. In the resulting thermogram, the dissolution gives rise to a broad endotherm similar to that of a melting. The temperature at which this endotherm stops marks the end of the dissolution process. This conveys that the composition of the equilibrium saturated material at this temperature is expected to be that of the initial physical mixture. As a consequence, the initial composition at this temperature produces a point of the solubility curve (186,188,189,191,192). However, the position of this dissolution peak appears to be very sensitive to the scanning rate. It shifts towards lower temperatures when the scanning rate decreases. This can be explained by the high viscosity of polymers which generally makes the time scale of the dissolution process much longer than the time scale of the DSC scan. The endpoint of the dissolution is thus systemically overestimated. This problem is generally overcome by extrapolating the end points measured for different heating rates, to a zero-heating rate. Clearly, this method is very time consuming due to the employment of many slow DSC scans. Additionally, it can also be considered as rather inaccurate since the points of the solubility curve are obtained by extrapolation (189,191–193).

Moreover, it is relevant to note this method becomes obsolete below the mixture's Tg, where the molecular mobility decreases substantially, preventing the completion of the dissolution in a reasonable time scale (192).

3.1.2. The annealing method

In order to increase the ease of obtaining the solubility equilibrium, Sun et al. (193) proposed a new technique. A mixture of an API and polymer with a predetermined concentration is now annealed for a sufficiently long time to achieve the equilibrium solubility (approximately 10 h) at a given annealing temperature (hereby defined as T_a). Posteriorly to the annealing process, the sample is scanned in the DSC. If is detected a residual dissolution endothermic peak in the resulting thermogram,

it can be concluded that the dissolution process was not completed and the dissolution temperature is higher than T_a. Conversely, the absence of the dissolution endotherm shows the accomplishment of the total dissolution. Hence, the temperature at which it is possible to obtain the equilibrium dissolution is below T_a. Lastly, by annealing the sample at different temperatures or by altering its composition keeping the same T_a, it is possible to obtain the solubility curve. Nevertheless, this method displays a major drawback: although it is precise, it is also highly time-consuming due to the large annealing times and DSC experiments (192–195).

3.1.3. The recrystallization method/Demixing of the API in the polymer

In this technique, first described by Mahieu et al. (192), the saturated equilibrium is now reached by the recrystallisation of a supersaturated glass solution, prepared by a milling process. The latter force the mixing of the two chemical species, directly in the solid-state giving rise to an amorphous solid solution possibly highly supersaturated. This solution is then annealed in the DSC, in a temperature larger than its Tg in order to attain the equilibrium dissolution concentration by recrystallization of the excess dissolved drug. The Tg displayed in the final thermogram, corresponding to the demixed product, is measured and the API dissolved in the polymer at the equilibrium solubility is calculated using the Gordon-Taylor curve of the mixture. By varying the annealing temperatures, it is possible to obtain the solubility curve of the API in the polymer (189,192,195).

This method is more advantageous when compared to the previous dissolution methods once it allows to faster achieve the saturated equilibrium state. This can be explained by the fact the Tg of the polymer matrix during the recrystallization process is always higher than that of the polymer matrix during the dissolution process. The molecular mobility is thus much higher in the first case than in the second one so that the saturated equilibrium state is reached much faster. However, the recrystallisation method can only be efficient in systems where the API acts as a plasticizer, leading to a higher molecular mobility (189,192,195).

Finally, in order to obtain a complete phase diagram of the API/polymer system, it is essential to better understand the evolution of the amorphous mixture's Tg depending on its initial composition. To do so, the Gordon-Taylor equation can be employed. The combination of the latter two curves (solubility and Gordon-Taylor) will split the phase diagram into four different areas (**Figure 20**):

1. Area I: the blend is above the solubility curve (undersaturated) and the temperature below the glass transition. This combination leads to a glass solution, being

thermodynamically and kinetically stable. As a consequence, it is not observed demixing or recrystallisation of the compounds.

2. Area II: the mixture is both surpassing the solubility curve (undersaturated) as well as the Gordon-Taylor curve, producing a liquid solution where, once again, no demixing or recrystallisation take place.
3. Zone III: the blend is now positioned below the solubility curve. To this extent, it represents a supersaturated state in API hence, possibly promoting the drug's partial recrystallisation. On the other hand, it is also located under the Gordon-Taylor curve, displaying sufficiently low molecular mobility thus, decreasing the demixing or recrystallisation rate. As a result, this is considered to be a kinetically stable glass.
4. Zone IV: lastly, the blend can be located below the solubility curve (supersaturated) and above the Tg evolution curve (where it is verified a high molecular mobility). This area becomes problematic once it leads to the formation of a both thermodynamically and kinetically unstable solution thus, promoting a higher rate of demixing or recrystallization of the API. It is generally the worst zone for the formulation.

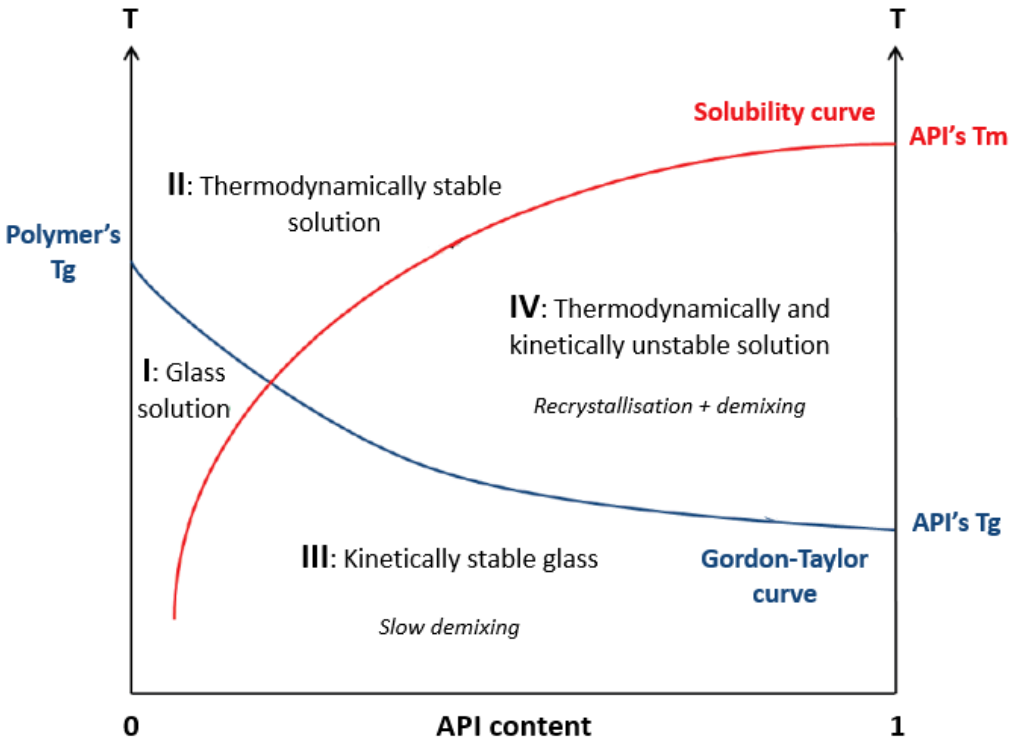


Figure 20: Phase diagram of an API/polymer system. The employment of both solubility and Gordon-Taylor curves allows the formation of four distinct zones on the graph with strictly defined properties.

3.2. Solubility of ibuprofen in PLGA 502H

In order to determine the solubility of ibuprofen in PLGA using the melting point depression method, several physical mixtures with different compositions of the crystalline drug and the amorphous polymer were co-milled. The milling is expected: i) to reduce the particle size, ii) to increase the sample's homogeneity, iii) to induce a partial dissolution of the API within the polymer, and iv) to increase the molecular mobility due to ibuprofen's plasticizing effect in PLGA. All these effects are expected to improve the dissolution of the remaining crystallites of ibuprofen in PLGA upon heating, leading to an easier and better determination of the endpoint of the dissolution process.

It is relevant to note that the amorphization of a compound, when employing a milling process, is a consequence of the competition between i) the effective amorphization due to the mechanical impact of the milling ball on the compound and, ii) the thermal recrystallization of the formed amorphous material between two mechanical impacts. Hence, the success of the process is then directly linked to the milling temperature, which influences the re-crystallization rate of the amorphous compound (196). Briefly, the amorphization is only possible when the milling is carried out sufficiently below the glass transition temperature of the compounds, namely at temperatures where recrystallization is protracted compared to the amorphization rate (196–198). As characterized in the previous sections, ibuprofen's glass transition temperature is roughly - 43.6 °C while PLGA's Tg is located at approximately 42.0 °C. To expect a co-amorphization upon milling, the latter should be performed at a temperature noticeably lower than those of the glass transition temperatures of the pure compounds. As a consequence, the co-milling was here performed at the liquid nitrogen's temperature (T = - 196 °C), employing a cryomill.

To do so, sample sizes of 500 to 700 mg were loaded into a 10 mL grinding jar with a 10 mm milling ball (both of zirconium oxide). Posteriorly, the jars were immersed in a liquid nitrogen bath (T = 77 K) for approximately 5 minutes. The samples were then placed in a Mixer Mill MM400 where the vibration frequency was set to 30 Hz. Effective grinding periods (5 min) were alternated with pause periods (5 min) so as to avoid the sample's heating due to the collisions throughout the process. During pauses, the milling jars were immersed in the liquid nitrogen bath to maintain a temperature close to 77K. The samples were milled for a range of effective milling times from 10 minutes to 15 minutes.

Finally, the blends were analysed in a DSC device at a heating rate of 5 °C/min. In the resulting thermogram, the dissolution of the API within the polymer should produce a broad endothermic peak (similar to the one of a melting process). The endpoint of the latter (T_{end}) indicates the complete API dissolution and displays the equilibrium solubility temperature of the initial given composition. Lastly, this API composition: T_{end} generates a point in the ibuprofen solubility curve.

Figure 21 shows the thermograms of both ibuprofen and PLGA individually as well as their co-milled mixtures. All scans were obtained at a heating rate of 5 °C/min.

Run 1 corresponds to the first heating of the crystalline ibuprofen. It shows an endothermic peak ranging from 70.7 °C to 83.1 °C representative of the drug's melting. The corresponding melting temperature and enthalpy of melting are, respectively, 77.2 °C and 135.4 J/g.

Run 2 displays the first heating scan of PLGA. As observed in section 2.1.1., this curve depicts an evident endothermic peak superimposing the specific heat capacity's jump characteristic of the glass transition. This reveals the presence of specific structural relaxations occurring during storage at room temperature (below Tg). As a result, the peak corresponds to the enthalpy recovery. As a consequence, the polymer's second heating cycle is also shown (Run 3). In the latter, it is possible to identify a Tg taking place at 34.81 °C.

Runs 4 to 7 depict mixtures of PLGA:Ibuprofen whose composition vary from (85:15) to (98:2). All mixtures were subjected to effective cryomilling times fluctuating between 10 and 15 minutes. It is observed, for all scans, a slight but clear depression of the glass transition temperature when compared to pure PLGA. In fact, this is highlighted by the dash vertical black line. This Tg depression reveals the plasticizing effect of ibuprofen in the polymer hence, a partial dissolution of the API within the PLGA was induced by the cryomilling process. Since the shift of Tg is quite constant and close to that of run 7, it can be concluded that the fraction of IBU molecularly dispersed in the PLGA does not exceed 2%, independently of the mixture's initial composition. In fact, it is likely that a larger amount of IBU is co-amorphized during the cryomilling process however, a significant part of it recrystallizes during the unavoidable time spent by the sample at room temperature between the end of the cryo-milling and the beginning of the DSC analysis. This potentially large recrystallization already suggests that the solubility of IBU in PLGA is very weak.

Interestingly, the superimposing relaxation endotherm observed for PLGA alone is considerably weaker after the employment of cryomilling. Briefly, the latter process promotes the fast rejuvenation of the amorphous polymer (i.e., it erases the calorimetric signatures of aging verified during storage) (199).

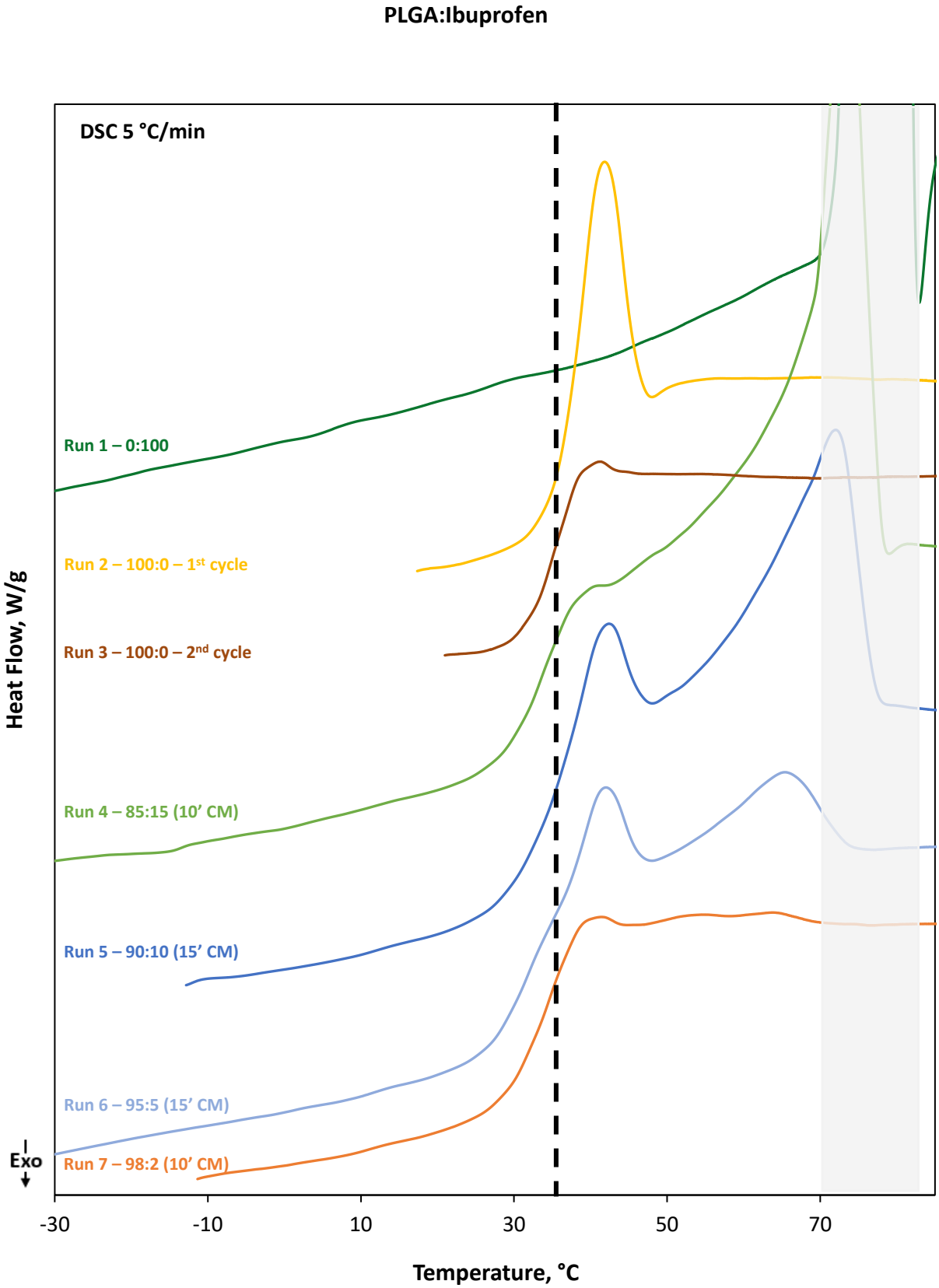


Figure 21: DSC scans of both ibuprofen and PLGA individually as well as their co-milled mixtures. All scans were obtained at a 5 °C/min heating rate.

Additionally, all mixtures show a broad and sluggish endothermic peak which starts just above the glass transition and stops abruptly at higher temperature. Such a peak is characteristic of a dissolution process which starts above Tg when the molecular mobility is high enough to allow it, and stops when there is no more crystalline drug to dissolve. The endpoints of these endotherms are reported in *Table 9*. They range from 79.0 °C for the 85:15 mixture to 70.7°C for the 98:2 mixture, indicating that the endpoint of dissolution decreases with the fraction of drug in the mixture. However, except for the 98:2 mixture, it must be noted that the endpoint of dissolution is located above the onset of the pure IBU's melting (this is clearly evidenced by the grey rectangle present in **Figure 21**). It is then possible to conclude that the time scale of the dissolution process is longer than the time scale of the DSC scan, which leads to a severe overestimation of the dissolution's endpoints. Consequently, these data cannot be considered for the determination of the solubility curve of IBU in PLGA.

Table 9: Melting, glass transition and dissolution endpoint temperatures of the studied blends of PLGA 502H and ibuprofen, determined by DSC scans at a heating rate of 5 °C/min

PLGA:IBU Composition	Tm, °C	Tg, °C	T_{end}, °C
0:100	77.2	---	---
100:0	---	39.3	---
85:15 (10' CM)	---	33.5	79.0
90:10 (15' CM)	---	39.2	78.6
95:5 (15' CM)	---	39.3	76.1
98:2 (10' CM)	---	34.6	70.7

To better estimate the solubility curve of IBU in PLGA, it was employed a thermal activity monitor (TAM III, TA instruments, France) which allows the use of considerably smaller heating rates. This system presents an exceptionally high heat flow sensitivity as well as a long-term temperature stability, being able to determine many processes which are imperceptible when using other techniques. Moreover, the combination of remarkably slow heating rates (2 °C/hour at maximum) and precisely controlled scanning conditions yields enhanced resolution of phase transformations when compared to traditional DSC devices.

Sample sizes of 500 to 700 mg were loaded into a 10 mL grinding jar with a 10 mm milling ball (both of zirconium oxide). The jars were then immersed in a liquid nitrogen bath (T = - 196 °C) for approximately 5 minutes. Subsequently, the samples were placed in a Mixer Mill MM400 where the vibration frequency was set to 30 Hz. The effective grinding period (5 min) was alternated with 5 min pause periods to avoid the sample's heating due to the collisions throughout the process. All samples

were milled for 10 minutes of effective milling. Finally, the blends were analysed in TAM III at a heating rate of 1 °C/hour, which is 300 times slower than the heating rate used for the previous DSC scans (5°C/min). Once more, the dissolution of the API within the polymer should produce a broad endothermic peak in the resulting thermogram. The endpoint of the latter (T_{end}) indicates the complete API dissolution and displays the equilibrium solubility temperature of the initial given composition.

Figure 22 shows the thermograms of ibuprofen and blends of this compound with PLGA 502H. All samples were treated in the same manner (10 minutes of effective cryomilling) and the scans were obtained at a heating rate of 1 °C/h.

Run 1 corresponds to the crystalline ibuprofen. It is observed an endotherm located between 74.1°C and 76.1°C, illustrative of the API's melting. Interestingly, this interval is narrower in comparison with the previous DSC studies, demonstrating the higher sensitivity and resolution of the TAM III (when employing a heating rate of 1 °C/h).

Runs 2-5 correspond to the heating scans of different blends of PLGA and IBU, presenting compositions ranging from 90:10 to 99:1. Each scan shows a glass transition between 20°C and 30 °C, immediately followed by a broad endotherm representing the dissolution of the API within the polymer. It should be noticed that when the temperature run is started in a TAM device, it is observed a larger transient effect, when compared to a DSC. Hence, in the current analysis, this is positioned very close to the mixture's glass transition, making it challenging to observe this phenomenon with a high resolution. The temperatures at which the dissolution endpoints stop are reported in **Table 10**. They range from 74.2 °C, for the composition of 90:10, to 50.9 °C for the 99:1 blend. Remarkably, these temperatures are significantly lower than those obtained in the previous DSC investigations, which were all situated above 70 °C for similar compositions. This confirms, *a posteriori*, that the dissolution rate of IBU in PLGA 502H is rather slow to be analysed with heating rates usually employed for DSC experiments (typically 5 °C/min). It must also be noted that the endpoints of dissolution determined by TAM experiments are located below the melting of the pure API thus, surpassing the drawback verified with the DSC studies (overlap of the dissolution and melting processes).

The determined endpoints indicate the complete API dissolution and display the equilibrium solubility temperature of the initial given composition. Consequently, it was possible to estimate the solubility curve of ibuprofen within PLGA 502H (**Figure 23**).

Figure 23 showcases the experimental solubility curve of IBU in PLGA 502H, derived from the TAM experiments. While the data is scarce, it distinctly depicts the very rapidly solubility reduction at the same time as the temperature decreases. The analysis of the results leads to the conclusion the solubility of the API within the polymer at body temperature is lower than 1%.

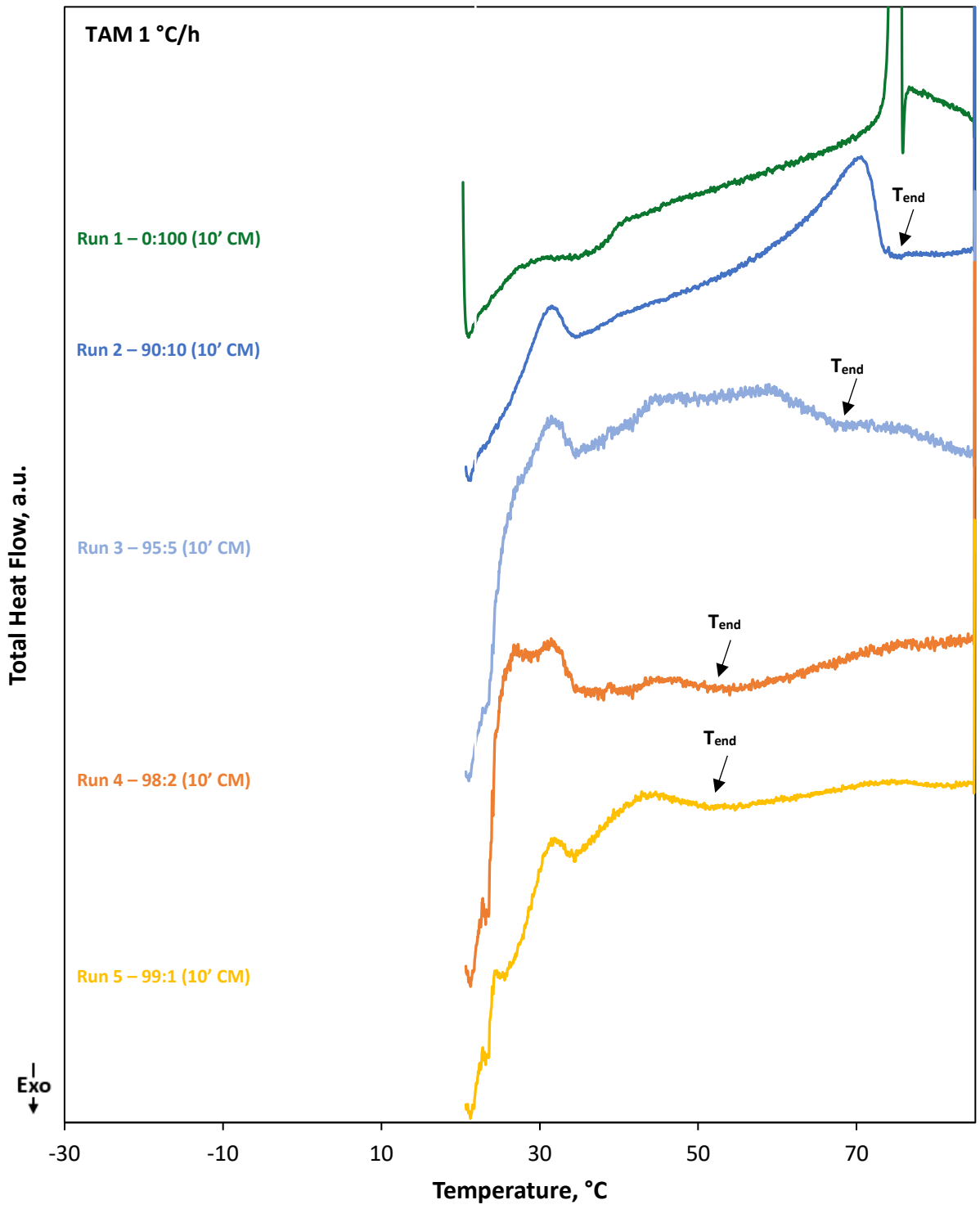


Figure 22: TAM III thermograms of pure ibuprofen and blends of this compound and PLGA 502H, performed at a heating rate of 1 °C/h. All samples were subjected to an effective cryomilling of 10 minutes. The glass transition temperature (Tg) and the dissolution endpoint (Tend) are illustrated.

Table 10: Dissolution endpoint temperatures of the studied blends of PLGA 502H and ibuprofen, determined by TAM III at a heating rate of 1 °C/h.

PLGA:IBU Composition	Tm, °C	T_{end}, °C
0:100	75.2	---
90:10	---	74.2
95:5	---	67.9
98:2	---	52.6
99:1	---	50.9

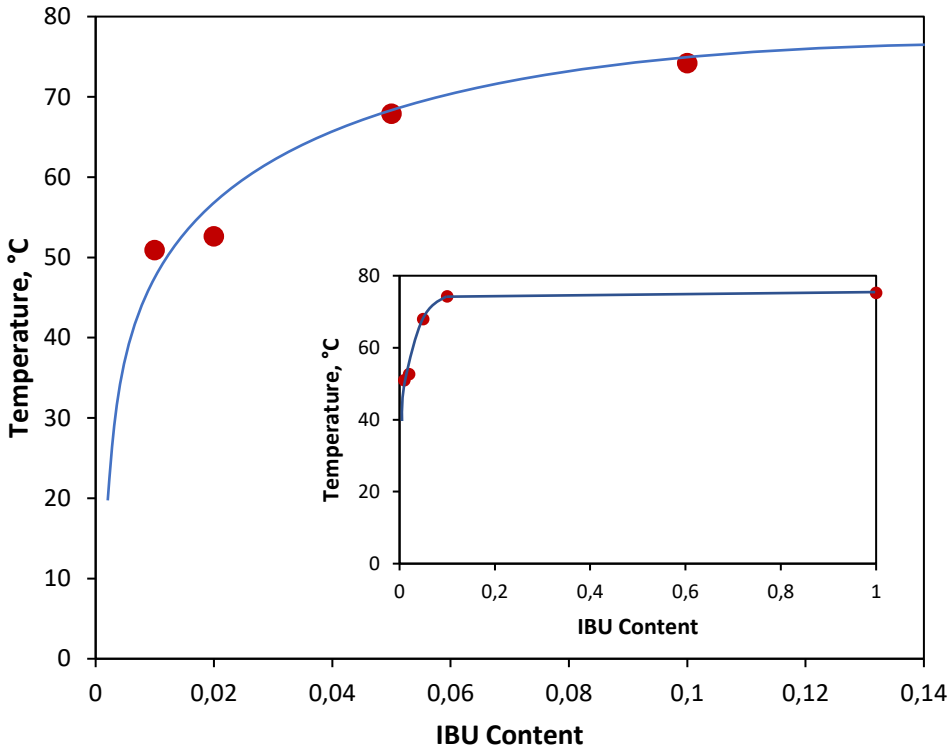


Figure 23: Solubility curve of ibuprofen in PLGA 502H.

Finally, it was attempted to determine the evolution of the amorphous mixture's Tg depending on its composition through the employment of the Gordon-Taylor curve. The combination of these two curves (solubility and Gordon-Taylor) allows to obtain a complete phase diagram of the API/polymer system.

To determine the Gordon-Taylor curve, blends of ibuprofen and PLGA 502H in different ratios were amorphized. It has been widely reported that the amorphization of molecular materials can be attained under mechanical grinding. Once again, and because the glass transition temperature of

ibuprofen is located at approximately – 43.6 °C, liquid nitrogen was used as a coolant. Moreover, at such temperature it is expected a low molecular mobility hence, largely decreasing the rate of demixing or recrystallisation of the API (provided that the material is maintained at the temperature of liquid nitrogen after grinding).

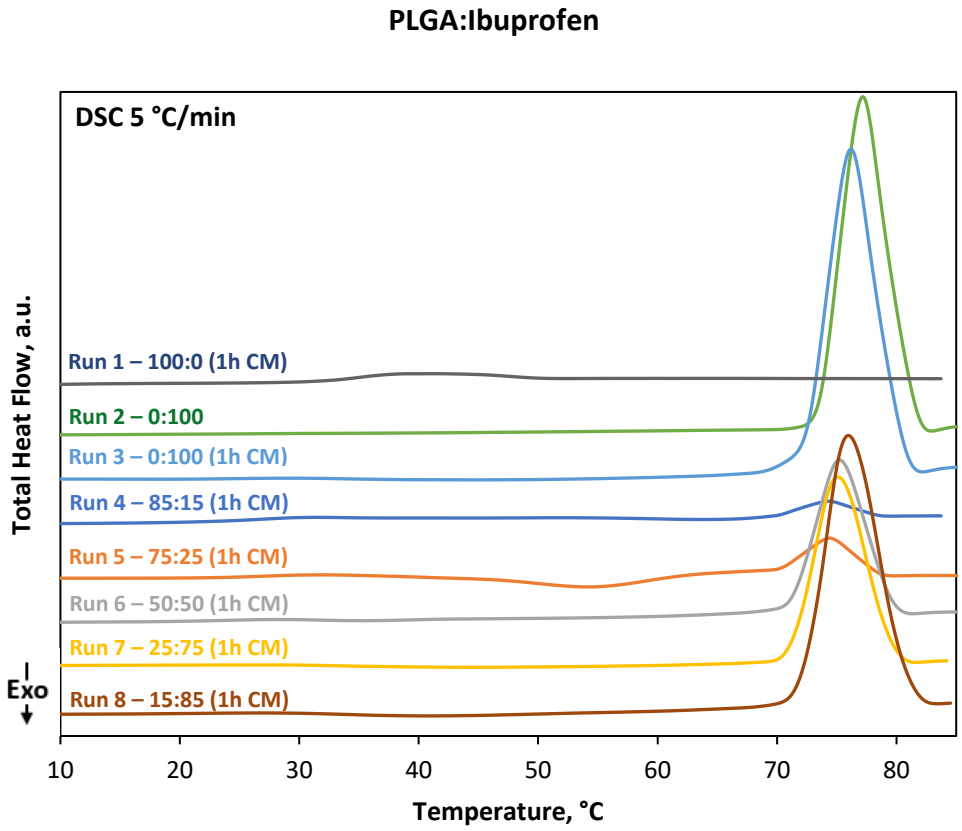
To this extent, the ibuprofen and PLGA 502H blends were accurately weighed (final mass of approximately 1 g) and placed into a 50 mL grinding jar with a 15 mm diameter zirconium oxide grinding ball. The milling jar was positioned in a CryoMill device (Retsch GmBH, Haan, Germany), precooled for 30 s at 5 Hz, cryo-milled (T = - 196 °C) for 15 min at 30 Hz and intermediately cooled for 5 min to avoid heating of the system. The samples were milled for an effective grinding time of 60 mins which is generally enough to amorphized and coamorphize materials. Finally, the blends were analysed in a DSC device at a heating rate of 5 °C/min. The results are shown in **Figure 24**.

Figure 24 depicts the first heating scans, reported at 5 °C/min, of ibuprofen and PLGA individually as well as blends of both compounds after an effective cryomilling process of 60 minutes. Run 1 represents 100% of PLGA (anteriorly subjected to a 1h cryomilling process). It displays a distinct jump on the specific heat capacity, characteristic of its glass transition temperature at 35.0 °C.

The following curves (Runs 2 and 3) illustrate 100% ibuprofen, having the second one been subjected to a 1h effective cryomilling. Interestingly, both exhibit an endotherm representative of the API's melting at 77.2 °C and 76.2 °C, respectively, as well as similar melting enthalpies (ΔH = 136.0 J/g vs $\Delta H_{cryomilled}$ = 137.2 J/g). This possibly shows the totality of the drug is in its crystalline state. In summary, this can either demonstrate that the 60 min-cryomilling process did not amorphize the sample or, most likely, ibuprofen was amorphized but recrystallizes when no longer at a temperature of 77 K. Additionally, the similar melting enthalpies are intriguing: it was expected that the cryomilled sample would present a slightly lower energy as a result of crystal's defects promoted by the milling process. However, that was not verified.

Several co-milled mixtures of the API and polymer are also represented in **Figure 24**. It is noteworthy to notice all of them are characterized by an endothermic peak, typical of ibuprofen's melting, suggesting part of the drug is in its crystalline form. The curves composed by 85:15 and 75:25 PLGA:IBU were enlarged to provide a clearer view of the observed phenomena (**Figure 24 b**). In both cases, it is observed a Cp jump characteristic of a glass transition temperature ($Tg_{85:15}$ = 26.5 °C; $Tg_{75:25}$ = 27.8 °C). It is identified a noticeable depression of this number when compared to PLGA 502H alone, conveying some part of ibuprofen was dissolved in the polymer during the milling method. The glass transition temperature is then followed by an exotherm, evidently showing a recrystallisation process, and finally, the melting of the crystalline API.

a)



b)

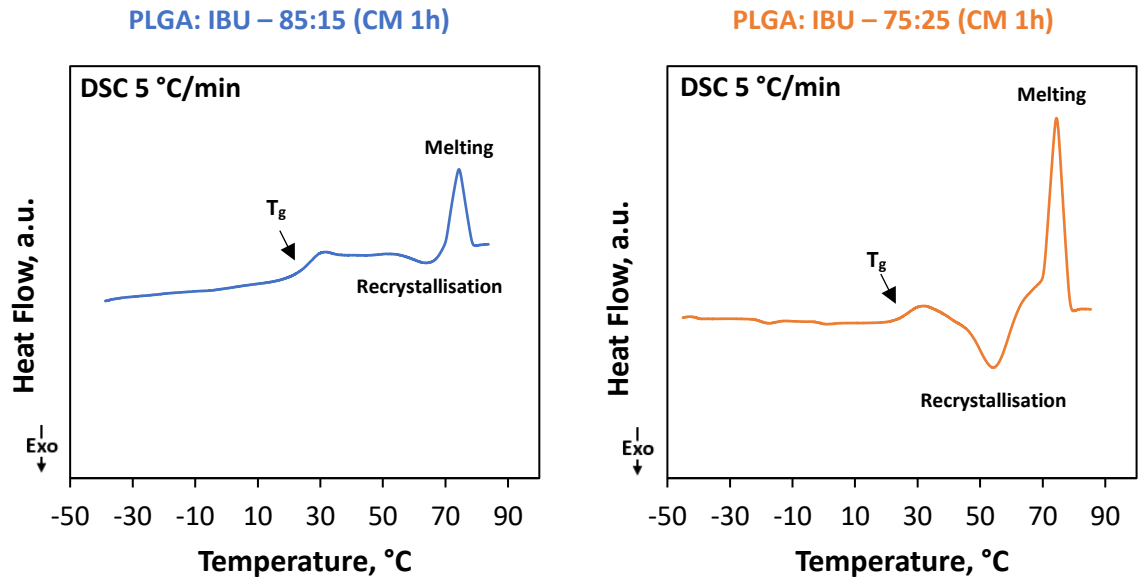


Figure 24: a) DSC thermograms of PLGA, ibuprofen and PLGA:ibuprofen mixtures subjected to a 1h cryomilling process, reported at 5 °C/ min. b) Enlargement of 85:15 and 75:25 PLGA:ibuprofen mixtures to provide a clearer view of the phenomena taking place. The glass transition temperature, recrystallisation and melting are identified

In summary, it was not possible to obtain the Gordon-Taylor curve of the PLGA 502H:ibuprofen system once it was not verified an efficient amorphization process. Ibuprofen's glass transition temperature is approximately of - 43.6 °C while PLGA's Tg is located nearly at 39.30 °C. Consequently, in order to guarantee the success of the milling, the latter should be performed at an adequate low temperature (- 196 °C), where the molecular mobility is decreased and thus the recrystallisation rate is slow when compared with the amorphization. Nevertheless, the previous thermograms undoubtedly show the recrystallisation of the API when the temperature condition (T = - 196 °C) is no longer met.

Although it is challenging to precisely determine the phase diagram of PLGA and ibuprofen systems, it is possible to point out the weak solubility of the crystalline drug within the polymer, being expected to be incredibly low at body temperature.

3.3. Solubility of chlorhexidine dihydrochloride in PLGA 502H

The solubility of chlorhexidine dihydrochloride in PLGA 502H was determined. The results are represented in **Figure 25**.

Firstly, chlorhexidine dihydrochloride was accurately weighted and scanned on a DSC device, at a heating rate of 5 °C/min between 20 °C and 280 °C (Run 1). As previously discussed, it is observed a narrow endotherm consistent with the API's melting followed by a sharp exotherm peak, indicating a strong thermal degradation (in accordance with the thermogravimetric results obtained in **Figure 17**). PLGA 502H was also scanned in the same conditions and its first heating cycle is shown in Run 2 (**Figure 25**). The latter curve exhibits a jump of the specific heat capacity (ΔC_p = 0.28 J /(g °C)), characteristic of the glass transition of PLGA at Tg = 39,3 °C.

Posteriorly, a physical mixture of 50:50 PLGA 502H and chlorhexidine dihydrochloride was analysed (Run 3). It reveals a single glass transition temperature at Tg = 38.5 °C. Furthermore, the jump on the specific heat capacity (ΔC_p = 0.16 J /(g °C)) corresponds to roughly 50% of the C_p of PLGA 502H alone. No other events are observed until approximately 246 °C, where it is seen an exotherm peak, consistent with the API's thermal degradation. It is relevant to note there is no sign of a sluggish increasing endothermic signal above Tg (as it was the case for PLGA:IBU blends: **Figure 22**, Runs 3-5) which would indicate the dissolution of chlorhexidine into the polymer upon heating. This strongly suggests that the solubility of chlorhexidine in PLGA is rather weak.

Finally, a second physical mixture of chlorhexidine and PLGA was co-milled, recurring to a solid-state amorphization process, in order to "force" the API's dissolution into the polymer. The mixture

was accurately weighed and placed into a 50 mL grinding jar with a 15 mm diameter zirconium oxide grinding ball. The milling jar was positioned in a CryoMill device (Retsch GmBH, Haan, Germany), precooled for 30 s at 5 Hz, cryomilled (T = - 196 °C) for 15 min at 30 Hz and intermediately cooled for 5 min to reduce the mechanical heating of the system. The sample was milled for an effective grinding time of 60 mins. It was then placed in a DSC device at 50 °C for 10 minutes to promote the evaporation of water, possibly absorbed by the sample during the cryomilling process. Lastly, it was scanned and rescanned at a heating rate of 5 °C/min. Both heating cycles were enlarged in **Figure 25 b)** to better comprehend the occurring phenomena. Please be aware the temperature axis in the latter Figure is now between 20 °C and 180 °C.

Run 4 corresponds to the first heating scan. It shows a single glass transition at Tg = 50.8 °C which is noticeably higher than that of PLGA 502H alone (Tg = 39.3°C). This indicates the anti-plasticization of PLGA by chlorhexidine (Tg = 93 °C (185)) hence, demonstrating the dissolution of the API during the milling process. At higher temperature, it is possible to observe a two-step exotherm similar to that shown in reference (185) when heating pure CHX DiHCl, previously amorphized by milling. The first one has been attributed to the recrystallization toward the polymorphic form II, and the second to the polymorphic transformation II to III. In the present study, the strong recrystallisation above 90 °C indicates that the co-amorphous mixture obtained after co-milling is highly supersaturated so that the solubility of chlorhexidine dihydrochloride into PLGA at room temperature is clearly very weak. Additionally, Elisei et al. (185) reported that the recrystallisation enthalpy of pure CHX DiHCl towards its form II is 34 J/g. In the current analysis, this enthalpy is of approximately 17.24 J/g, roughly half of the verified in the previous study, which is consistent with the 50:50 PLGA:CHX DiHCl proportion. Briefly, this demonstrates once again the little or lack of miscibility of the API within the polymer.

The second heating scan (Run 5) shows a single glass transition very close to that of pure PLGA. This confirms that the fraction of CHX DiHCl still dissolved into PLGA after the first heating scan is very weak and that nearly all the API mechanically dispersed into the polymer during the comilling process has recrystallized during the first heating scan. This evidently proves the rather frail solubility of chlorhexidine in PLGA 502H.

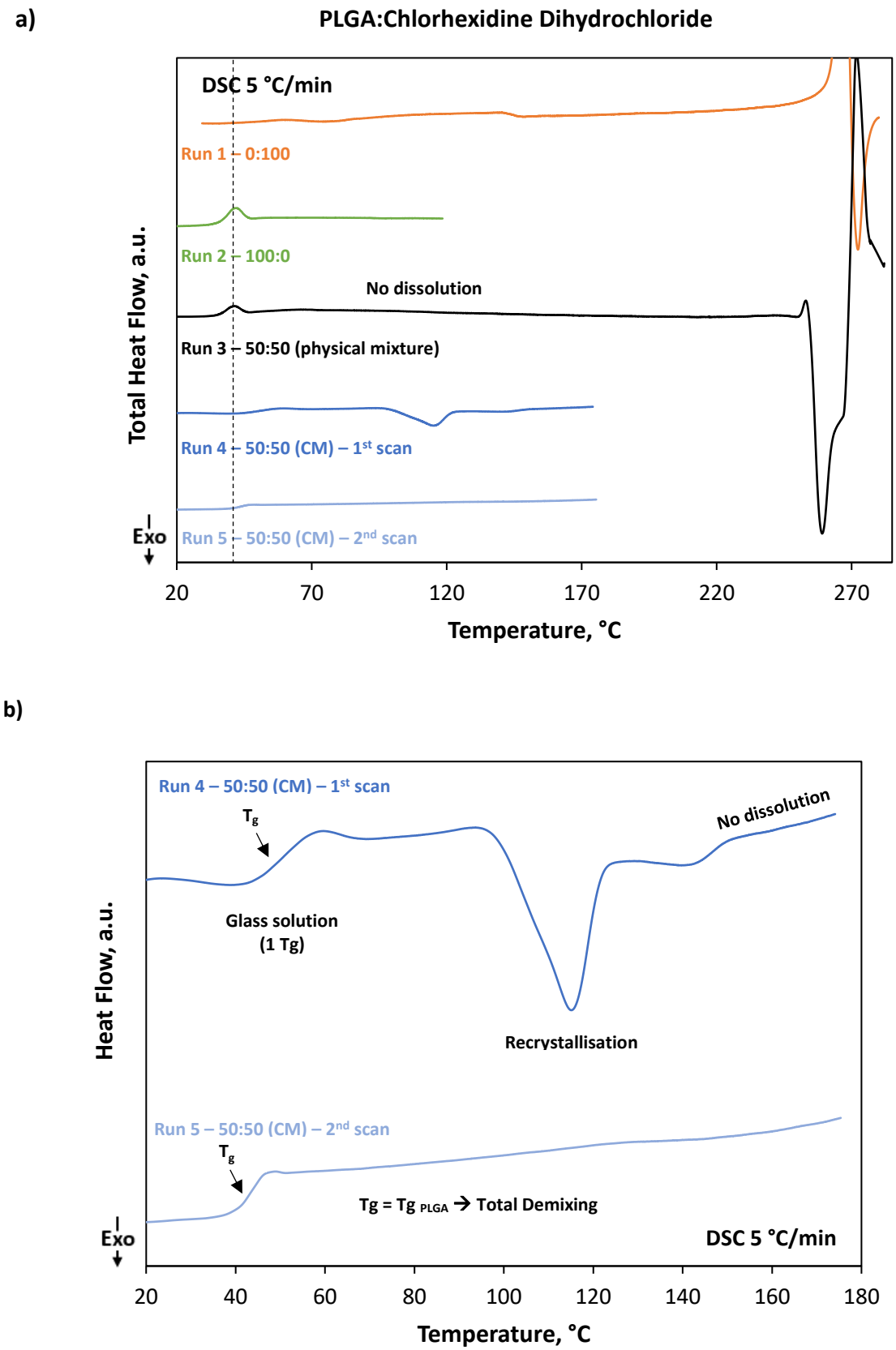


Figure 25: a) DSC thermograms of chlorhexidine dihydrochloride, PLGA 502H, a 50:50 physical mixture of both compounds and a 1h cryomilled blend of chlorhexidine dihydrochloride and PLGA (50:50). b) Enlargement of the cryomilled sample to provide a clearer view of the phenomena taking place. The most important events are marked. All scans were performed at a heating rate of 5 °C/min

4. Conclusion

The current chapter aimed to physically characterize the pure compounds employed in the current project (PLGA 502H, ibuprofen and chlorhexidine dihydrochloride) as well as attempted to determine the solubility of the APIs within the polymer.

Initially, several physical mixtures of ibuprofen and the amorphous polymer were shortly cryomilled (10 to 15 minutes) and analysed in a DSC device, at a heating rate of 5 °C/min. This method was proved to be inadequate for such task due to the very slow dissolution rate of IBU which leads the mixture into the melting zone of the API before the end of the dissolution process.

Subsequently, a thermal activity monitor was employed. The latter is well known for its high heat flow sensitivity as well as a long-term temperature stability, being able to determine many processes which are unnoticeable when using other techniques. Again, several blends of the API and PLGA 502H were cryomilled for an effective grinding period of 10 minutes and analysed at a heating rate of 1 °C/h. This allowed to obtain the endpoint of the dissolution endotherms thus, originating several points in the solubility curve. The latter evidently displayed the weak solubility of ibuprofen in PLGA 502H. Undoubtedly, it is observed a reduction in solubility as the temperature decreases. As a consequence, it is expected an extremely low solubility of ibuprofen in PLGA 502H at body temperature.

Finally, the solubility of chlorhexidine dihydrochloride in PLGA 502H was also determined. To this effect, the API, polymer and a physical mixture of both were analysed through a DSC equipment, at a heating rate of 5 °C/min. The mixture revealed a single glass transition temperature, corresponding to PLGA's Tg. In addition, the specific heat capacity showed to be approximately 50% of the ΔC_p of PLGA alone, conveying the lack of solubility of the API within the polymer. Lastly, a second mixture of chlorhexidine dihydrochloride and PLGA were cryomilled for 60 minutes so to "force" the API's dissolution into the polymer. The last-mentioned was scanned in DSC at the same heating rate as before. The sample showed a total demixing of the API clearly demonstrating the lack of solubility of the chlorhexidine dihydrochloride within the polymer.

As previously discussed, the physicochemical properties of all the ISFIs' compounds greatly affect the final formulation and thus, the release kinetics. Consequently, the low solubility (or lack of) of both APIs within the polymer will play a key role on the previous processes. Although this is clear, it is extremely reductive to base the release kinetics solely on this parameter. Other factors should be taken into consideration such as: the polymer's molecular weight, APIs' solubility, particle size, pH, loading and stability.

Chapter 4: *In-situ* forming PLGA implants – Towards less toxic solvents

*Part of this chapter has been submitted to the *International Journal of Pharmaceutics*

F. Ramos, J-F. Willart, C. Neut, K. Agossa, J. Siepmann, F. Siepmann., In-situ forming PLGA implants – Towards less toxic solvents

1. Solvent Screening through the application of the Hansen Solubility Parameters

1.1. General introduction

Substantial amounts of solvent are employed in the production of *in-situ* forming implants, leading to the formation of a polymeric solution. As a consequence, and being the solvent a critical parameter in this type of systems, it must meet some requirements namely, the ability to dissolve the selected biodegradable polymer, adequate water affinity and, suitable viscosity. When the final formulation is ultimately introduced into the human body, the solvent dissipates into the surrounding tissues. As a consequence, it must be non-toxic and biocompatible so as to guarantee the safety of the treatment (138,147–150). This seems to be one of the major concerns when it comes to the formulation of ISFI once there is limited toxicological data regarding organic solvents' parenteral use (150).

Up until this moment, both hydrophilic solvents (such as N-methyl pyrrolidone (NMP), dimethyl sulfoxide (DMSO) and 2-pyrrollidone) as well as hydrophobic ones (including triacetin, ethyl acetate, benzyl benzoate, benzyl alcohol) have been reported (138,148,150,151). NMP and DMSO are pointed out as the most favourable, not only because of their pharmaceutical precedence in approved parenteral products but also due to their large solvating ability, allowing to dissolve an extensive variety of polymers (138,148–151,155). However, according to the ICH Guidance for Industry Q3C, NMP is classified as a Class 2 solvent and should be restricted in pharmaceutical products owing to its inherent toxicity (151,163). On the other hand, DMSO is placed in Class 3 and although it presents fewer toxicity risks to human health, there is scarce data on its long-term toxicity (151,155,163). Finally, both solvents are freely miscible with water. Upon injection, they rapidly dissipate into the surrounding tissues leading to a fast solvent and drug burst. This release of significant quantities of solvent and drug within a brief time span is unfavourable once it could lead to tissue irritation or systemic side effects not foreseen by an estimated average dose, initially thought to be consistent throughout the entire drug delivery period (138,150).

In order to overcome these drawbacks, there is a need to find less hazardous solvents for the formulation of *in-situ* forming implants. To proceed to solvents selection, Hansen solubility parameters (HSP) were employed in the present chapter as an initial theoretical approach, avoiding the trial-and-error method. The latter is challenging, tedious and costly thus, using HSP, as a scientific screening

comprising a large understanding of chemical composition and intermolecular interactions, allows the saving of resources (200–203).

Hansen solubility parameters were first developed by Charles Hansen as an extension to the Hildebrand's theory (200,204), allowing to forecast the compatibility between materials. (202–205). The HSP is defined by the cohesive energy density holding a liquid's molecules together. Briefly, it represents the molar energy change required to separate the molecules from the compound's condensed state to an ideal gas (206). The cohesive energy density can then be divided into 3 contribution forces: dispersion (London or van der Waals) (δ_D), polar (δ_P), and hydrogen bonding (δ_H) (200,204,206–209). These intermolecular interactions offer a detailed numerical manner to characterise molecules (209) and their sum gives rise to the total Hansen solubility parameter (δ_{total}) (Equation 1) (200,202,204–208):

$$\delta_{total}^2 = \delta_D^2 + \delta_P^2 + \delta_H^2 \qquad \text{Eq. 1}$$

The Hansen Solubility Parameter theory has been commonly described as "like seeks like". Consequently, materials with similar solubility parameters (SP) are compatible (translating into miscibility, solubility, …). Nevertheless, it is necessary to quantitatively define this qualitative concept (202,204). Each compound's HSP can be represented as a coordinate (δ_D, δ_P, δ_H) in a 3D plot and the compatibility of two materials is measured by the distance between them (R_a). The latter is calculated by Equation 2 (204,206,209). A low R_a coveys the similarity of the compounds and hence, it results in a mutual solubility between the materials (204,206,209).

$$R_a^2 = 4\,(\delta_{D1} - \delta_{D2})^2 + (\delta_{P1} - \delta_{P2})^2 + (\delta_{H1} - \delta_{H2})^2 \qquad \text{Eq. 2}$$

It is relevant to note that, although the factor of 4 has generated controversy, it has been well established and proven valid for both theoretical reasons as well as for the extremely large amount of experimental data produced over the years (210).

Finally, another valuable parameter is the relative energy difference (RED), characterized by the ratio between R_a and R_0, the maximum value of the expected solubility (as known as interaction radius) (Equation 3) (205,206).

$$RED = \frac{R_a}{R_0} \qquad \text{Eq. 3}$$

RED numbers below 1 (and progressively closer to zero) indicate high affinity between materials. On the contrary, RED values larger than 1 depicts the increasingly lack of compatibility between the materials (204–206).

Lastly, the HSPs of a blend of compounds is directly acquired from the volume-weighted average of the HSP of the solvents alone (209).

1.2. Solvent Screening

Hansen Solubility Parameters have already been assigned to a significantly large number of materials. In fact, the HSPs of approximately 1200 chemicals are described in the second edition of "*Hansen Solubility Parameters – A User's Handbook*" (204).

The detailed analysis of this list of chemicals represents the starting point of the solvent screening tests. To this extent, only the materials that are liquid at room temperature were considered. Posteriorly, the potential toxicity of the resulting 625 materials was evaluated recurring to the open chemistry database, PubChem. For instance, the compounds' acute toxicity, health and environmental hazard as well as their corrosive, irritant and flammable nature were assessed.

It is important to note that the toxicity of a material depends on numerous factors, namely the exposure's route (oral, dermal, respiratory) and level, combined with individual susceptibility and health conditions. However, several instructions had to be implemented in order to obtain a generally non-toxic solvent system.

Firstly, when any compound was suspected or confirmed of causing health hazards, they were automatically removed from the screening phase. This includes products presenting a risk of i) carcinogenicity, ii) mutagenicity, iii) reproductive toxicity, and iv) specific target organ toxicity. As a result, 187 compounds were removed from the initial test.

Posteriorly, and being the ISFI directly injected into the periodontal pocket, even if in reduced amounts, it was decided to eradicate from the screening test all the solvents which present some warning or danger regarding their oral toxicity. This led to the removal of 225 compounds. The same rationale was used for dermal toxicity, including the serious corrosive danger of the material, leading to the abandonment of 31 more solvents. Lastly, 2 more substances were eliminated due to their toxicity when inhaled.

Finally, it was possible to reduce the initial 625-solvents list to 180. However, some of the solvents included in the final list showcase limited information regarding their toxicity. Although there is insufficient toxicological data, some of the compounds contain molecular groups (e.g., chlorinated compounds) that are frequently associated with potential side effects. Consequently, some well-known non-toxic compounds were selected to proceed to further studies, namely:

1. Isopropanol
2. Polyethylene glycol (PEG) (grades 200, 300, 400)
3. Propylene glycol
4. Ethanol
5. Glycerol
6. Acetyl triethyl citrate
7. Dibutyl sebacate
8. Triacetin
9. Tributyl Citrate
10. Triethyl citrate
11. Tri-n-butyl acetyl citrate

Posteriorly, the Hansen Solubility Parameters theory was employed to evaluate the previous solvents. The workbooks developed by Professor Steven Abbot (a more simplistic adaption of the very well recognised software "Hansen Solubility Parameters in Practice" (HSPiP)) were used to calculate the distance and the relative energy density between the solvents and PLGA. It should be noted that SPs are not directly measured for polymers. However, Madsen et al. (203) calculated PLGA 502H's SPs by determining its intrinsic viscosity in different solvents. **Table 11** depicts the Hansen Solubility Parameters of the previous solvents and their relative energy density. Briefly, it is possible to observe most of the classical solvents present a RED larger than 1, suggesting they are outside of the solubility sphere of PLGA thus, not dissolving the biodegradable and biocompatible polymer alone. However, all of the plasticizers are represented by a RED smaller than 1, indicating their solvating power towards PLGA. Notably, it is not mandatory to use only a single solvent to dissolve the PLGA. Also blends of different solvents might be used. The advantage of such mixtures is that the properties of the resulting solvent mixture might be easily adjusted by simply varying the amounts of the single solvents. As a consequence, blends of 2 to 4 compounds, were defined, plotted in a 3D-graph, employing OriginLab 2022, their RED calculated and, in case it was smaller than 1.05, tested in practice. To do so, the solvent blend (70 %) was added to 30% PLGA 502H (*100% = solvent mixture + polymer*) and incubated overnight

at 37 °C and 80 rpm (to accelerate the process). At predetermined timepoints, within the next 24h, the blends were evaluated in order to assess the dissolution of PLGA. Clear, homogenous, and liquid solutions at room temperature were selected to test implant formation and other macroscopic properties were observed, such as elasticity and brittleness.

Table 11: Hansen Solubility Parameters of the selected non-toxic solvents.

Solvents	δ_D	δ_P	δ_H	**RED**
Ethanol	15.8	8.8	19.4	1.52
Glycerol	17.4	12.1	29.3	2.76
Isopropanol	15.8	6.1	16.4	1.21
PEG 200	16.7	5.6	16.7	1.23
PEG 300	16.6	4.4	14.5	1.08
PEG 400	16.6	3.7	13.3	1.01
PLGA 502H	*16.38*	*9.13*	*7.12*	---
Propylene Glycol	16.8	9.4	23.3	1.99
Acetyl Triethyl Citrate	16.6	3.5	8.6	0.72
Dibutyl Sebacate	16.7	4.5	4.1	0.68
Triacetin	16.5	4.5	9.1	0.62
Triethyl Citrate	16.5	4.9	12	0.82
Tri-n-Butyl Acetyl Citrate	16.7	2.5	7.4	0.75
Tri-n-Butyl Citrate	16.6	3.8	10.1	0.79

This screening analysis led to the final selection of PEG 400, triethyl citrate and ethanol. Although PEG 400 is able to dissolve PLGA alone, it does not readily form an implant when in contact with an aqueous medium. Additionally, it was verified that the use of plasticizers led to the production of softer implants, presenting higher elasticity as well as less brittle appearance. Finally, the employment of ethanol revealed to have a positive impact on the viscosity of the final liquid formulation. Besides the fact PEG 400 has already been widely reported in literature as a solvent for PLGA 502H (211), all of these compounds are FDA-approved for parenteral use (139,140).

Finally, in addition to the non-toxic nature of these solvents, PEG 400 and triethyl citrate are known to produce slow phase inversion ISFIs. As a consequence, the resulting implants will be formed in a longer period of time, possibly decrease the burst effect that one would be observed with NMP-based ISFIs.

2. In-situ forming PLGA implants – Towards less toxic solvents

2.1. General introduction

PLGA-based *in-situ* forming implants provide a promising potential for the treatment of several pathologies, including periodontitis, (129,138,212–215) due to their ability to locally control the drug release for prolonged periods of time as well as the biodegradable and biocompatible nature of the systems (212,216–218).

Albeit the existence of numerous trigger mechanisms that can induce the implant solidification after injection into the administration site, the current project aims to produce ISFIs based on solvent exchange. To this extent, a water-insoluble biocompatible and biodegradable polymer (e.g., PLGA) is dissolved in a water-miscible solvent. Commonly, the drug is posteriorly added and can either be dissolved and/or dispersed within the system. Once the liquid formulation is injected into the action site, the solvent diffuses out of the formulation while water penetrates into the system. This results in the polymer precipitation, trapping of the API, and solidification of the implant (147,219–221). Finally, the drug is released from the implant at a controlled rate (138,222–224). Numerous physicochemical phenomena can be involved in the control of drug release from PLGA-based ISFIs (225), including solvent diffusion into the surrounding tissue, water diffusion into the system, polymer precipitation, drug dissolution and diffusion, polymer degradation, the creation of local drops in micro-pH (226,227), autocatalytic effects (228,229), limited drug solubility effects within the implant and/or within the surrounding environment (230), system swelling (231), drug-polymer interactions (232), and osmotic effects (233), to mention just a few.

As a result, it seems clear that ISFIs' components (polymer, drug and solvent) can strongly affect the final drug release mechanisms. For instance, the variation of a formulation parameter can lead to unpredictable effects on the implant's key features. Hence, it is helpful to comprehend how a specific product controls drug release.

The previous section identified three promising non-toxic solvents, possibly able to provide an alternative to the potentially toxic NMP: i) polyethylene glycol with a molecular weight of approximately 400 Da (PEG 400), triethyl citrate (TEC) and ethanol. Finally, in this section, several tertiary blends of the previous solvents are studied. Ibuprofen and chlorhexidine dihydrochloride are selected for the treatment of periodontitis (22). Lastly, the implant formation, drug release kinetics, dynamic changes in the systems' wet mass, release medium pH and mechanical and antibacterial properties are assessed.

2.2. Drug Release from the in-situ forming implants

The release of ibuprofen and chlorhexidine dihydrochloride from the *in-situ* forming implants was assessed. To that extent, liquid formulations were produced employing different solvent systems and 100 µL of each of the latter was placed in 1.5 mL Eppendorf vials. Posteriorly, 1 mL of preheated (37 °C) phosphate buffer pH 6.8 (PB) was carefully added, allowing for solvent exchange and thus, implant formation. The vials were horizontally shaken at 80 rpm and 37 °C.

At predetermined time points, the release medium was completely replaced with fresh PB; the withdrawn bulk fluids were filtered and the API content was determined by HPLC-UV analysis. Moreover, the pH of the release medium and the change of the implants' wet mass were measured at each sampling time point. All experiments were conducted in triplicate.

2.2.1. Ibuprofen Release

Liquid formulations containing 30 % PLGA and 2 % ibuprofen were produced. Additionally, the selected solvents (PEG 400, TEC, ethanol) were varied within the solvent blend and their impact on the drug release was evaluated (**Figure 26 - Figure 28**). In **Figure 26**, ethanol is kept at a constant ratio of 5 % (100 % = solvent mixture), while PEG 400 and TEC ratios are altered as displayed. In **Figure 27 and Figure 28**, the ethanol is set to 10 % and 15 % ratios, respectively. The ibuprofen release kinetics is represented in the top rows, followed by the dynamic changes in the implants' (apparent) wet mass and the release medium pH (middle and bottom rows). Evidently, all formulations present a 3-phasic drug release pattern. Firstly, it is clearly depicted a burst release during the first days followed by a zero order API release (approximately constant release rate) and finally, a rapid drug release phase (resulting in the complete drug exhaust). It is important to note the solvent system ratio influences not only the duration of the different phases but also the amount of ibuprofen being released in each one of them.

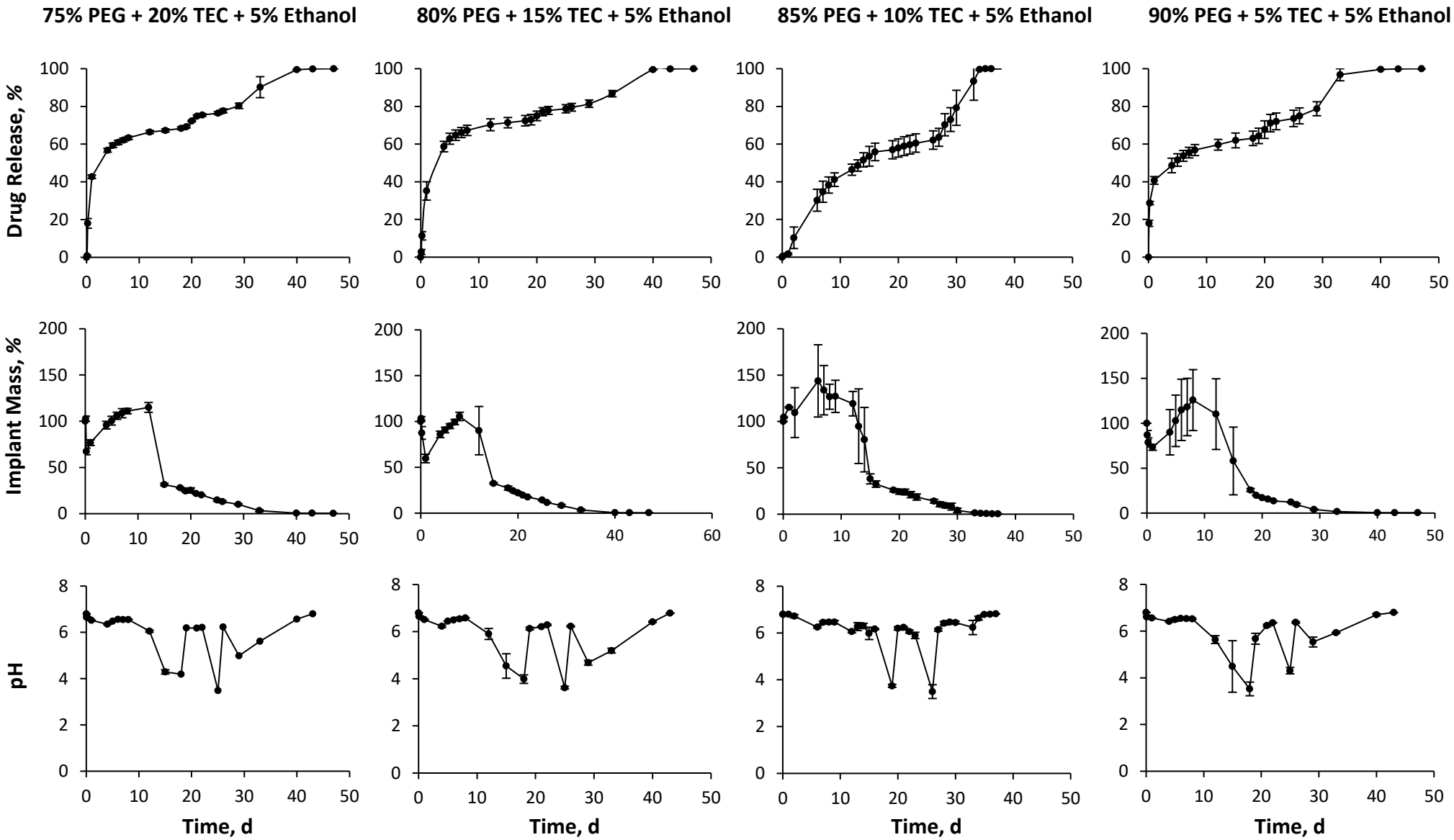


Figure 26: In-situ forming implants prepared from liquid formulations containing **30 % PLGA** and **2 % ibuprofen**: Impact of the type of solvent system on drug release, dynamic changes in the implants' wet mass and pH of the release medium. The **ethanol** content was kept constant at **5 %**.

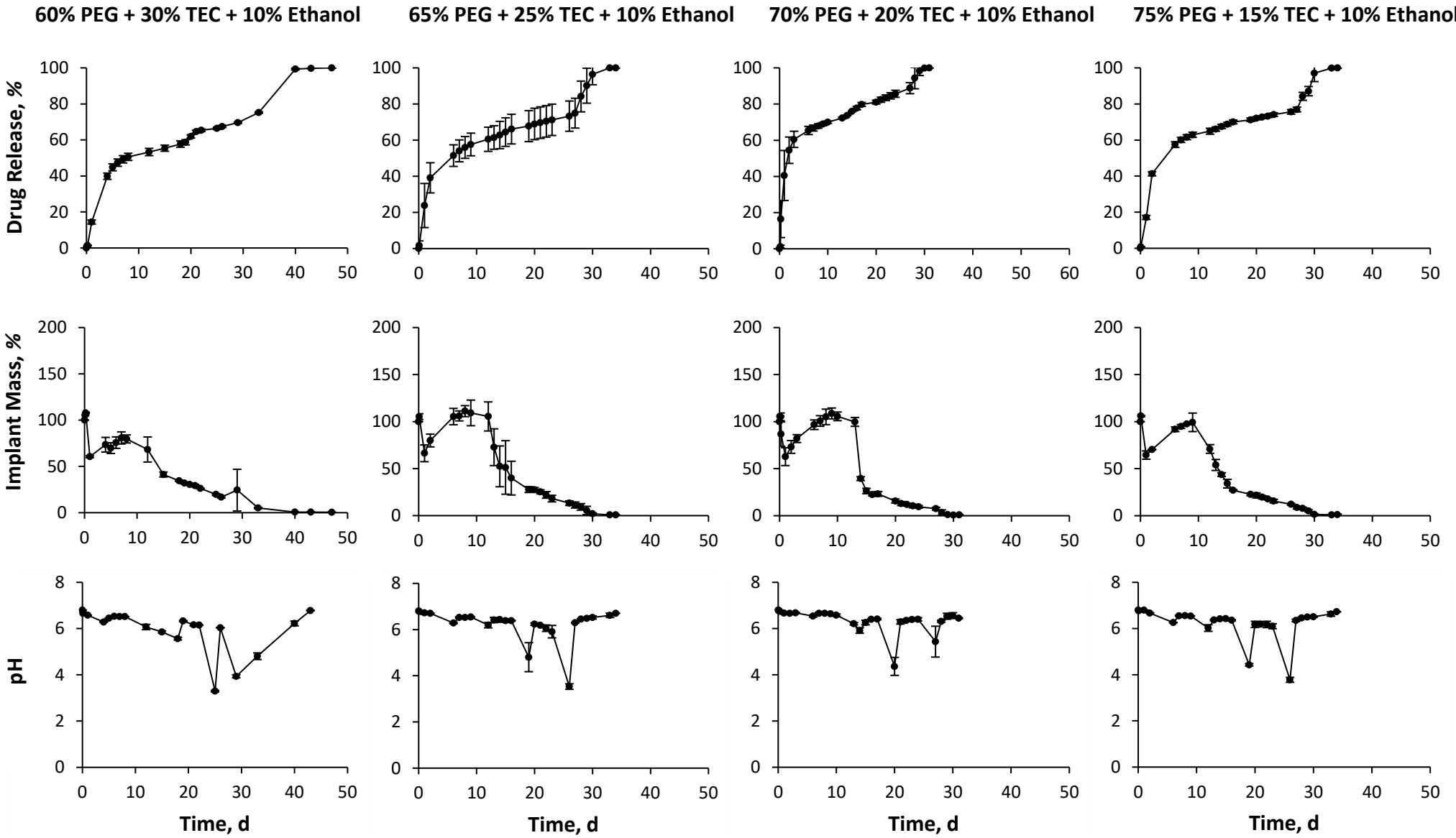


Figure 27: In-situ forming implants prepared from liquid formulations containing **30 % PLGA** and **2 % ibuprofen**: Impact of the type of solvent system on drug release, dynamic changes in the implants' wet mass and pH of the release medium. The **ethanol** content was kept constant at **10 %**.

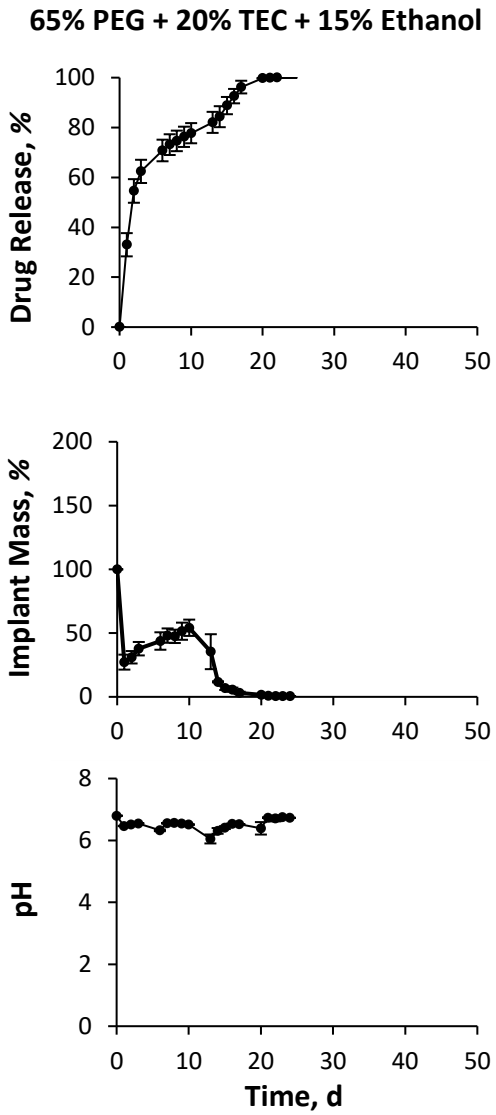


Figure 28: In-situ forming implants prepared from liquid formulations containing **30 % PLGA** and **2 % ibuprofen**: Drug release, dynamic changes in the implants' wet mass and pH of the release medium. The solvent system consisted of 65 % PEG 400, 20 % TEC and **15 % ethanol**.

During the first days, and being these IFSIs characterized as slow inversion systems, the polymer is not completely precipitated. As a result, ibuprofen's portions, dissolved in the solvent system, leach out from the formulation together with the solvent, leading to the first phase of the drug release kinetics: the burst effect. The latter is impacted by several factors, namely: i) the API's solubility in the solvent mixture, ii) the polymer's solubility in the system and, iii) the exchange rate between the aqueous medium penetrating the formulation and the diffusion of the solvents into the surrounding tissues.

The following phase, "zero order release", may be strongly explained by ibuprofen's diffusion. The decrease in the drug concentration gradient over time is partially compensated by an increase in

drug mobility due to the degradation of PLGA. Additionally, the experiments were performed under sink conditions, allowing for approximately constant ibuprofen's release rates. Moreover, it is relevant to mention it is observed important changes in the implant's wet mass during this phase however, they do not appear to largely influence the "zero order release". In fact, **Figure 26 – Figure 28** (middle rows) display an increase in the implants' "apparent" wet mass at early time points, followed by a pronounced reduction of this parameter after roughly 10 days. The former observation is possibly explained by the increasingly PLGA's hydrophilicity, upon hydrolysis. An -OH and a -COOH groups (hydrophilic) are formed every time an ester bond is cleaved, leading to a higher water uptake. Moreover, the solvent system first starts to dissipate out of the formulation at the interface "liquid formulation – release medium" leading to a lower PLGA's solubility (insoluble in water) and thus, to the polymer's precipitation at this interface. The latter defines the limits of the solid *in-situ* forming implant. In addition, the polymer's mass remaining to precipitate is generally limited and does not fill all the "implant's volume", resulting in the formation of "water pockets". **Figure 29** depicts optical macroscopic pictures of a representative ISFI (composed of 30 % PLGA (*100 % = PLGA + drug + solvents*), 2 % ibuprofen (*100 % = PLGA + drug*) and based on a "85% PEG 400/10% TEC/5% ethanol" blend (*100 % = solvent mixture*), where a red rectangle emphasises a "water pocket". ***Figure S 1* – *Figure S 17*** display photos of all the investigated formulations (exhibiting a rather identical behaviour). After a period of time of roughly 10 days, the implants become mechanically fragile and the "water pocket" content is rapidly released into the bulk fluid (green rectangle in **Figure 29**). As a consequence, it is observed a clear decrease in the implants' "apparent" wet mass (**Figure 26 – Figure 28**, middle rows). It is noteworthy to remark the term "apparent" is employed in order to highlight that the mass of the liquid in the discussed structure is accounted for the implant's wet mass. Notably, the implant's geometry and mass do not significantly impact the "zero order release" phase, as seen by an approximately constant ibuprofen release in **Figure 26 – Figure 28** (top rows). Therefore, the release of the API in study into the water pockets does not appear to be significantly important. Finally, it is observed a steep reduction in the release medium pH alongside the opening of the water pockets, independently of the solvent system. **Figure 26 – Figure 28** (bottom rows) show that the release medium pH is roughly constant throughout the entire analysis period, except for i) an initial drop, which is coincident with the "water pockets" opening (decrease in implants' "apparent" wet mass), and ii) a second steep decrease, usually preceding the final drug release phase. The former is caused by the release of the acidic content present in the water pocket (pH 4.5, as measured experimentally). This acidic content is explained by PLGA's degradation, which produces short chain water-soluble acids into the water pocket. Importantly, this drop in pH also limits ibuprofen's release into this structure: being this an acidic API is not very soluble at low pH hence, the opening of the pockets does not largely influence ibuprofen's release.

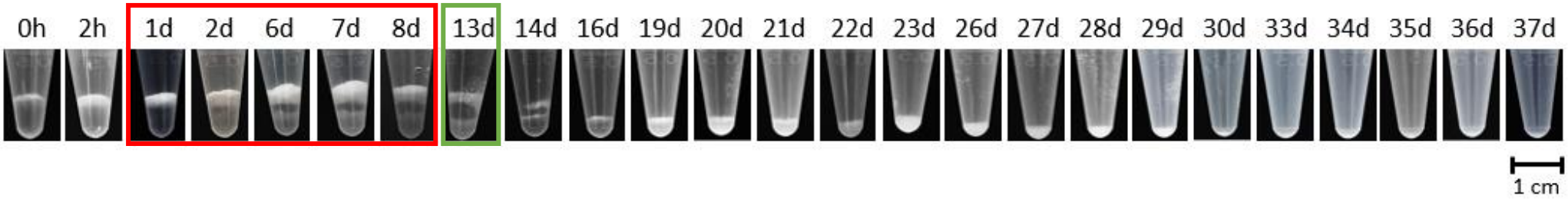


Figure 29: Optical macroscopy pictures of *in-situ* formed implants after different exposure times to the release medium (indicated at the top). The liquid formulation contained 30 % PLGA (100 % = PLGA + drug + solvents), 2 % ibuprofen (100 % = PLGA + drug) and was based on a "85 % PEG 400/10 % TEC/5 % ethanol" blend (100 % = total solvent system). The red rectangle highlights a "water pocket", the green rectangle indicates the opening of the pocket after about 10 d.

The third phase corresponds to a rapid drug release likely promoted by the formation of a highly swollen polymeric gel, which can no longer entrap ibuprofen. According to literature, PLGA implants can swell substantially once a critical polymer molecular weight is attained, leading to an accelerated drug release and complete API exhaust (231). To this extent, when a highly swollen PLGA gel is formed, it is observed the system's higher permeability for the generated short chains acids, leading to a fast acid release into the bulk fluid and decrease in the pH, coinciding with the depicted "second pH drops" (**Figure 26 – Figure 28**, bottom rows). Nevertheless, it is noteworthy to mention the physicochemical phenomena controlling the drug release from preformed PLGA implants can be fundamentally different when compared to the API release from ISFIs (231,234). Briefly, the latter generally presents a much more porous inner structure and an importantly larger water content, possibly affecting drug mobility and polymer degradation. As a consequence, the underlying causes limiting the drug release phases can differ.

Lastly, two solvents systems were selected for further studies: "85 % PEG 400, 10 % TEC, 5 % ethanol" and "60 % PEG 400, 30 % TEC, 10 % ethanol". As observed in **Figure 26 – Figure 28**, the use of this blends led to less variable drug release rates over the total analysis time.

2.2.2. Chlorhexidine Dihydrochloride's Release

Figure 30 depicts the release kinetics of chlorhexidine dihydrochloride's in phosphate buffer pH 6.8, from the *in-situ* forming implants (top row). The showcased formulations were prepared employing the previously selected solvent mixtures however, this time, the PLGA content was varied: 30 % (as in **Figure 26 – Figure 28**), or 25 % (*100 % = PLGA + drug + solvents*). Interestingly, it is displayed important differences when comparing the release kinetics of both drugs. Contrarily to ibuprofen (**Figure 26 – Figure 28**), it is ***not*** observed a chlorhexidine's burst release, independently of the formulation. In fact, the release is negligible until approximately day 10, in all cases (at this time point, CHX DiHCl release is inferior to 2%, irrespective of the ISFI). However, there are no significant discrepancies regarding the dynamic changes in the implants' "apparent" wet mass and in the bulk fluid pH when compared to the ibuprofen-charged ISFIs (middle and bottoms rows in **Figure 30** versus **Figure 26 – Figure 28**). The lack of a burst effect, associated with similar swelling and acid release, could be explained by the fact that chlorhexidine, contrarily to ibuprofen, is not dissolved but rather dispersed in the liquid formulations in the form of tiny particles. As a result, chlorhexidine does not leach out of the formulation with the solvent blend, when the implants are formed. Alternatively, the polymer precipitates around the particles of chlorhexidine dihydrochloride, and effectively traps the drug, preventing the extensive API release at the beginning of the study.

Remarkably, it is observed a rapid partial chlorhexidine release upon the opening of the "water pockets", after approximately 10 days. It is relevant to note the solubility of chlorhexidine is higher at a low pH (235) (when compared to ibuprofen (236)). Therefore, the antiseptic agent is mostly released into the "water pockets", where the pH is lower when compared to the bulk fluid, due to the presence of PLGA's degradation products. In fact, it was measured a drug concentration of 51 +/- 17 µg/mL after 7 days, in the water pockets of ISFIs formed from liquid formulations consisting of 30 % PLGA (*100 % = PLGA + drug + solvents*), 2 % chlorhexidine dihydrochloride (*100 % = PLGA + drug*), and a "85 % PEG 400/10 % TEC/5 % ethanol" blend (*100 % = total solvent system*). This fast chlorhexidine release starting roughly at day 10 is followed by an approximately "zero order drug release phase" and a final rapid API release. The lengths of the latter two phases are generally similar to the ones observed for ibuprofen-loaded implants (**Figure 30** versus **Figure 26 – Figure 28**), illustrating the possible similarity of the underlying release mechanisms when using either API.

Interestingly, the use of different polymer's ratios (25% versus 30%) does not appear to substantially affect the drug release kinetics, neither the implants' mass or the release medium pH, independently of the system employed (**Figure 30**).

2.2.3. Implants containing both ibuprofen and chlorhexidine

Figure 31 showcases the release kinetics from *in-situ* forming implants when employing a combination of ibuprofen (IBU) and chlorhexidine dihydrochloride (CHX DiHCL). Once more, the drug release rates into PB 6.8 is displayed in the top row, followed by the implants' "apparent" wet mass and dynamic changes in the pH of the bulk fluid (represented in the middle and bottom rows, respectively). The drug loading was set at 2% of ibuprofen and chlorhexidine dihydrochloride (*100 % = PLGA + drugs*) and the polymer content was either 25 or 30 % (*100 % = PLGA + drug + solvents*). Notably, it is not observed any significant discrepancies in the drug release, changes in implants' wet mass and medium pH, when compared to the implants charged with each API individually. As a result, it is possible to conclude the presence of either drug (in a 2% ratio) does not largely affect the underlying release mechanisms for any of the drugs, neither the implants' swelling or acid release kinetics.

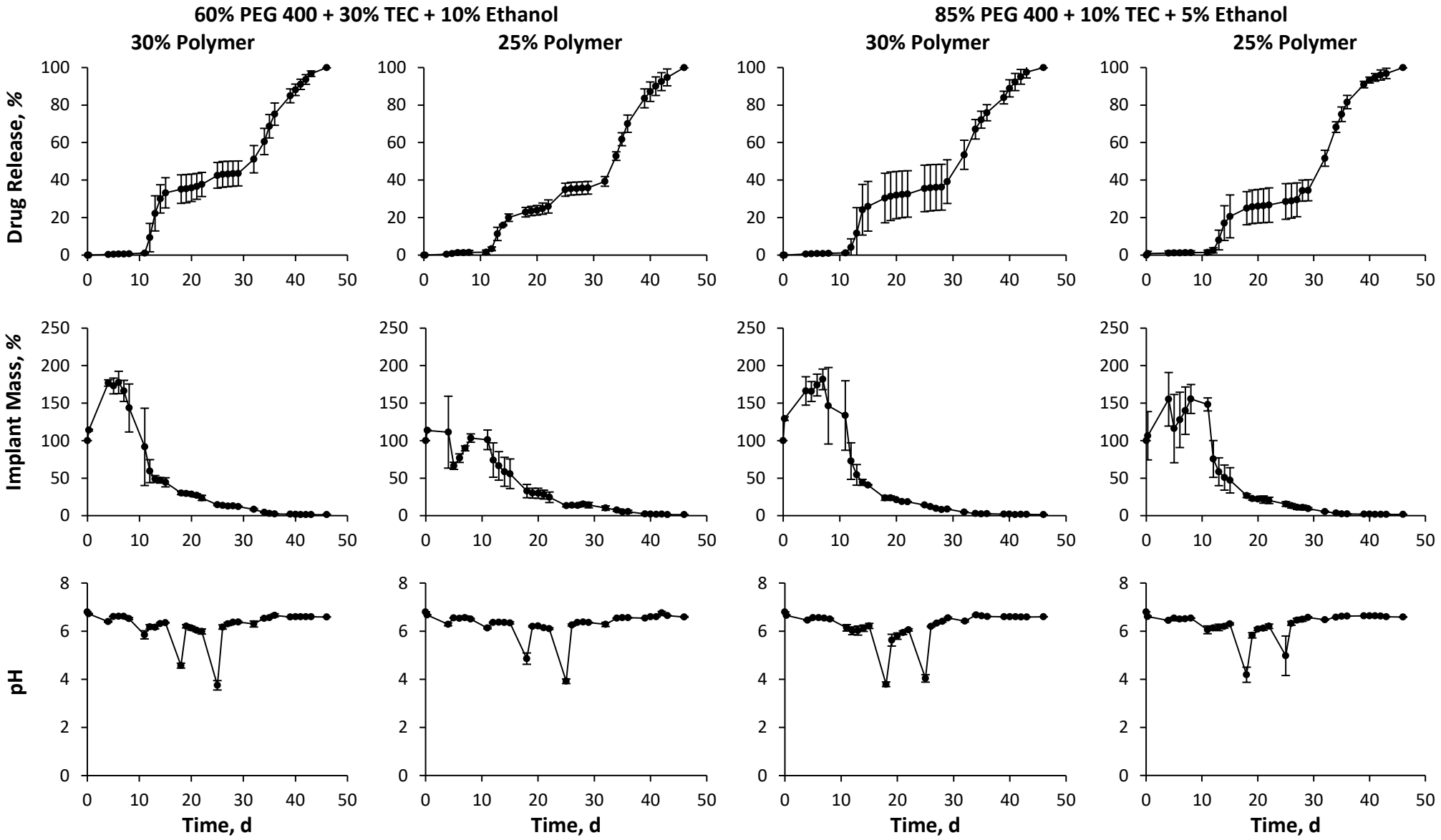


Figure 30: *In-situ* forming implants prepared from liquid formulations containing **2 % chlorhexidine dihydrochloride**: impact of the type of solvent system and polymer content on drug release, dynamic changes in the implants' wet mass and pH of the release medium.

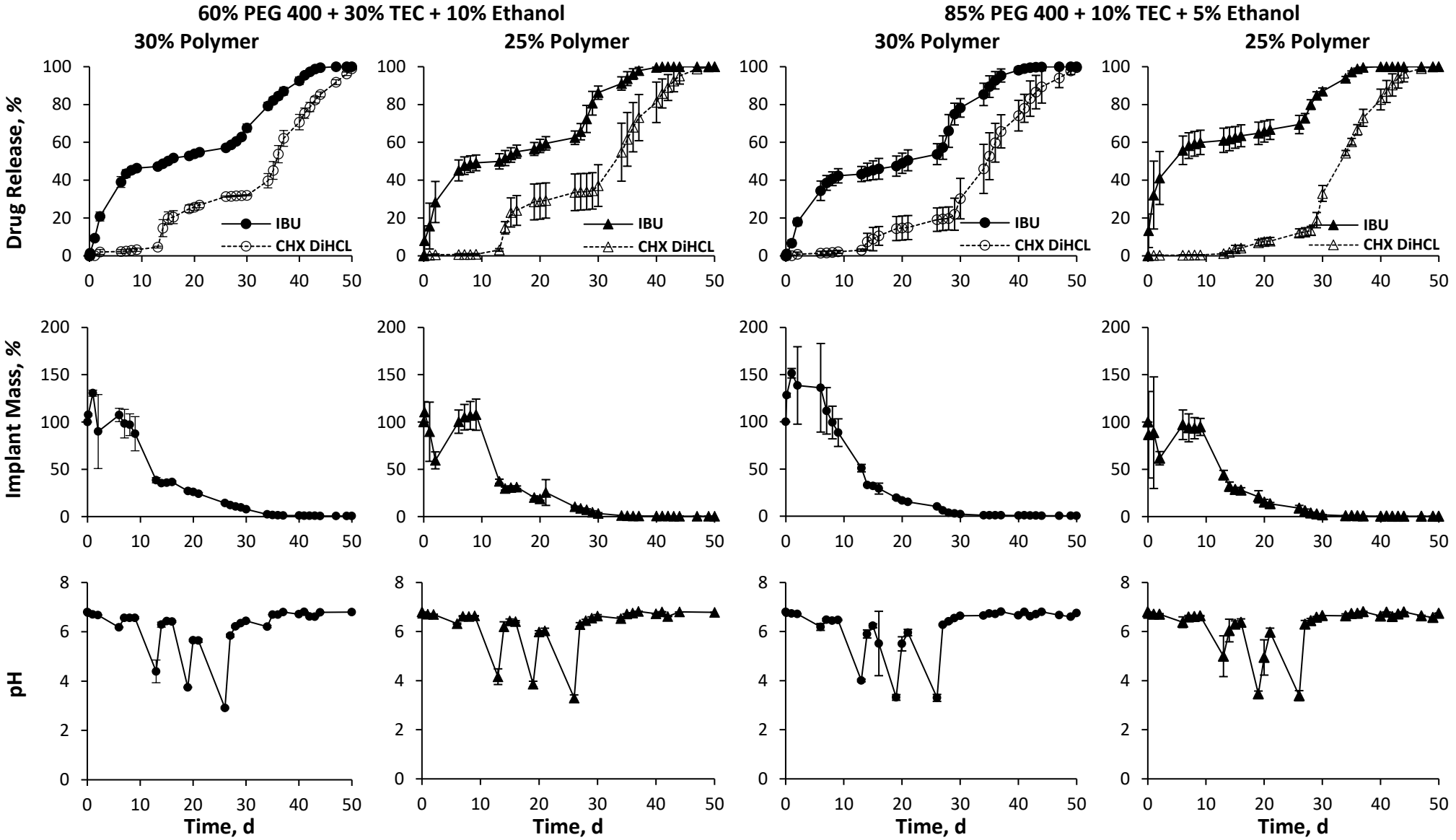


Figure 31: *In-situ* forming implants prepared from liquid formulations containing **2 % chlorhexidine dihydrochloride and 2 % ibuprofen**: Impact of the type of solvent system and polymer content on drug release, dynamic changes in the implants' wet mass and pH of the release medium.

Similarly to what is observed for the chlorhexidine only-loaded ISFI (**Figure 30**), **Figure 31** does not depict any important differences concerning the API release, implant's wet mass and medium pH when varying the PLGA ratio of the liquid formulation (25 % versus 30 %)

Finally, it should be noted a time-limited decrease in several implants' wet mass, in the first days of the release (**Figure 26 – Figure 28**, **Figure 30** and **Figure 31**). This can possibly result from the presence of small "water pockets", which opened early. At such early timepoints, these structures do not show large concentrations of the acidic degradation products or API, leading to negligible changes in the drug release and pH of the release medium.

2.3. Mechanical tests

2.3.1. Syringeability

The syringeability of a given liquid formulation is a key practical parameter for periodontitis treatment's success. The injection into the periodontal pocket should be simple and lead to the relatively fast formulation's deposition within the entire cavity. When these conditions are not met, the treatment becomes challenging, time-consuming and possibly, obsolete. Previous studies showed that it is required a force of approximately 150 N to expulse the marketed product, Parocline (composed by minocycline, Eudragit RS, hydroxyl ethylcellulose, magnesium chloride, triacetin and glycerol) from an Emdogain syringe, equipped with a 19 G cannula (35 mm length) (135).

The work required to expulse the investigated liquid formulations from a 2 mL syringe coupled with a 19 G needle is depicted in **Figure 32**. These studies were performed using a texture analyser, with a load cell of 50 kg. The syringe was filled with 1 mL formulation and fixed in a universal syringe rig. A syringe plunger clamp was used to drive the piston of the syringe downward at a constant speed of 1 mm/s.

The curves displayed in **Figure 32** are relative to the investigated formulations mean values, while the grey areas correspond to the standard deviations (n = 3). Evidently, an increase in the PLGA content results in a larger syringeability values, due to an increase in the liquid formulations' viscosity. Importantly, the force required to inject the proposed liquid formulations was well below the liquid marketed product Parocline (150 N).

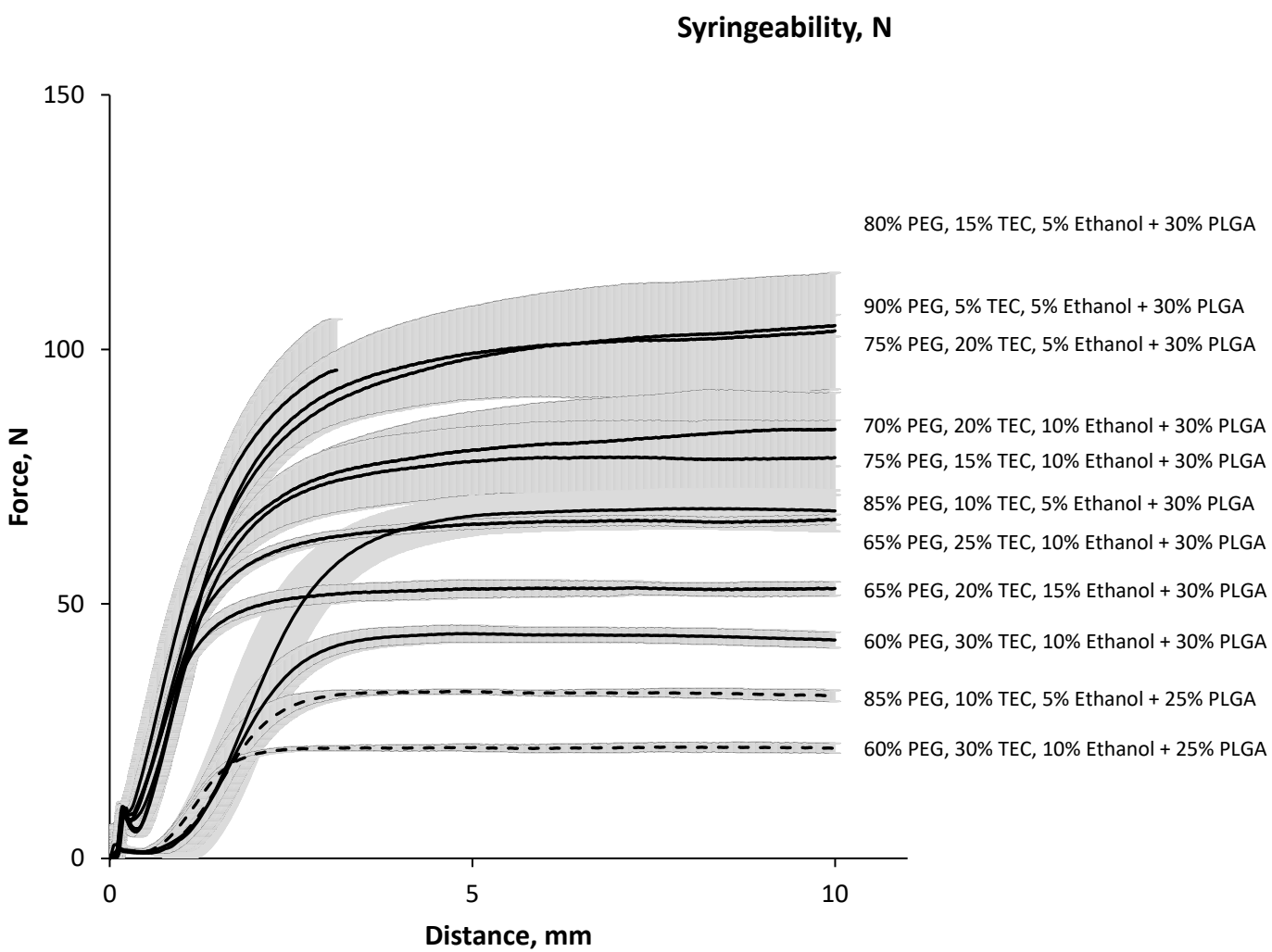


Figure 32: Syringeability of the investigated formulations. The curves illustrate mean values, the grey zones the respective standard deviations (n = 3). The compositions of the systems are indicated on the right-hand side.

2.3.2. Texture Profile Analysis

The textural properties of the selected *in-situ* forming implants were investigated. To do so, a texture profile analysis (TPA) was performed as a valuable mean to better understand the formulations' mechanical properties.

In summary, agarose gel 0.6% w/v was produced and cast into Petri dishes. Posteriorly, cylindrical holes were pierced, filled with the liquid formulations and incubated at 37°C for 24h to promote solvent exchange and hence, implant formation. Finally, the TPA test, characterized by two compression cycles, started: a spherical probe descended onto the sample. Once in contact with the formulation, force-displacement profiles were recorded. The probe moved downwards, at a constant speed (2 mm/s), until it reached a depth of half of the sample's height. Once this target distance was reached, the probe ascended until the position where it was first in contact with the ISFI. This position was held for 15 s to allow for the sample's recovery before a new compression cycle (identical to the first one) started. **Figure 33** depicts a typical force-time diagram obtained from a texture profile analysis.

Figure 34 illustrates the experimentally measured force-time curves for the previously selected ISFI systems. It is relevant to note all triplicates are represented so as to better understand the reproducibility of the study. Please note the y-axis scale differs when different solvent mixtures are employed. All recorded force-profiles are similar, irrespective of the formulation. Based on these data, it is possible to determine the *in-situ* forming implants' hardness, resilience and springiness (**Figure 35**). Finally, previous studies employing the same set-up calculated these parameters for the marketed products, Parocline and Chlosite (135).

Hardness

The hardness of the formulations is characterized as the peak force attained on the first compression cycle. Previous studies (135) demonstrated Parocline implants have a hardness of 232 +/- 30 mN, while the same parameter is of approximately 618 +/- 157 mN for Chlo-site formulations. **Figure 35a**, clearly shows the solvent system impacts the final hardness of the ISFI. As it can be observed, the systems produced with 60% PEG 400, 30% TEC and 10% ethanol (*100% = total solvent system*) result in substantially lower forces. In fact, the latter systems composed of either 25% or 30% PLGA depict comparable forces to the ones observed with Parocline® and Chlo-site®, respectively.

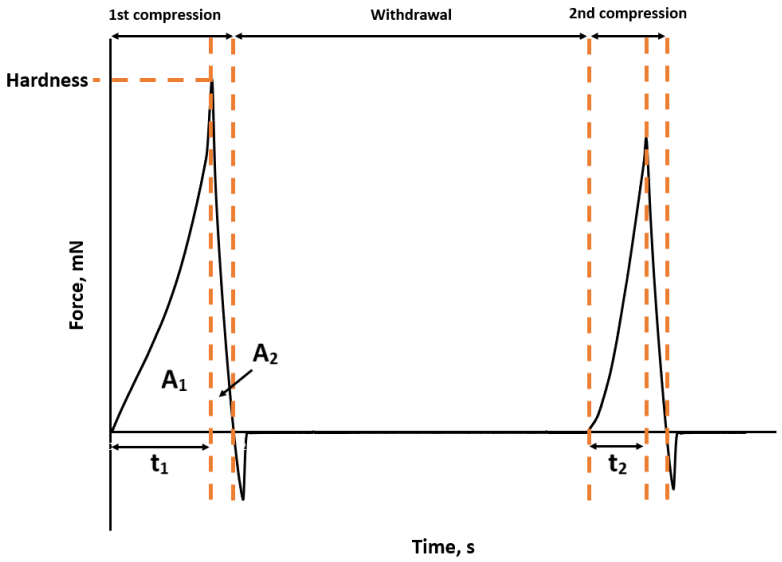


Figure 33: A typical force-time plot obtained from a texture profile analysis.

Resilience

The resilience is defined as the ability of a product to spring back to its original height, determined before the waiting period and second compression cycle. It can be calculated by the ratio between the upstroke and the downstroke energies, both occurring on the first compression cycle. Once the probe displacement speed was kept constant during the analysis, this parameter can simply be obtained by the ratio between A2 and A1 (**Figure 33**). Once again, previous studies showed the resilience of Parocline® and Chlo-site® is approximately 0.1 and 0.4, respectively (135). **Figure 35b** shows all the investigated formulations display resilience values in between the already marketed products, possibly indicating that the ISFIs in study could possess adequate properties to be used in practice.

Springiness

Finally, the springiness characterizes the ability of a material to spring back to its original shape, after being deformed and submitted to a waiting period. It is determined by the ratio between the probe's displacement during the second and first compression cycles. Once the test speed was constant, this parameter is simply given by the ratio between t2 and t1 (**Figure 33**). As it can be observed in **Figure 35c**, all tested formulations spring almost completely back to their original form. This could be beneficial once it can translate that the formulations are not susceptible to mechanical stress (e.g., chewing and tooth brushing). However, such large springiness can also be associated with

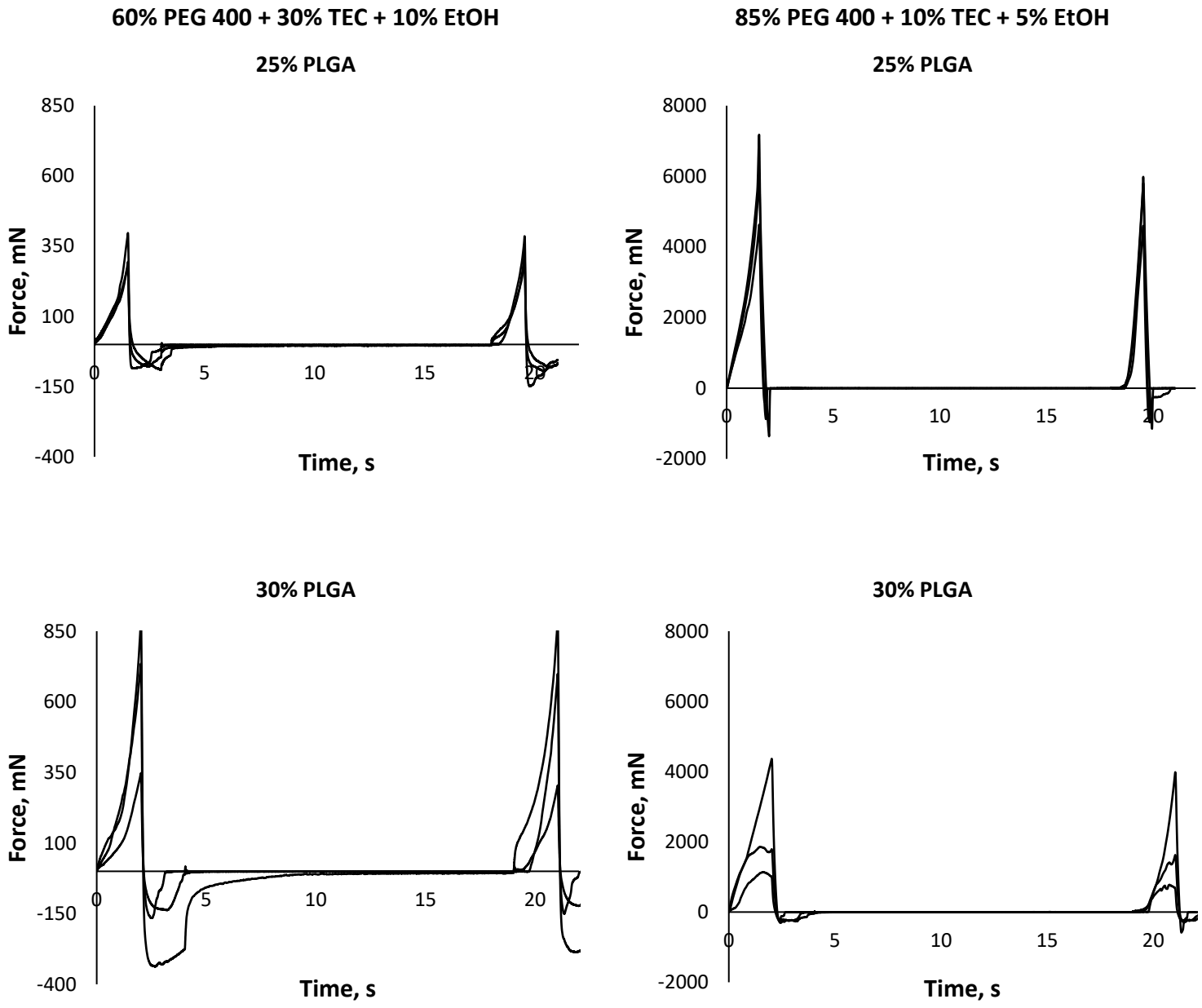


Figure 34: Force-time plots resulting from the texture profile analysis of the previously selected formulations.

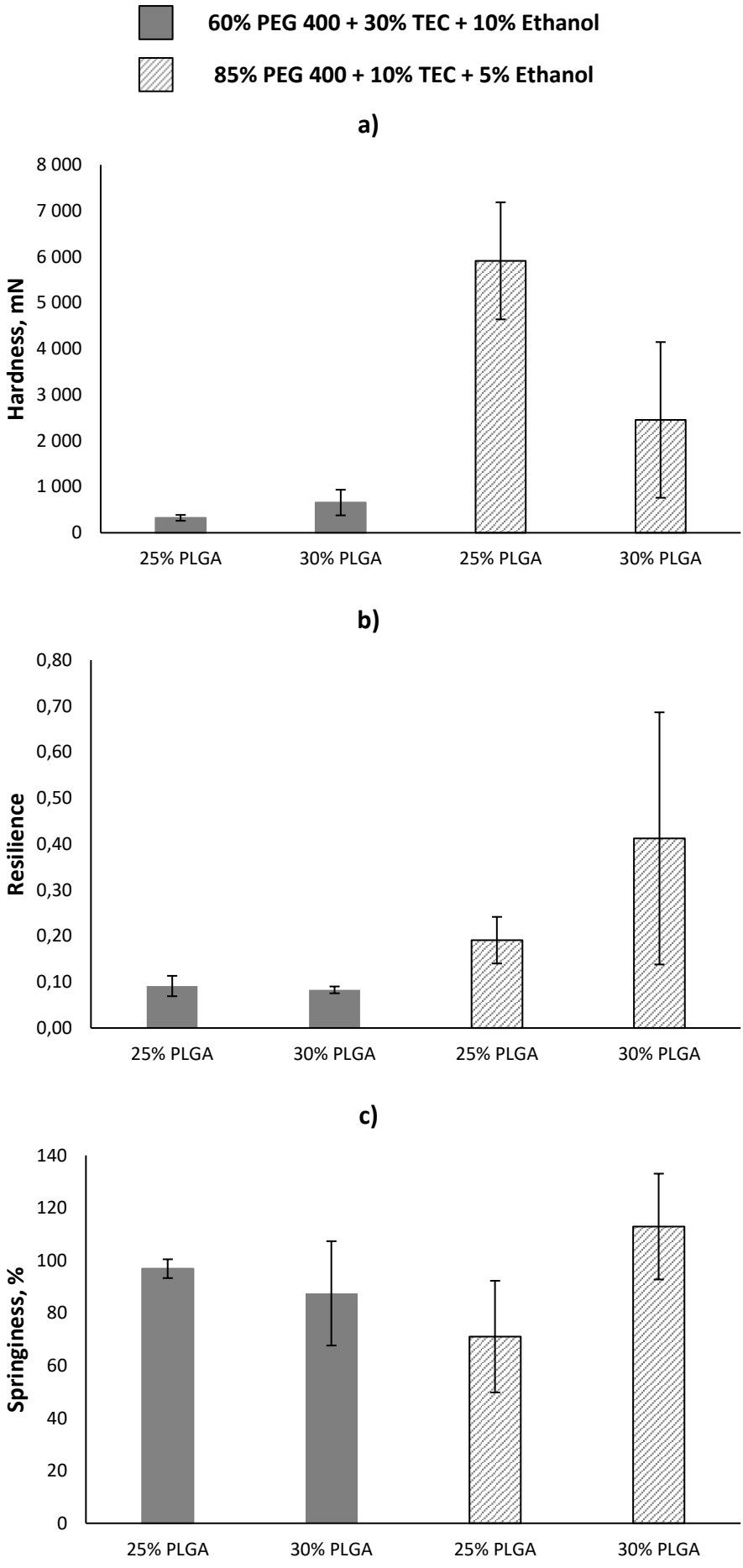


Figure 35: Mechanical properties of the investigated formulations obtained by texture profile analysis: a) Hardness, b) Resilience, and c) Springiness.

a weak adaptability to the periodontal pocket as it scares. Lastly, both the solvent system and PLGA content do not substantially affect this parameter. Chlo-site® and Parocline® revealed springiness values of roughly 42 and 85%, respectively (135).

2.4. Antimicrobial activity

It is clear that a fast control of the bacteria infection is of great interest for the achievement of periodontitis treatment. Consequently, **Figure 36** displays the antibacterial activity of the investigated ISFI, based on the previously selected solvent blends. The formulations are composed of 25% or 30 % PLGA (*100 % = PLGA + APIs + solvents*) and 2 % ibuprofen as well as optionally 2 % chlorhexidine dihydrochloride (*100 % = PLGA + drugs*). The schemes at the bottom part of **Figure 36** represent the experimental set-up.

Firstly, 1 mL of the liquid formulations were exposed to 9 mL Wilkins-West liquid medium (WWL medium), promoting solvent exchange. After 24 h incubation at 37 °C, the implants were formed and *the bulk fluid is fully withdrawn* and replaced with 8 mL WWL medium as well as 1 mL of the bacterial inoculum (*Streptococcus parasanguinis* strain). For reasons of comparison, the inoculum alone was also incubated with the WWL medium. The mixtures were finally incubated at 37 °C under anaerobic conditions, and the Colony Forming Units (CFU) were counted at different time points. **Figure 36a** clearly depicts the growth curve of the *Streptococcus parasanguinis* strain (black curve). All the antiseptic-free formulations do not modify the proliferation of the bacterial strain, independently of the solvent blend. This can partially illustrate the latter's lack of a pronounced toxicity, under this test conditions. On the contrary, all the formulations which possess chlorhexidine dihydrochloride in their composition lead to a reduction of the number of bacteria throughout the trial duration. Interestingly, it seems that the implants release adequate amounts of the antiseptic, able to kill the *Streptococcus parasanguinis* strain, known to play a significant role in the development of dental plaque (237). It is noteworthy to mention the conditions employed in this study are different from the ones used in the *in vitro* drug release analysis, previously discussed in detail. Additionally, it is expected for the microorganisms to sediment directly onto the implant's surface, during incubation. As a result, and identically to what is observed in a patient's periodontal pocket, the bacteria are in close contact with chlorhexidine. This likely elucidates the reason why the antiseptic-charged ISFI kill the bacterial strain, although chlorhexidine dihydrochloride's release rates seem to be insignificant during the first 10 days of the release (**Figure 30** and **Figure 31**).

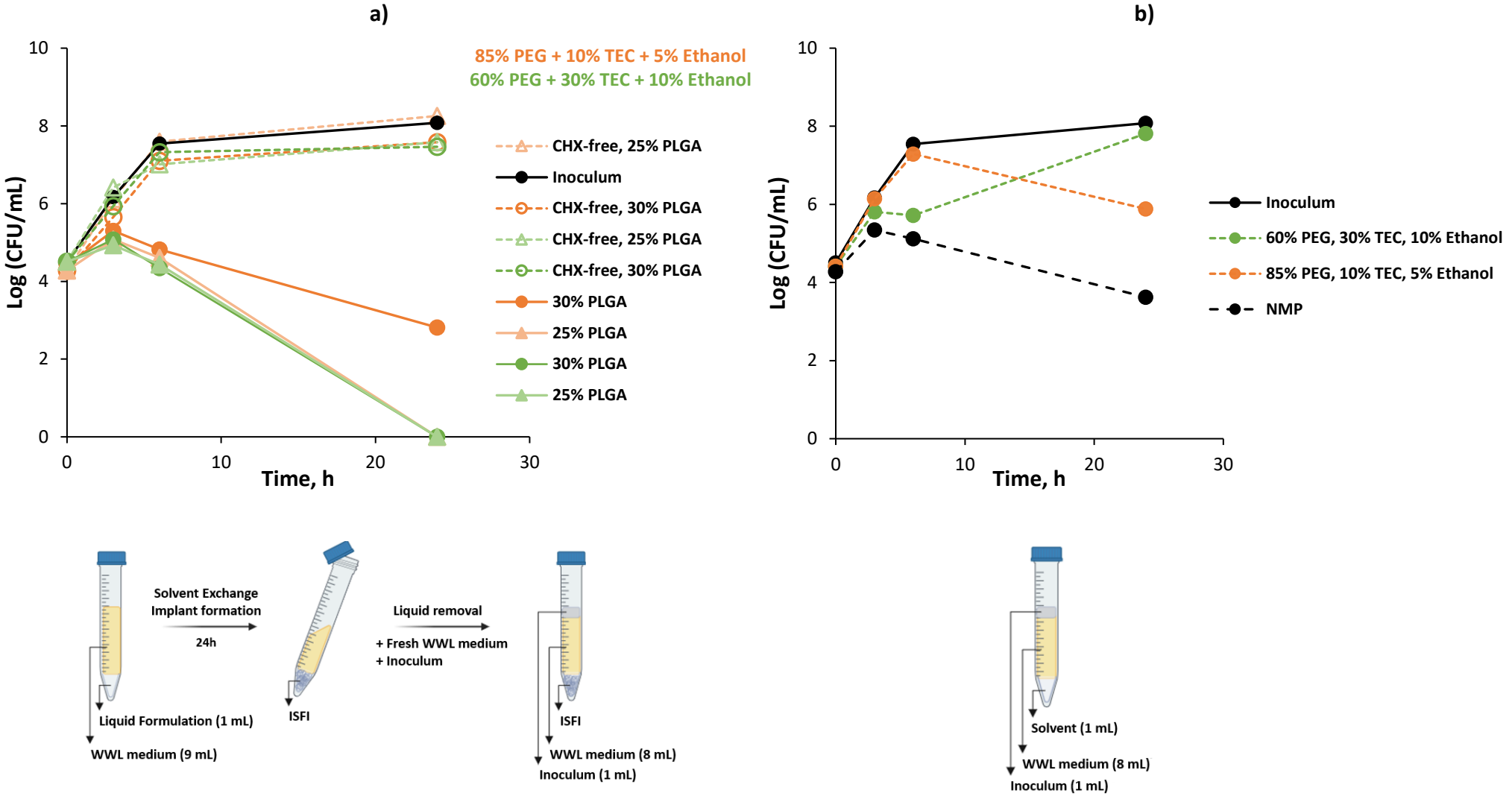


Figure 36: **a)** Antibacterial activity of the investigated formulations: Implants were formed upon exposure of the liquids to WWL medium for 24 h, followed by complete bulk fluid replacement by fresh WWL medium and bacterial inoculum. The samples were incubated and the Colony Forming Units (CFU) counted after different time periods. **b)** For reasons of comparison, also the antibacterial activity of the solvents was studied: Samples were exposed to WWL medium and bacterial inoculum, followed by inoculation and CFU counting. The compositions of the solvent systems are indicated in the diagrams. All implants contained 2 % ibuprofen and 2 % chlorhexidine dihydrochloride (CHX), unless otherwise stated.

The potential toxicity of the selected solvent systems was also assessed. To this extent, 1 mL of the solvent sample was simply exposed to 8 mL WWL medium and 1 mL bacterial inoculum (*Streptococcus parasanguinis*). NMP as well as the inoculum were evaluated under the same test conditions, as a mean of comparison. As aforementioned, the mixtures were incubated at 37 °C under anaerobic conditions, and CFU were counted at different time points. **Figure 36b** shows the newly proposed solvent blends are less toxic to the *Streptococcus parasanguinis* strain when compared to NMP, which is commonly employed for the formulation of ISFIs. Importantly, although the aim of the formulation is to completely eliminate all the bacteria, this should not be accomplished by the solvent system but by the API once, in case the solvent (or solvent blend) is toxic, it will likely lead to the to the damage of the patient's healthy tissues.

3. Conclusion

The current chapter focused on the better understanding of the tertiary solvent blend composed of polyethylene glycol 400, triethyl citrate and ethanol. These solvents are considered as non-toxic FDA-approved for parenteral use, possibly serving as an alternative to the potentially toxic NMP. In order to confirm if a blend of the three solvents can indeed replace NMP in the development of ISFIs, further studies have to be implemented: this was the aim of the present chapter.

The tertiary solvent blend was assessed to better understand its role on the implant formation, drug release kinetics, dynamic changes in the systems' wet mass, release medium pH and mechanical and antibacterial properties. Moreover, the ratio of each solvent within the blend was varied and two polymer:solvent mixture ratios were tested (30%:70% and 25%:75%).

The resulting analysis identified new solvent systems, which show a promising potential for PLGA-based *in-situ* forming implants, with the advantage of possessing a lower toxicity when compared to the already used NMP. Importantly, it was possible to form solid implants upon contact with an aqueous media while it was verified the effective controlled drug release of both ibuprofen and chlorhexidine dihydrochloride for over several weeks. Interestingly, although the antiseptic release is scarce for the first 10 days, it was still observed the removal of the *Streptococcus parasanguinis* strain. This can possibly be explained by sedimentation of the microorganisms directly onto the implant's surface. As a result, and similarly to what is observed in a patient's periodontal pocket, the bacteria are in close contact with the antiseptic agent. However, it should be noted that the conditions employed in the antibacterial study are not the same as the ones used in the *in vitro* drug release analysis, which can also contribute to the observed differences.

Moreover, the formulations exhibit adequate mechanical properties. In particular, the TPA analysis mostly revealed similar results to the marketed products, Chlo-site® and Parocline ®. Finally, all of the ISFIs in study revealed a syringeability force lower than the marketed product, Parocline®.

In summary, when loaded with ibuprofen and chlorhexidine dihydrochloride, this type of *in-situ* forming implants, employing new solvent systems, could be used for improved local periodontitis treatments.

Chapter 5: General conclusion and future perspectives

Periodontitis is a highly prevalent chronic inflammatory disease of the tooth supporting tissues. It is considered the 6th most prevalent disease globally, having the World Health Organization estimated that 19% of the world's population suffered from its severe form in 2019.

Although the mechanisms leading to the development of the disease are not fully understood yet, it is well established the persistent accumulation of supra- and subgingival biofilms initiates a host immune response, leading to inflammation and tissue destruction. As a consequence, the treatment of periodontitis aims to manage both the bacterial dysbiosis and the inflammation process. To do so, the first line of treatment corresponds to the mechanical removal of the pathogenic biofilm and calculus. However, the latter is challenging, dependent on many variables and does not eradicate all the bacteria due to a highly colonized oral cavity. As a result, it has been proposed to combine this mechanical treatment with advanced local drug delivery systems, able to control the release of both antiseptics and anti-inflammatory agents for prolonged periods of time.

Poly(lactic-co-glycolic acid) (PLGA)-based *in-situ* forming implants (ISFIs), formed by solvent exchange, offer an interesting potential for the treatment of periodontitis. A water-immiscible biocompatible and biodegradable polymer is dissolved in a water-soluble organic solvent. The selected drug is posteriorly added. The final formulation is an injectable solution or dispersion. Following administration into the site of action (e.g., the periodontal pocket), the water-miscible solvent dissipates into the surrounding tissues at the same time as aqueous fluids penetrate into the injected system. As a result, the polymer precipitates entrapping the drug and forming a solid implant, which releases the API in a controlled manner.

Up to date, N-methyl pyrrolidone (NMP) is the most commonly employed solvent in the development of ISFIs. However, its parenteral administration raises toxicity concerns. Moreover, NMP is freely miscible with water, leading to the production of fast phase inversion systems, where the solid implant is formed within seconds or minutes. As a result, it is verified a release of significant quantities of solvent and drug within a brief time span, possibly leading to tissue irritation or side effects not initially foreseen.

The aim of this study was to identify less toxic alternative solvent systems, which can replace NMP in the development of PLGA-based ISFIs, contributing to sustainability in drug release.

It is relevant to note that the physicochemical properties of all the components encompassing the ISFI (e.g., polymer, solvent and drug) greatly affect the final formulation and thus, the system's release kinetics. As a consequence, it was first intended to better characterize the pure compounds

employed in the current project (PLGA 502H, ibuprofen and chlorhexidine dihydrochloride) and attempted to determine the solubility of the APIs within the polymer.

Firstly, the amorphous nature of PLGA 502H should be noted. It is well known that amorphous polymers generally present higher degradation rates when compared to their crystalline form. Consequently, it may be observed a faster degradation of the polymeric matrix, promoting the drug release. In addition, this amorphous nature may result in a better distribution of the API within the polymer, foreseeing more consistent (therefore, predictable) drug release kinetics.

Secondly, the solubility of the crystalline APIs (ibuprofen and chlorhexidine dihydrochloride) within PLGA 502H was determined. This solubility is largely important once it provides a strong indication on the fractions of drug which can be trapped within the matrix at the molecular level or in the form of crystallites. This structural composition of the implant is then expected to have a strong repercussion on the ISFI's drug release kinetics. The performed studies led to the conclusion that ibuprofen presents a rather weak solubility in the polymer. In fact, it was observed a reduction in solubility as the temperature decreased. As a consequence, it is expected an extremely low solubility of ibuprofen in PLGA 502H at body temperature. Lastly, chlorhexidine dihydrochloride showed to be insoluble in PLGA 502H. The low solubility (or lack of) of both APIs within the polymer are expected to play a key role on the drug release profiles. Although this is clear, it is reductive to base the release kinetics solely on this parameter. Other factors should be taken into consideration such as: the polymer's molecular weight, APIs' solubility, particle size, pH, loading and stability.

Posteriorly, the focus was then in the selection of the non-toxic solvent system. The Hansen Solubility Parameters theory was employed as a screening technique in order to identify solvents able to both dissolve PLGA 502H and replace NMP. This theory has been described as "like seeks like" and allows to forecast the compatibility between materials. Although it is required for the solvent to dissolve PLGA 502H, this is not a sufficient condition to select the final solvent. Additionally, the solvent should present an adequate water affinity, suitable viscosity, ability to create implants with appropriate mechanical properties, and it must be non-toxic and biocompatible so as to guarantee the safety of the treatment. Finally, three promising solvents were proposed: poly(ethylene glycol) 400 (PEG 400), triethyl citrate (TEC) and ethanol. These are considered as non-toxic FDA-approved for parenteral use, possibly serving as an alternative to the potentially toxic NMP.

Lastly, tertiary blends of the solvents previously identified were employed to prepare liquid formulations containing PLGA 502H, ibuprofen (as an anti-inflammatory drug) and/or chlorhexidine dihydrochloride (as an antiseptic agent). Implant formation, drug release kinetics, dynamic changes in the implants' wet mass, the release medium pH and mechanical and antibacterial properties were assessed. Once again, and given the fact that the components of ISFIs greatly affect the final dosage form, the ratio of each solvent within the blend was varied and two polymer:solvent mixture ratios were tested (30%:70% and 25%:75%).

The resulting analysis identified two solvent systems, which show a promising potential for PLGA-based *in-situ* forming implants, with the advantage of possessing a lower toxicity when compared to the already used NMP. These were composed of 85:10:5 and 60:30:10 PEG 400:TEC:ethanol blends. Importantly, it was possible to form solid implants upon contact with an aqueous media while it was verified the controlled drug release of APIs for over several weeks. Interestingly, although the antiseptic release is scarce for the first 10 days, it was still observed the eradication of the *Streptococcus parasanguinis* strain. This can possibly be explained by sedimentation of the microorganisms directly onto the implant's surface. As a result, and similarly to what is observed in a patient's periodontal pocket, the bacteria are in close contact with the antiseptic agent. However, it should be noted that the conditions employed in the antibacterial study were not the same as the ones used in the *in vitro* drug release analysis, which can also contribute to the observed differences.

Moreover, the formulations exhibited adequate mechanical properties. In particular, the TPA analysis mostly revealed similar results to the marketed products, Chlo-site® and Parocline®. Finally, all of the ISFIs in study revealed a syringeability force lower than the marketed product, Parocline®.

In summary, when loaded with ibuprofen and chlorhexidine dihydrochloride, this *in-situ* forming implant systems composed of 85:10:5 and 60:30:10 PEG 400:TEC:ethanol blends could be used for improved local treatment of periodontitis.

For future research, it is encouraged to vary PLGA's grade, molecular weight and end group (as well as test other biodegradable polymers) once it may result in different solubility parameters. Additionally, it is desirable to test model drugs which present higher solubility in the selected polymer so to evaluate their impact on the drug release kinetics.

Finally, although the advantages of the *in-situ* forming implants are undeniable, the development of such devices remains challenging, mainly due to the absence of standard in-vitro release testing methods. As a consequence, poor in-vitro/in-vivo correlations can potentially be

verified. However, the production of suited in-vitro release testing methods for this type of system is linked to rather specific challenges. The latter include the acquisition of reproducible implant shape and size during implant formation. As a result, efforts should be made in order to find a robust in-vitro release testing method.

Supplementary Material

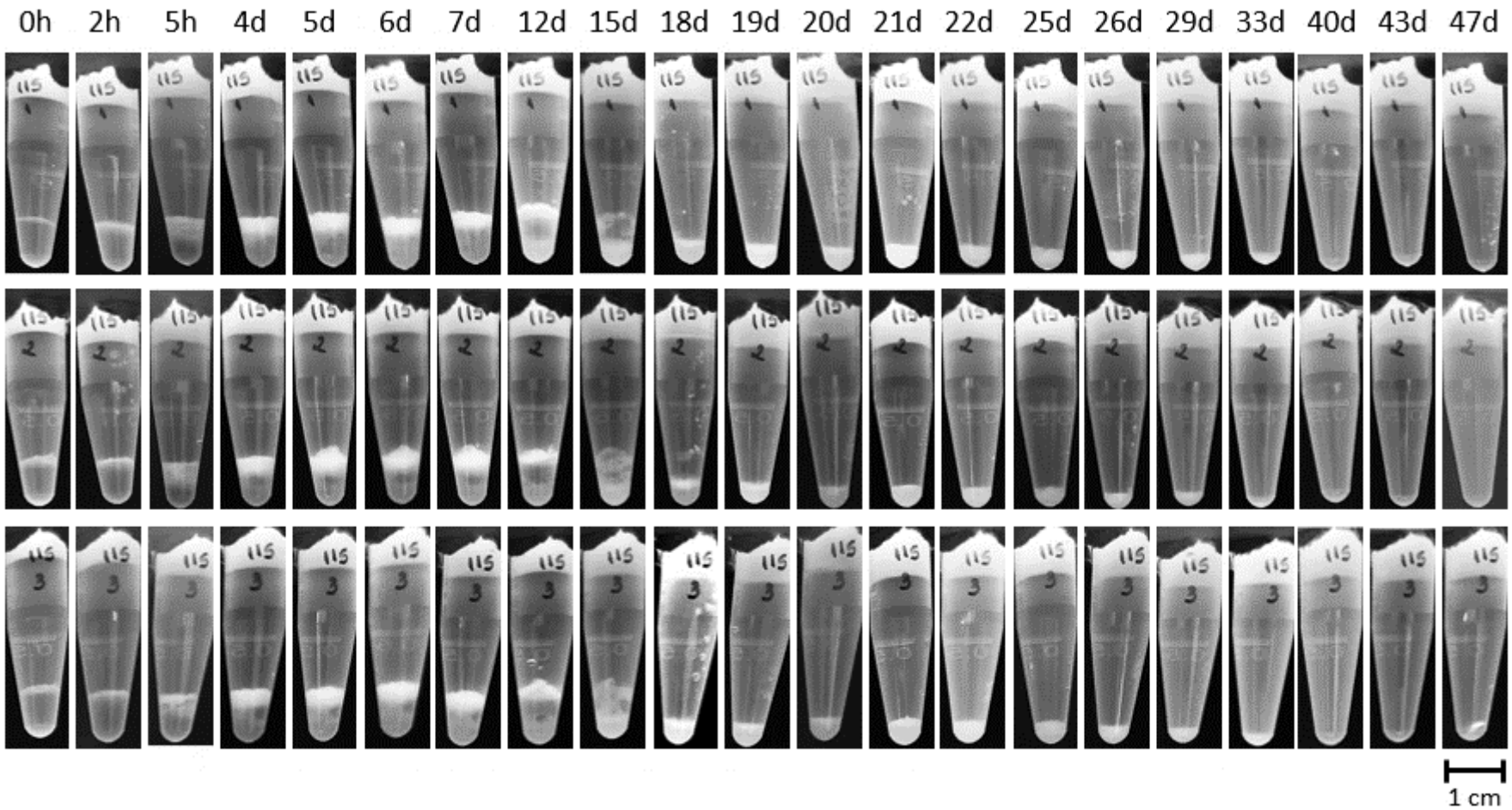


Figure S 1: Optical macroscopy pictures of in-situ formed implants at different time points. The experiment was performed in triplicate, each row shows one replicate. The liquid formulation contained **30 % PLGA** (100 % = PLGA + drug + solvents) and **2 % ibuprofen** (100 % = PLGA + drug). The solvent was a blend of **75% PEG 400, 20% TEC and 5% ethanol** (100 % = total solvent system).

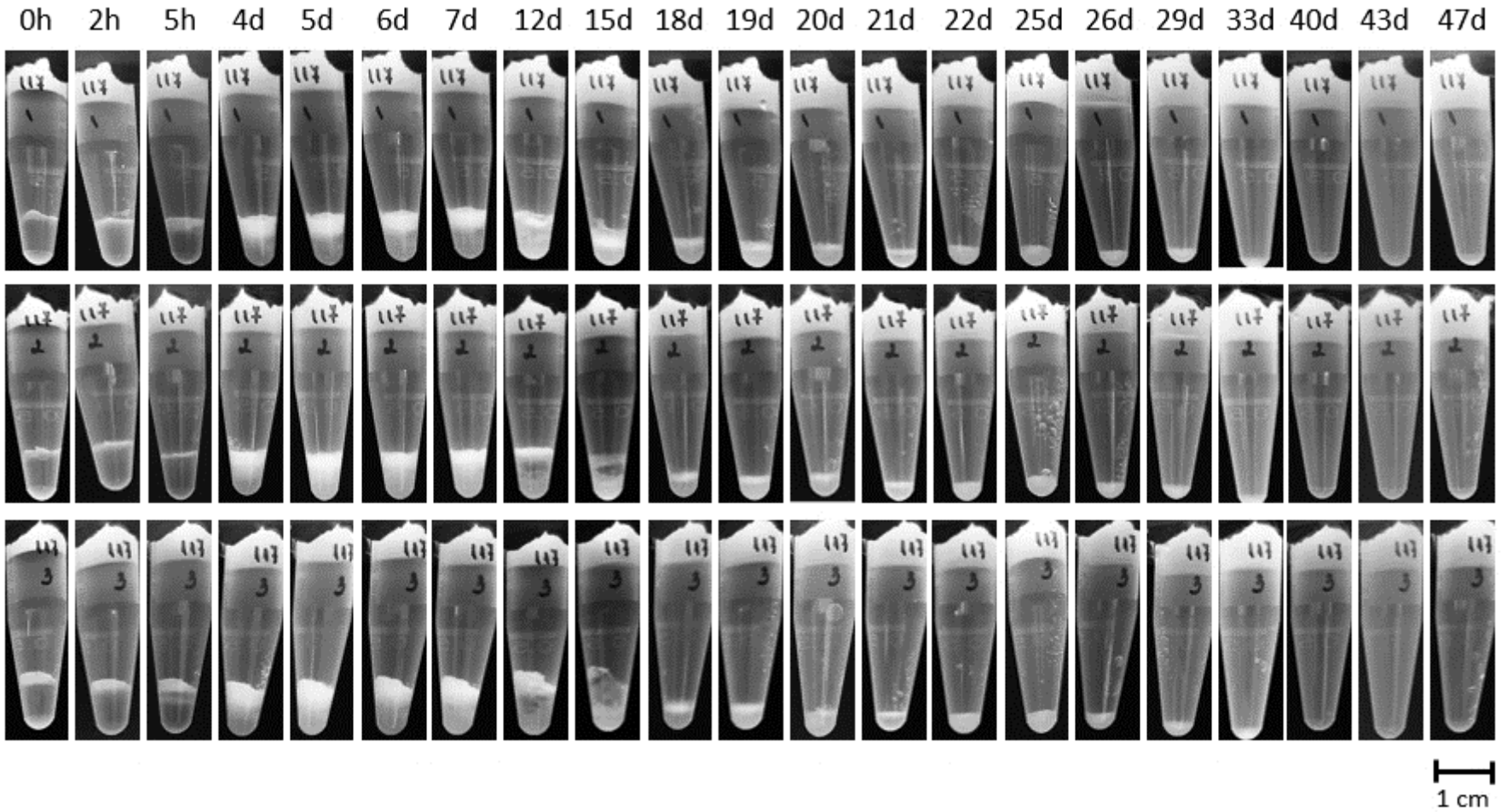


Figure S 2: Optical macroscopy pictures of in-situ formed implants at different time points. The experiment was performed in triplicate, each row shows one replicate. The liquid formulation contained **30 % PLGA** (100 % = PLGA + drug + solvents) and **2 % ibuprofen** (100 % = PLGA + drug). The solvent was a blend of **80% PEG 400, 15% TEC and 5% ethanol** (100 % = total solvent system).

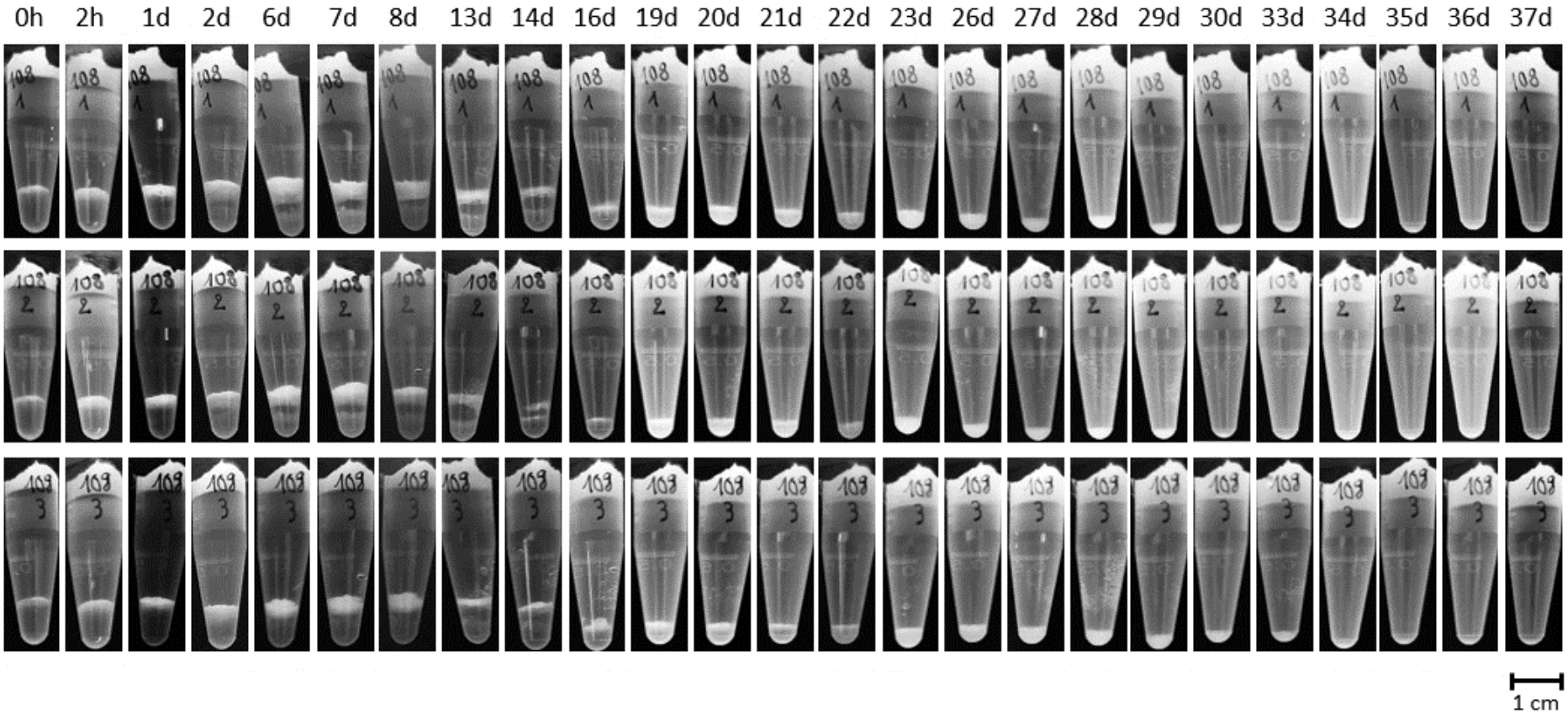


Figure S 3: Optical macroscopy pictures of in-situ formed implants at different time points. The experiment was performed in triplicate, each row shows one replicate. The liquid formulation contained **30 % PLGA** (100 % = PLGA + drug + solvents) and **2 % ibuprofen** (100 % = PLGA + drug). The solvent was a blend of **85% PEG 400, 10% TEC and 5% ethanol** (100 % = total solvent system).

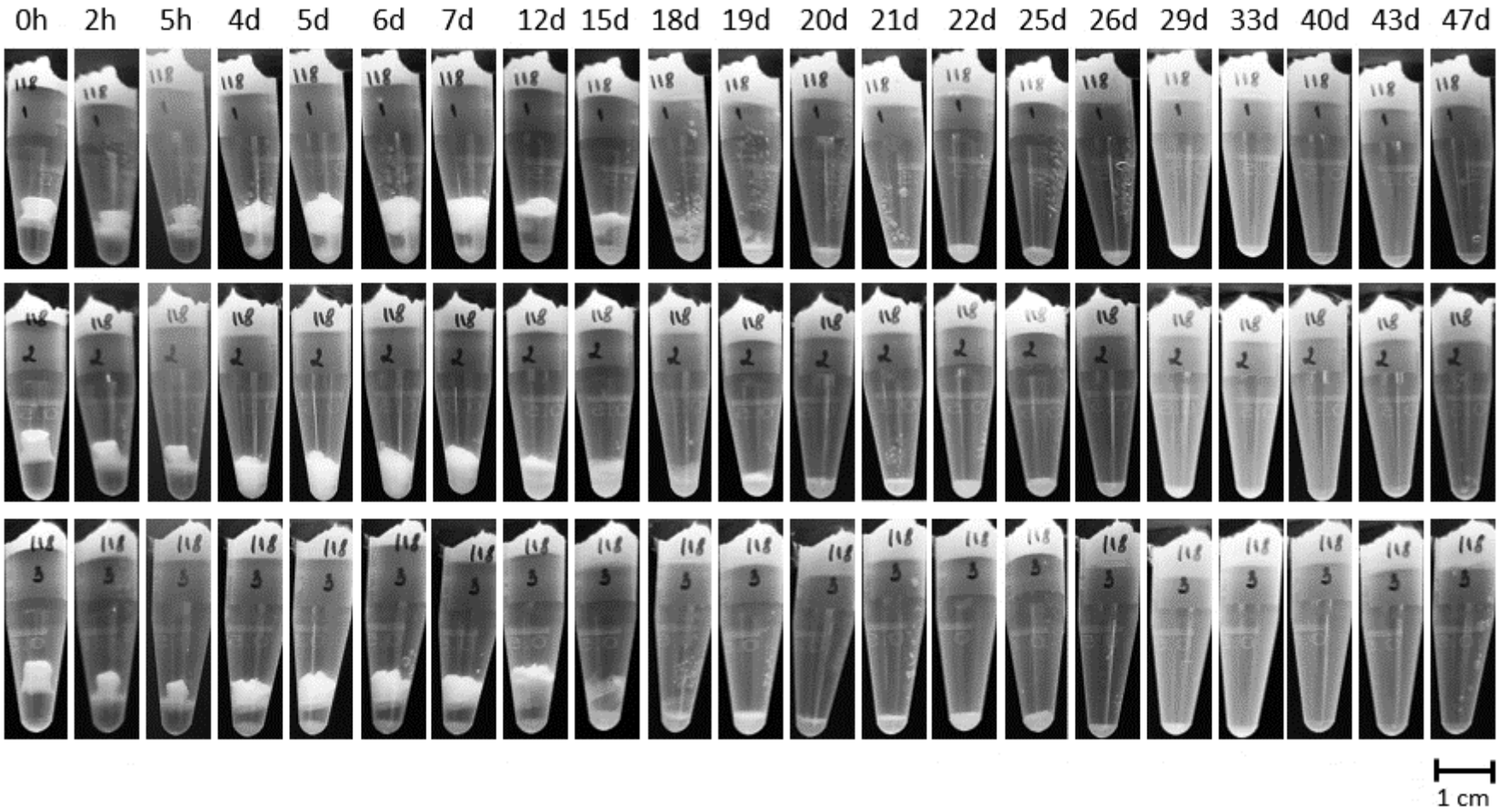


Figure S 4: Optical macroscopy pictures of in-situ formed implants at different time points. The experiment was performed in triplicate, each row shows one replicate. The liquid formulation contained **30 % PLGA** (100 % = PLGA + drug + solvents) and **2 % ibuprofen** (100 % = PLGA + drug). The solvent was a blend of **90% PEG 400, 5% TEC and 5% ethanol** (100 % = total solvent system).

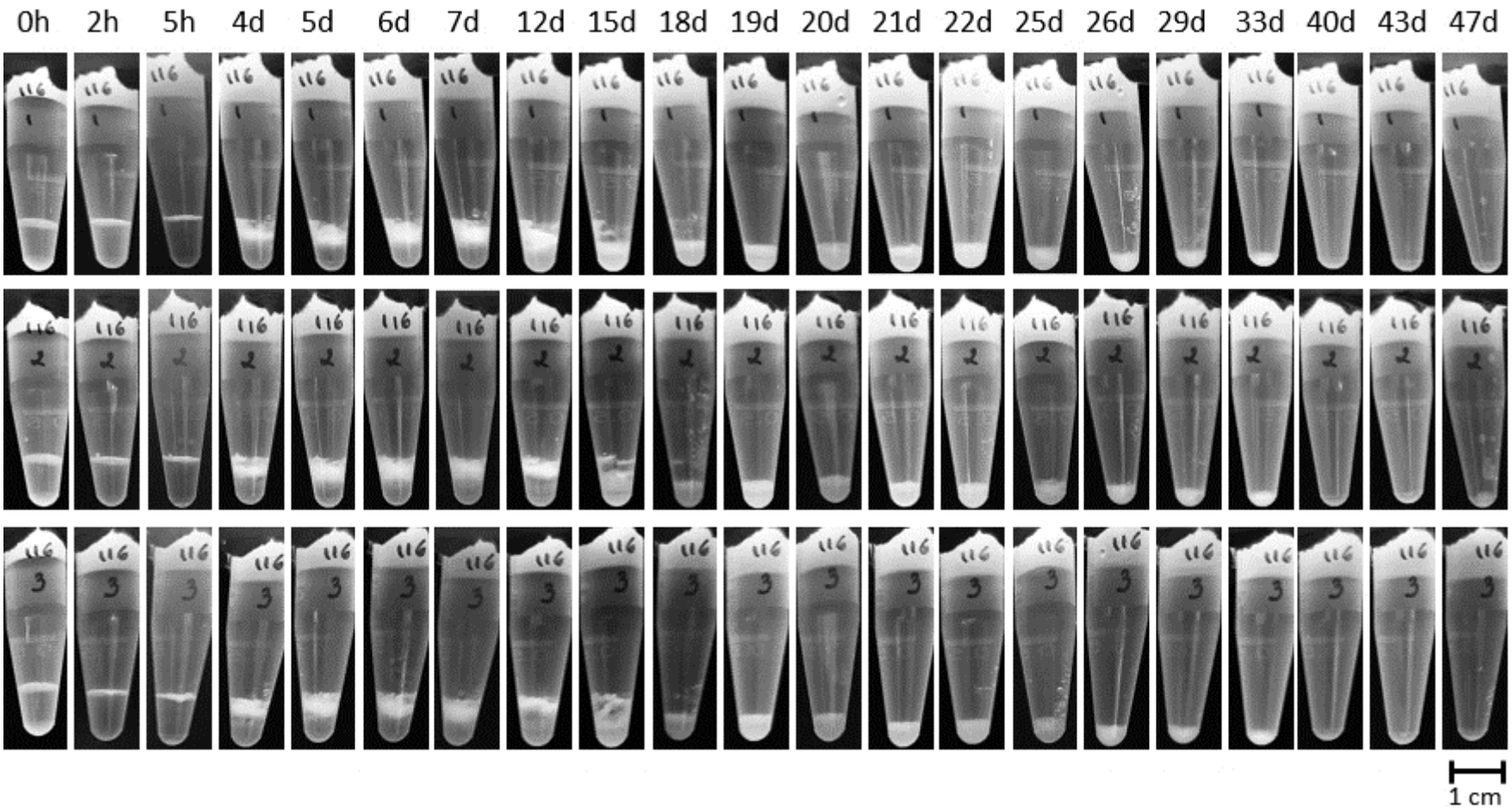


Figure S 5: Optical macroscopy pictures of in-situ formed implants at different time points. The experiment was performed in triplicate, each row shows one replicate. The liquid formulation contained **30 % PLGA** (100 % = PLGA + drug + solvents) and **2 % ibuprofen** (100 % = PLGA + drug). The solvent was a blend of **60% PEG 400, 30% TEC and 10% ethanol** (100 % = total solvent system).

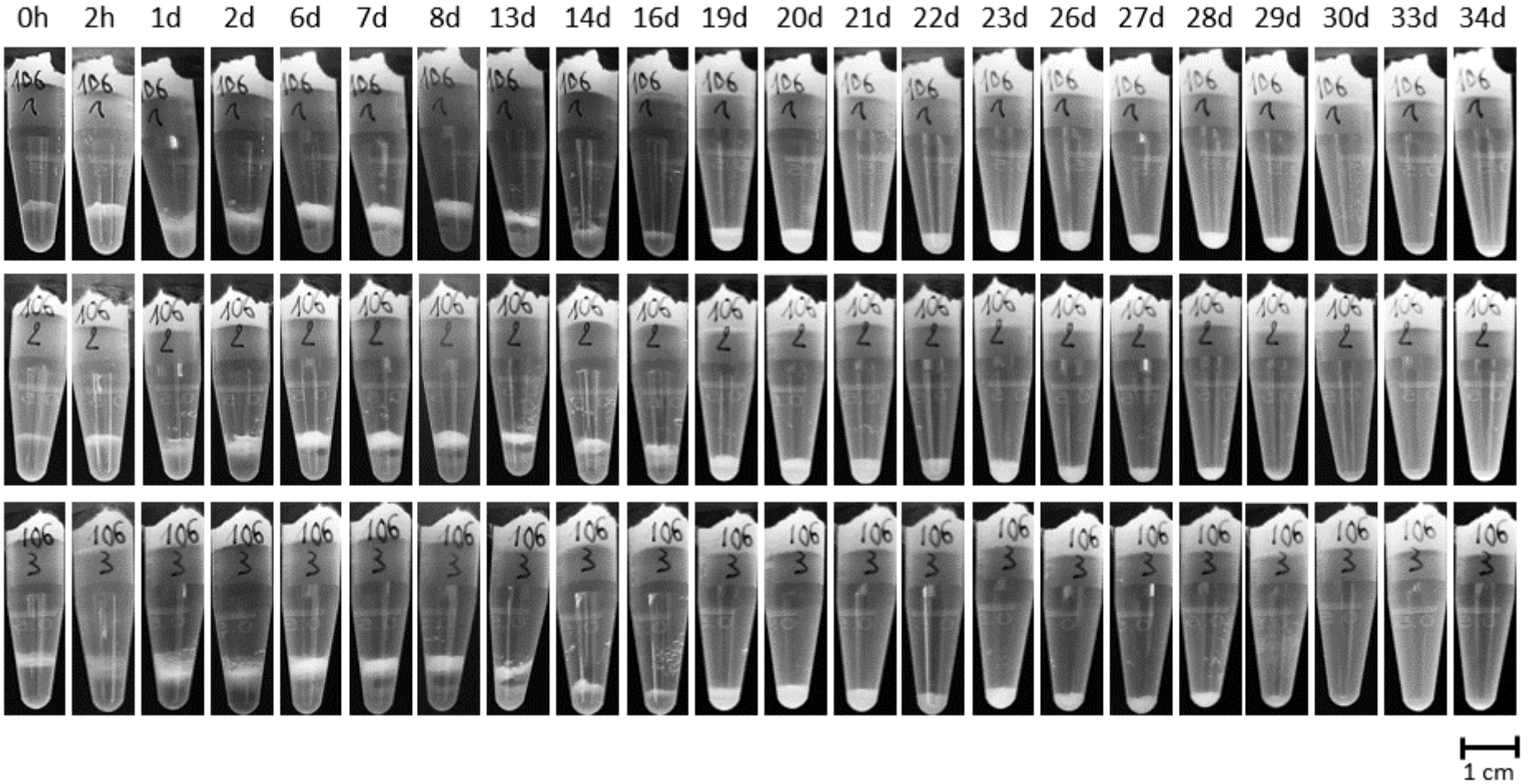


Figure S 6: Optical macroscopy pictures of in-situ formed implants at different time points. The experiment was performed in triplicate, each row shows one replicate. The liquid formulation contained **30 % PLGA** (100 % = PLGA + drug + solvents) and **2 % ibuprofen** (100 % = PLGA + drug). The solvent was a blend of **65% PEG 400, 25% TEC and 10% ethanol** (100 % = total solvent system).

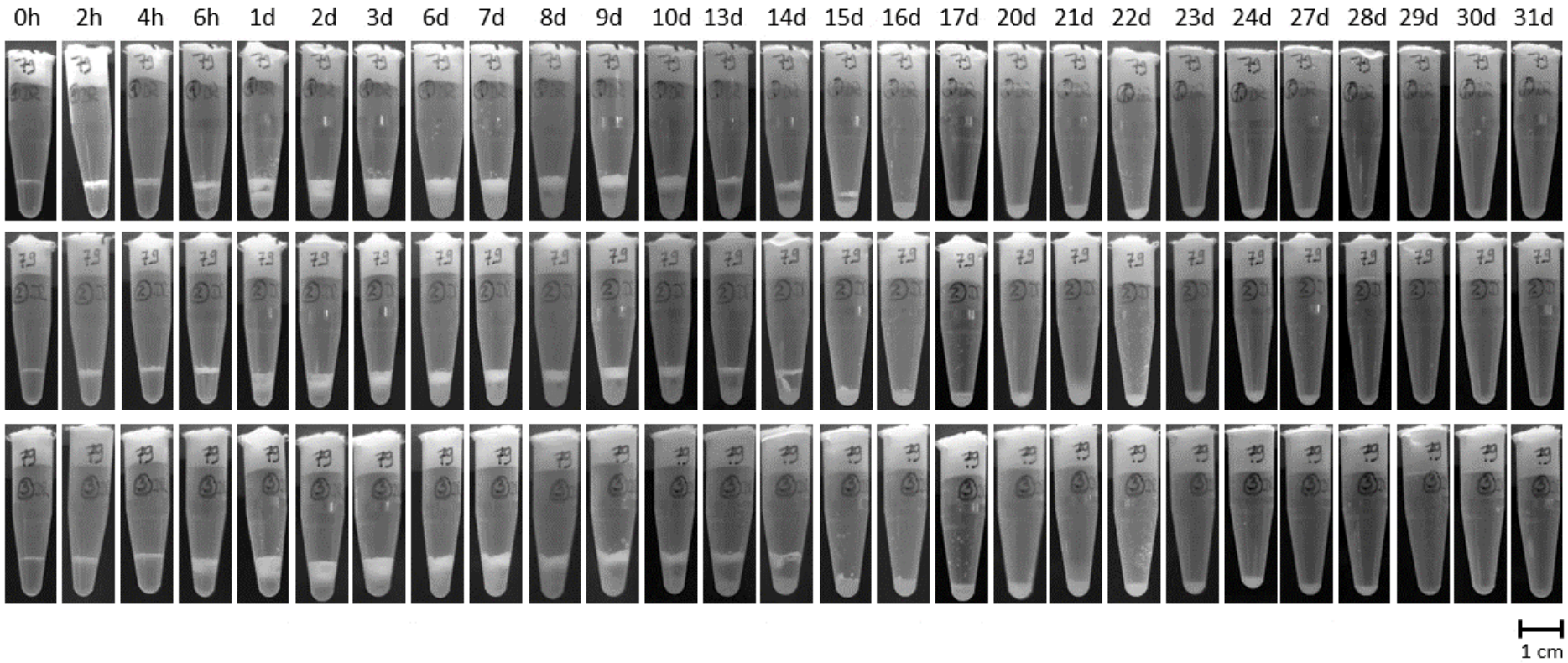


Figure S 7: Optical macroscopy pictures of in-situ formed implants at different time points. The experiment was performed in triplicate, each row shows one replicate. The liquid formulation contained **30 % PLGA** (100 % = PLGA + drug + solvents) and **2 % ibuprofen** (100 % = PLGA + drug). The solvent was a blend of **70% PEG 400, 20% TEC and 10% ethanol** (100 % = total solvent system).

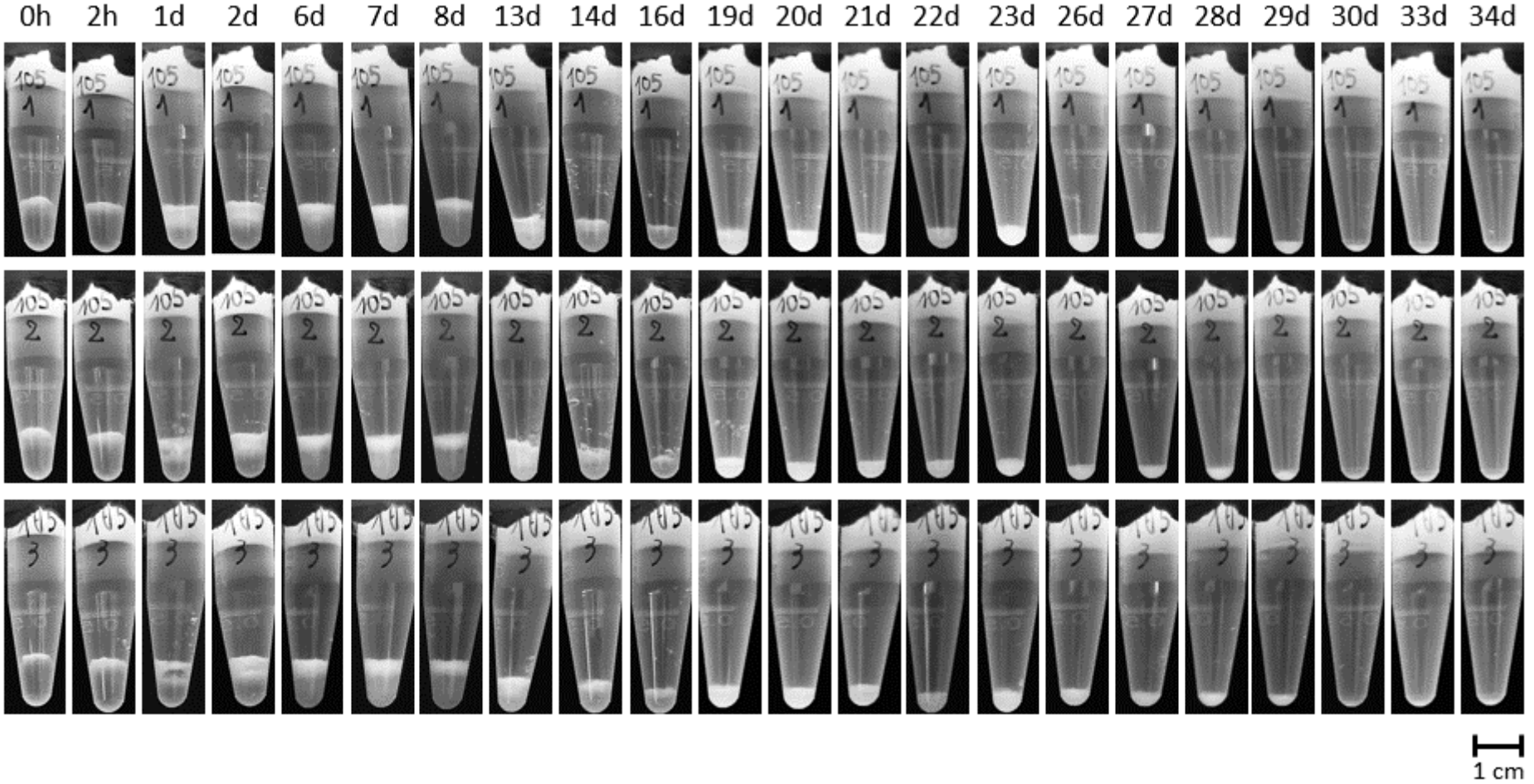


Figure S 8: Optical macroscopy pictures of in-situ formed implants at different time points. The experiment was performed in triplicate, each row shows one replicate. The liquid formulation contained **30 % PLGA** (100 % = PLGA + drug + solvents) and **2 % ibuprofen** (100 % = PLGA + drug). The solvent was a blend of **75% PEG 400, 15% TEC and 10% ethanol** (100 % = total solvent system).

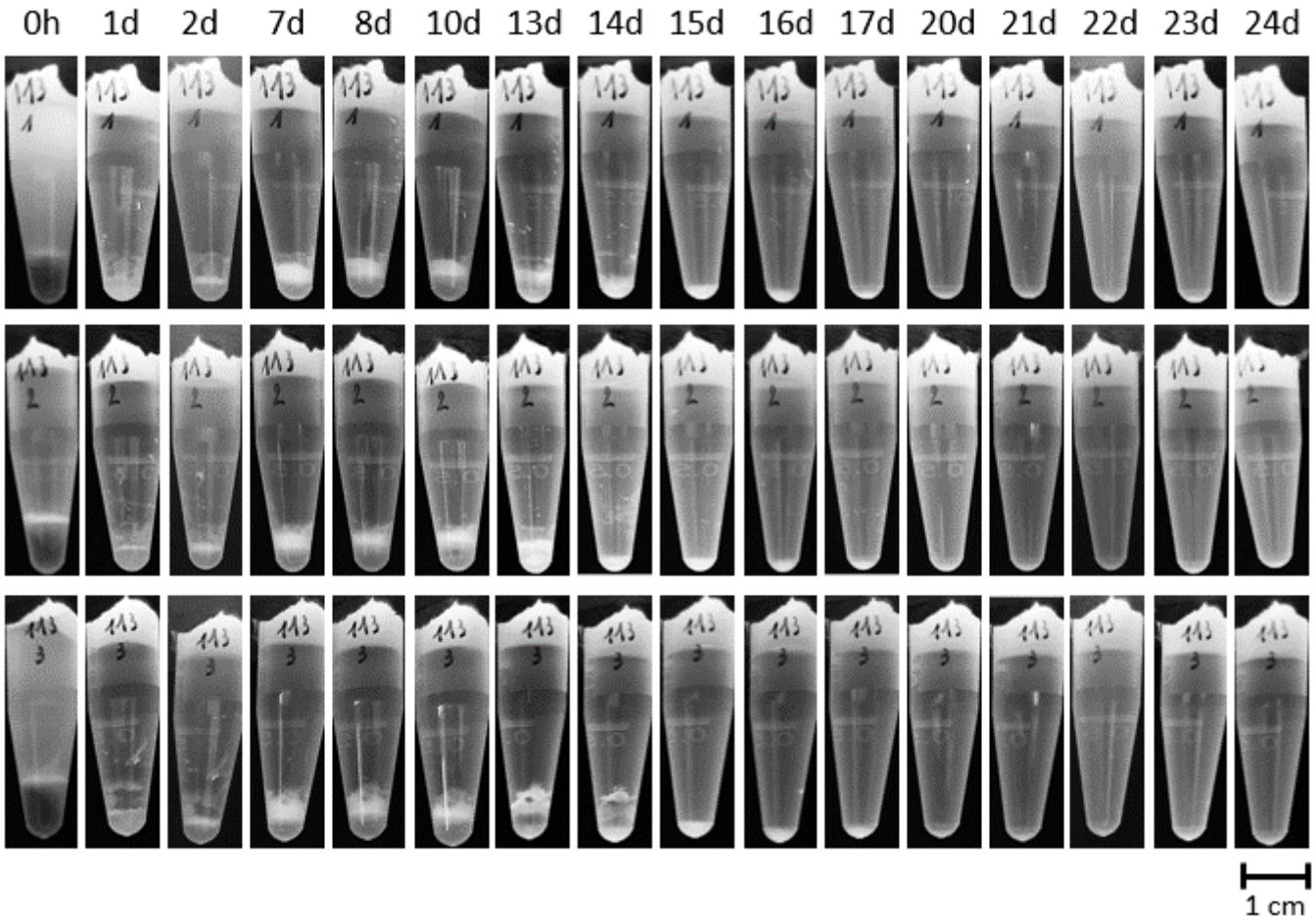


Figure S 9: Optical macroscopy pictures of in-situ formed implants at different time points. The experiment was performed in triplicate, each row shows one replicate. The liquid formulation contained **30 % PLGA** (100 % = PLGA + drug + solvents) and **2 % ibuprofen** (100 % = PLGA + drug). The solvent was a blend of **65% PEG 400, 20% TEC and 15% ethanol** (100 % = total solvent system).

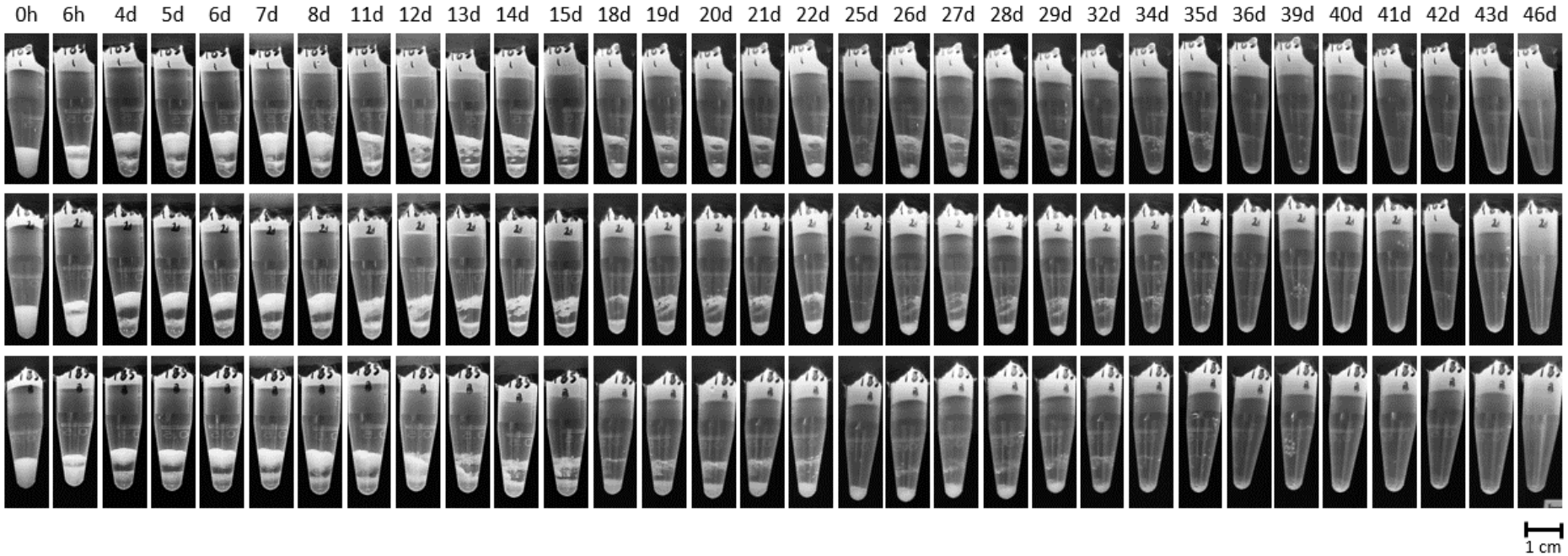


Figure S 10: Optical macroscopy pictures of in-situ formed implants at different time points. The experiment was performed in triplicate, each row shows one replicate. The liquid formulation contained **30 % PLGA** (100 % = PLGA + drug + solvents) and **2 % chlorhexidine dihydrochloride** (100 % = PLGA + drug). The solvent was a blend of **60% PEG 400, 30% TEC and 10% ethanol** (100 % = total solvent system).

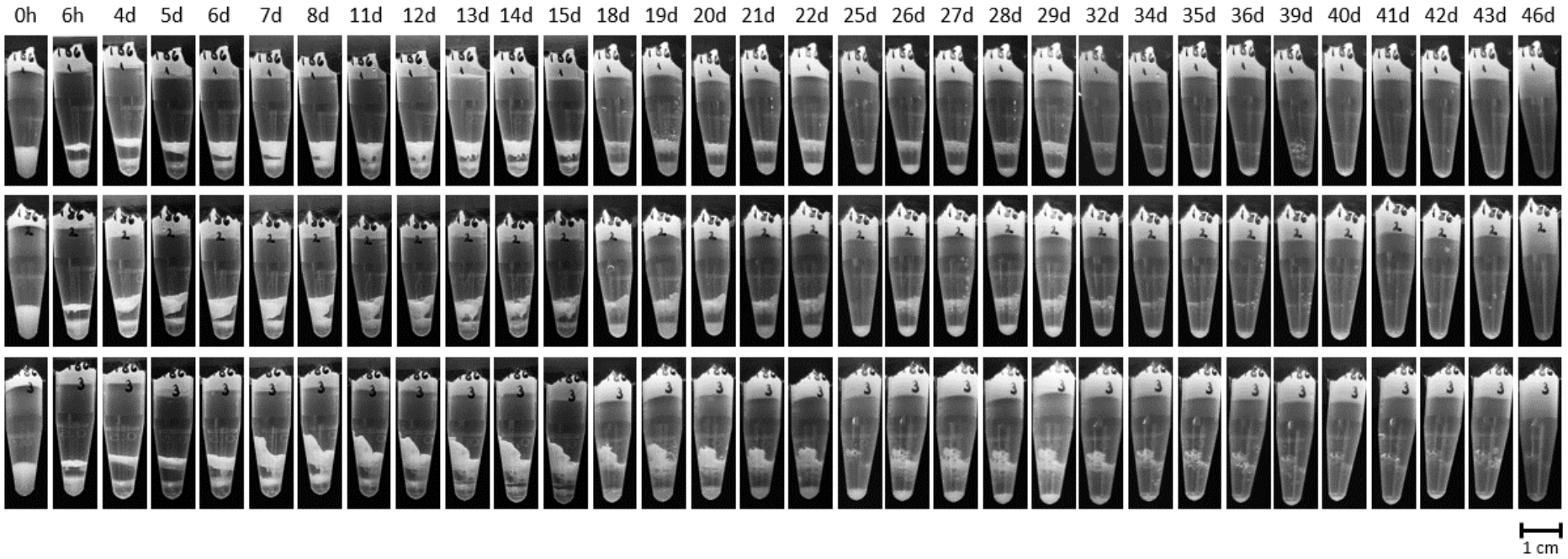


Figure S 11: Optical macroscopy pictures of in-situ formed implants at different time points. The experiment was performed in triplicate, each row shows one replicate. The liquid formulation contained **25 % PLGA** (100 % = PLGA + drug + solvents) and **2 % chlorhexidine dihydrochloride** (100 % = PLGA + drug). The solvent was a blend of **60% PEG 400, 30% TEC and 10% ethanol** (100 % = total solvent system).

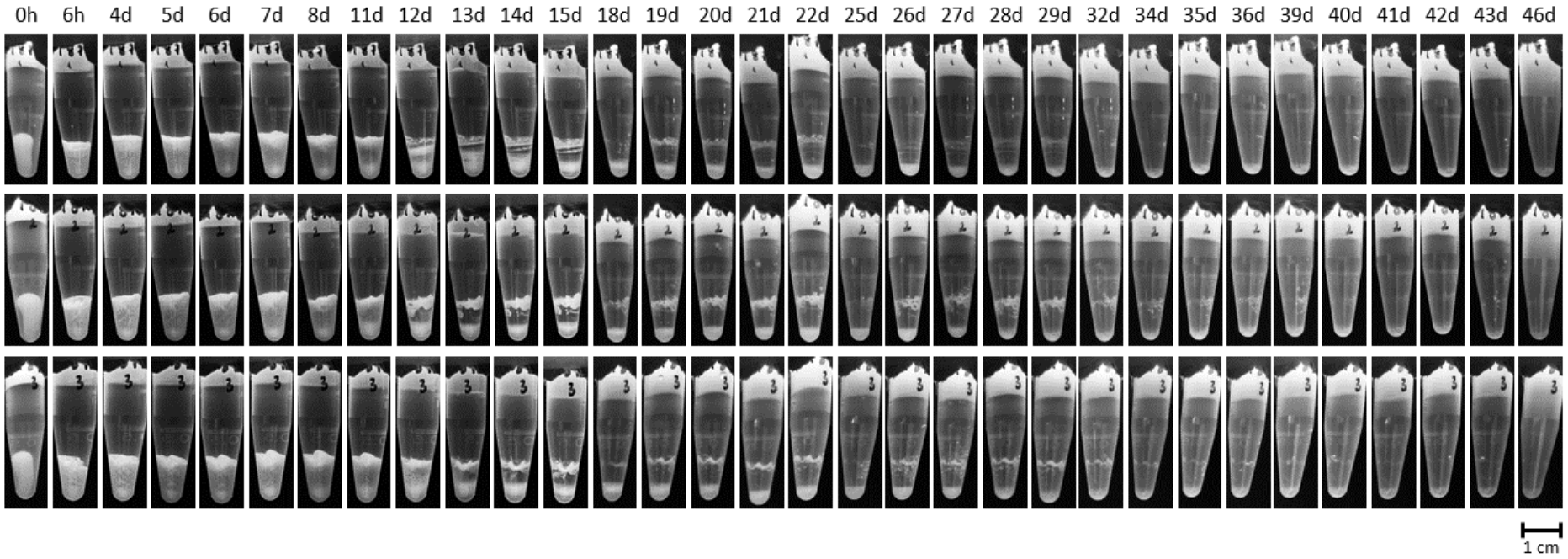


Figure S 12: Optical macroscopy pictures of in-situ formed implants at different time points. The experiment was performed in triplicate, each row shows one replicate. The liquid formulation contained **30 % PLGA** (100 % = PLGA + drug + solvents) and **2 % chlorhexidine dihydrochloride** (100 % = PLGA + drug). The solvent was a blend of **85% PEG 400, 10% TEC and 5% ethanol** (100 % = total solvent system).

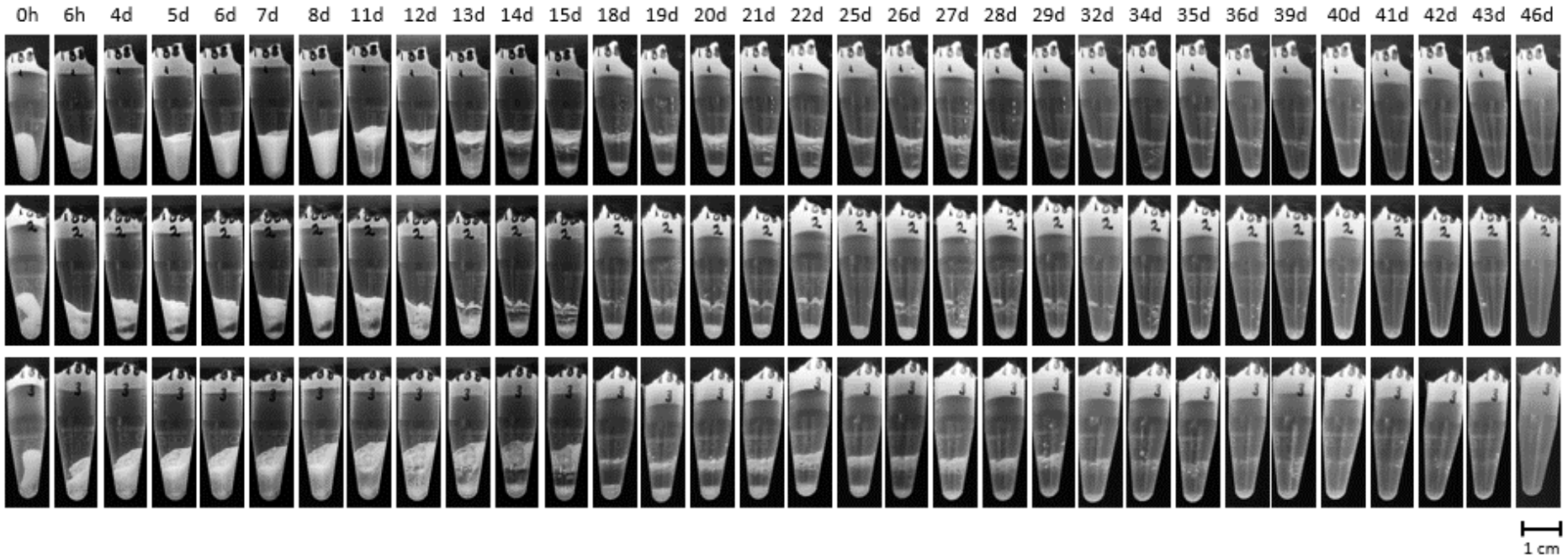


Figure S 13: Optical macroscopy pictures of in-situ formed implants at different time points. The experiment was performed in triplicate, each row shows one replicate. The liquid formulation contained **25 % PLGA** (100 % = PLGA + drug + solvents) and **2 % chlorhexidine dihydrochloride** (100 % = PLGA + drug). The solvent was a blend of **85% PEG 400, 10% TEC and 5% ethanol** (100 % = total solvent system).

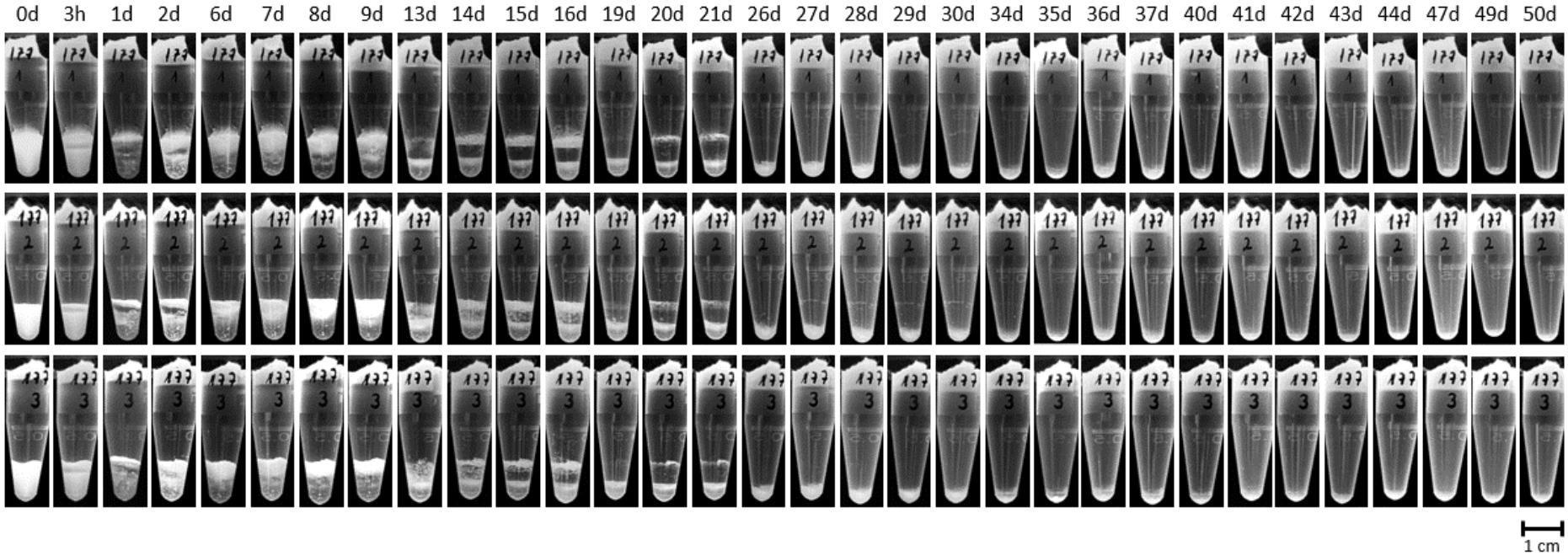


Figure S 14: Optical macroscopy pictures of in-situ formed implants at different time points. The experiment was performed in triplicate, each row shows one replicate. The liquid formulation contained **30 % PLGA** (100 % = PLGA + drug + solvents), **2 % ibuprofen and 2 % chlorhexidine dihydrochloride** (100 % = PLGA + drugs). The solvent was a blend of **60% PEG 400, 30% TEC and 10% ethanol** (100 % = total solvent system).

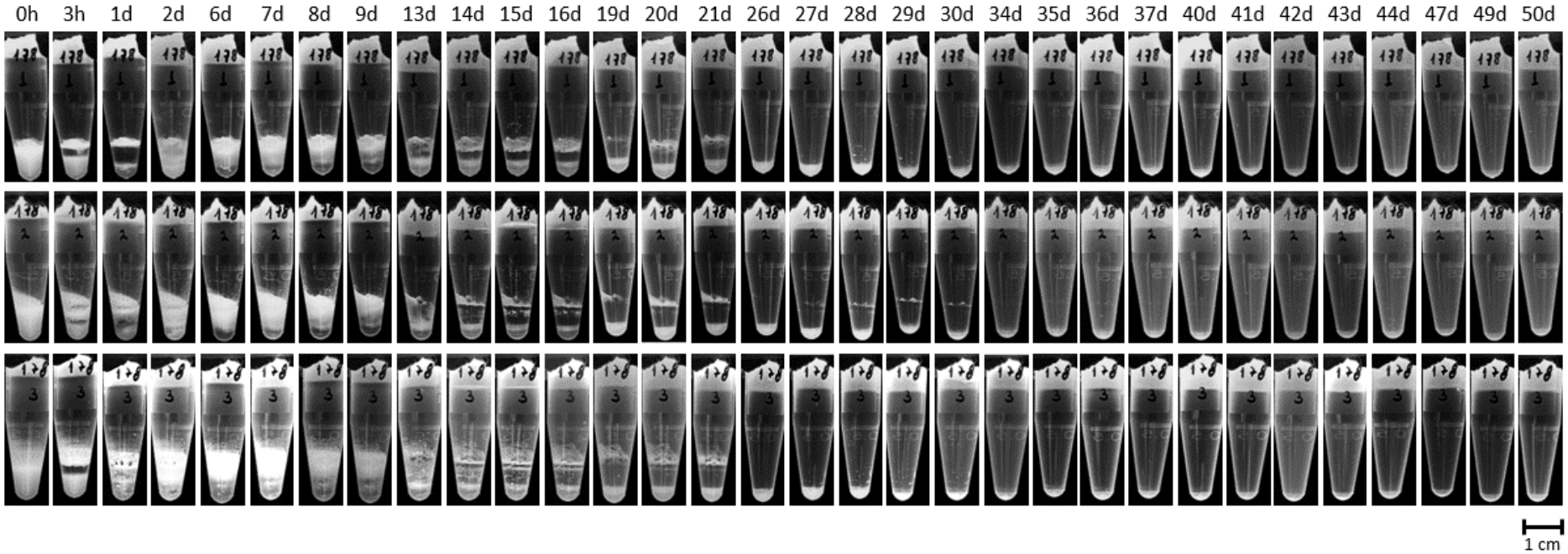


Figure S 15: Optical macroscopy pictures of in-situ formed implants at different time points. The experiment was performed in triplicate, each row shows one replicate. The liquid formulation contained **25 % PLGA** (100 % = PLGA + drug + solvents), **2 % ibuprofen and 2 % chlorhexidine dihydrochloride** (100 % = PLGA + drugs). The solvent was a blend of **60% PEG 400, 30% TEC and 10% ethanol** (100 % = total solvent system).

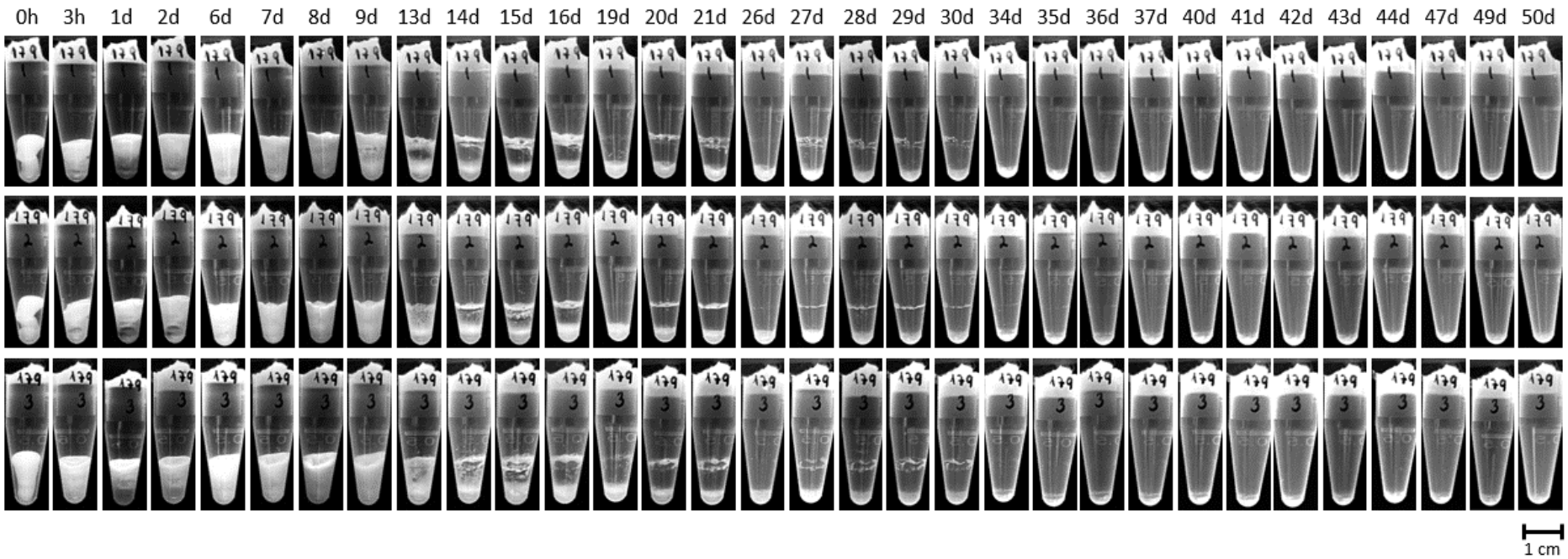


Figure S 16: Optical macroscopy pictures of in-situ formed implants at different time points. The experiment was performed in triplicate, each row shows one replicate. The liquid formulation contained **30 % PLGA** (100 % = PLGA + drug + solvents), **2 % ibuprofen and 2 % chlorhexidine dihydrochloride** (100 % = PLGA + drugs). The solvent was a blend of **85% PEG 400, 10% TEC and 5% ethanol** (100 % = total solvent system).

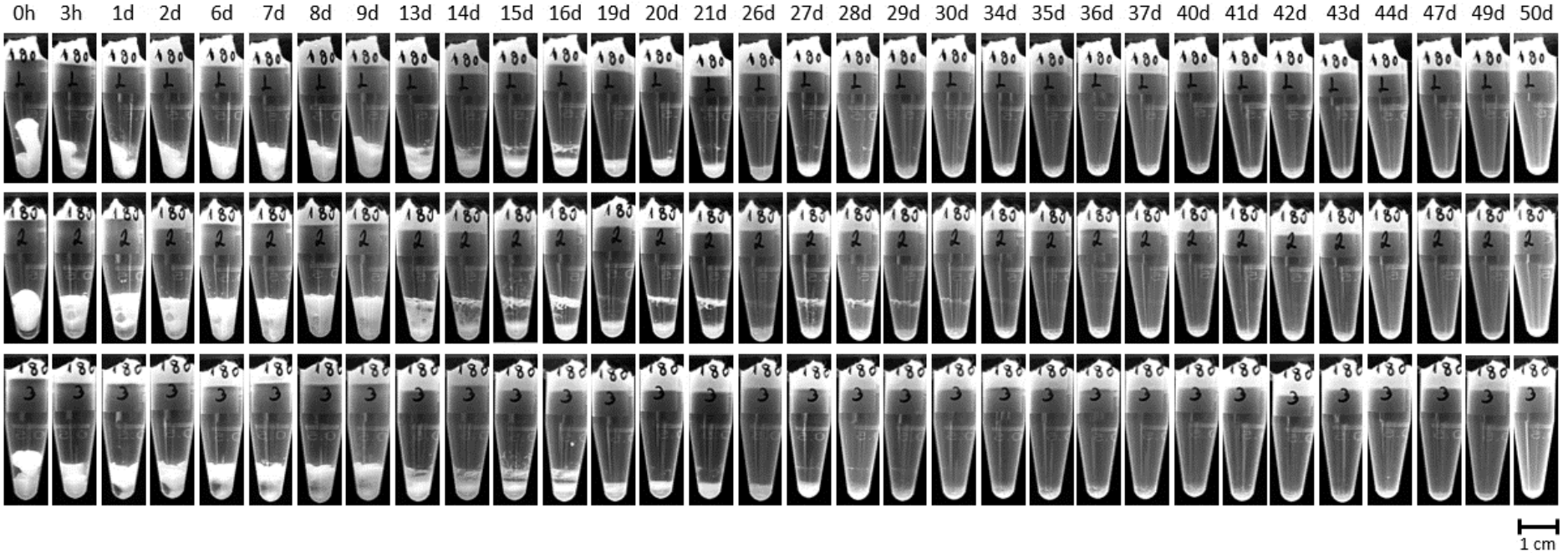


Figure S 17: Optical macroscopy pictures of in-situ formed implants at different time points. The experiment was performed in triplicate, each row shows one replicate. The liquid formulation contained **25 % PLGA** (100 % = PLGA + drug + solvents), **2 % ibuprofen and 2 % chlorhexidine dihydrochloride** (100 % = PLGA + drugs). The solvent was a blend of **85% PEG 400, 10% TEC and 5% ethanol** (100 % = total solvent system).

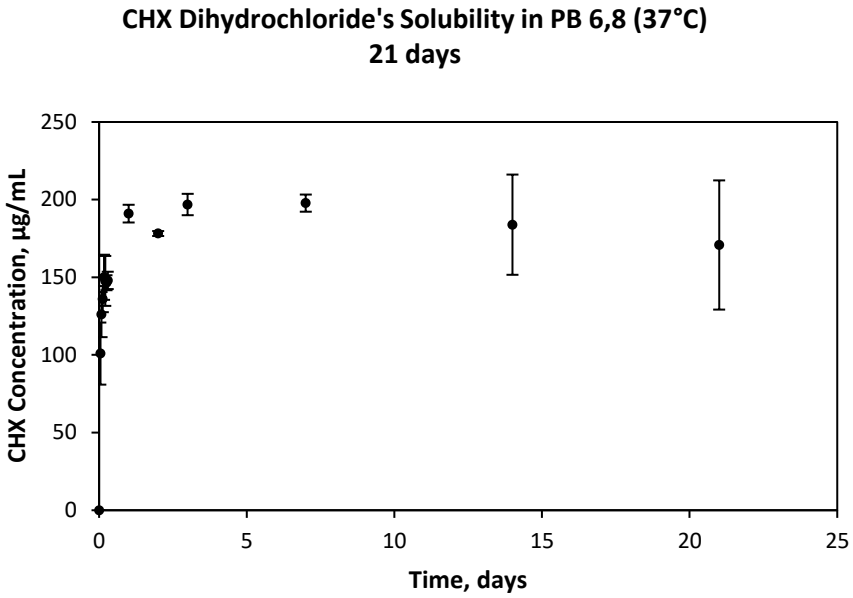


Figure S 18: Chlorhexidine solubility in phosphate buffer pH 6.8.

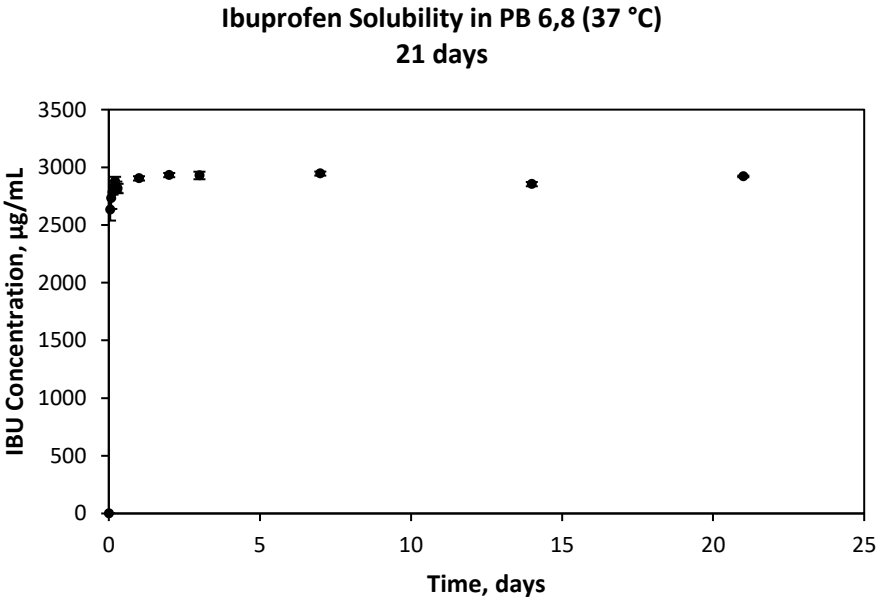


Figure S 19: Ibuprofen solubility in phosphate buffer pH 6.8.

References

1. Cho MI, Garant PR. Development and general structure of the periodontium. Periodontol 2000. 2000 Oct;24:9–27.

2. Katancik JA, Kumarswamy A, Branch-Mays G, Califano JV. 11 - Infections of the Periodontal Apparatus. In: Hupp JR, Ferneini EM, editors. Head, Neck, and Orofacial Infections [Internet]. St. Louis: Elsevier; 2016 [cited 2024 Feb 16]. p. 189–202. Available from: https://www.sciencedirect.com/science/article/pii/B9780323289450000119

3. Reed DA, Diekwisch TGH. Chapter 35 - Morphogenesis and Wound Healing in the Periodontium. In: Vishwakarma A, Sharpe P, Shi S, Ramalingam M, editors. Stem Cell Biology and Tissue Engineering in Dental Sciences [Internet]. Boston: Academic Press; 2015 [cited 2024 Feb 16]. p. 445–58. Available from: https://www.sciencedirect.com/science/article/pii/B9780123971579000394

4. Goudouri OM, Kontonasaki E, Boccaccini AR. 17 - Layered scaffolds for periodontal regeneration. In: Tayebi L, Moharamzadeh K, editors. Biomaterials for Oral and Dental Tissue Engineering [Internet]. Woodhead Publishing; 2017 [cited 2024 Feb 16]. p. 279–95. Available from: https://www.sciencedirect.com/science/article/pii/B9780081009611000177

5. Stark WD DDS, Smith DG PhD. Teeth. In: Salem Press Encyclopedia of Health. Salem Press; 2022.

6. Beertsen W, McCulloch CA, Sodek J. The periodontal ligament: a unique, multifunctional connective tissue. Periodontol 2000. 1997 Feb;13:20–40.

7. de Jong T, Bakker AD, Everts V, Smit TH. The intricate anatomy of the periodontal ligament and its development: Lessons for periodontal regeneration. J Periodontal Res. 2017 Dec;52(6):965–74.

8. Page RC, Kornman KS. The pathogenesis of human periodontitis: an introduction. Periodontology 2000. 1997;14(1):9–11.

9. Chapple ILC, Mealey BL, Dyke TE, Bartold PM, Dommisch H, Eickholz P, et al. Periodontal health and gingival diseases and conditions on an intact and a reduced periodontium: Consensus report of workgroup 1 of the 2017 World Workshop on the Classification of Periodontal and Peri-Implant Diseases and Conditions. Journal of Periodontology. 2018 Jun 3;89:S74–84.

10. Highfield J. Diagnosis and classification of periodontal disease. Aust Dent J. 2009 Sep;54 Suppl 1:S11-26.

11. Kinane DF. Causation and pathogenesis of periodontal disease. Periodontol 2000. 2001;25:8–20.

12. Pihlstrom BL, Michalowicz BS, Johnson NW. Periodontal diseases. The Lancet. 2005 Nov 19;366(9499):1809–20.

13. Kwon T, Lamster IB, Levin L. Current Concepts in the Management of Periodontitis. International Dental Journal. 2021 Dec 1;71(6):462–76.

14. Bascones-Martinez A, Matesanz-Perez P, Escribano-Bermejo M, González-Moles MÁ, Bascones-Ilundain J, Meurman JH. Periodontal disease and diabetes-Review of the Literature. Med Oral Patol Oral Cir Bucal. 2011 Sep 1;16(6):e722-729.

15. Papapanou PN, Sanz M, Buduneli N, Dietrich T, Feres M, Fine DH, et al. Periodontitis: Consensus report of workgroup 2 of the 2017 World Workshop on the Classification of Periodontal and Peri-Implant Diseases and Conditions. Journal of Periodontology. 2018;89(S1):S173–82.

16. Tonetti MS, Greenwell H, Kornman KS. Staging and grading of periodontitis: Framework and proposal of a new classification and case definition. Journal of Periodontology. 2018;89(S1):S159–72.

17. Do MP, Neut C, Metz H, Delcourt E, Siepmann J, Mäder K, et al. Mechanistic analysis of PLGA/HPMC-based in-situ forming implants for periodontitis treatment. European Journal of Pharmaceutics and Biopharmaceutics. 2015 Aug 1;94:273–83.

18. Silva-Boghossian CM, Neves AB, Resende FAR, Colombo APV. Suppuration-Associated Bacteria in Patients With Chronic and Aggressive Periodontitis. Journal of Periodontology. 2013 Sep;84(9):e9–16.

19. Silva-Boghossian CM, Luiz RR, Colombo APV. Periodontal Status, Sociodemographic, and Behavioral Indicators in Subjects Attending a Public Dental School in Brazil: Analysis of Clinical Attachment Loss. Journal of Periodontology. 2009 Dec;80(12):1945–54.

20. Agossa K, Delepierre A, Lizambard M, Delcourt-Debruyne E, Siepmann J, Siepmann F, et al. In-situ forming implants for dual controlled release of chlorhexidine and ibuprofen for periodontitis treatment: Microbiological and mechanical key properties. Journal of Drug Delivery Science and Technology. 2020 Dec;60:101956.

21. Lizambard M, Menu T, Fossart M, Bassand C, Agossa K, Huck O, et al. In-situ forming implants for the treatment of periodontal diseases: Simultaneous controlled release of an antiseptic and an anti-inflammatory drug. International Journal of Pharmaceutics. 2019 Dec;572:118833.

22. Batool F, Agossa K, Lizambard M, Petit C, Bugueno IM, Delcourt-Debruyne E, et al. In-situ forming implants loaded with chlorhexidine and ibuprofen for periodontal treatment: Proof of concept study in vivo. International Journal of Pharmaceutics. 2019 Oct;569:118564.

23. The Global Status Report on Oral Health 2022 [Internet]. [cited 2023 Nov 28]. Available from: https://www.who.int/team/noncommunicable-diseases/global-status-report-on-oral-health-2022

24. Tonetti MS, Jepsen S, Jin L, Otomo-Corgel J. Impact of the global burden of periodontal diseases on health, nutrition and wellbeing of mankind: A call for global action. Journal of Clinical Periodontology. 2017;44(5):456–62.

25. Deo P, Deshmukh R. Oral microbiome: Unveiling the fundamentals: Journal of Oral and Maxillofacial Pathology. Journal of Oral and Maxillofacial Pathology. 2019 Jan 1;23(1):122.

26. Sedghi LM, Bacino M, Kapila YL. Periodontal Disease: The Good, The Bad, and The Unknown. Frontiers in Cellular and Infection Microbiology [Internet]. 2021 [cited 2024 Feb 16];11. Available from: https://www.frontiersin.org/articles/10.3389/fcimb.2021.766944

27. Hajishengallis G, Lamont R j. Beyond the red complex and into more complexity: the polymicrobial synergy and dysbiosis (PSD) model of periodontal disease etiology. Molecular Oral Microbiology. 2012;27(6):409–19.

28. Holt SC, Ebersole JL. Porphyromonas gingivalis, Treponema denticola, and Tannerella forsythia: the ‘red complex’, a prototype polybacterial pathogenic consortium in periodontitis. Periodontol 2000. 2005 Jun;38(1):72–122.

29. Rosan B, Lamont RJ. Dental plaque formation: Microbes and infection. Microbes Infect. 2000 Nov;2(13):1599–607.

30. Mark Welch JL, Rossetti BJ, Rieken CW, Dewhirst FE, Borisy GG. Biogeography of a human oral microbiome at the micron scale: Proceedings of the National Academy of Sciences of the United States of America. Proceedings of the National Academy of Sciences of the United States of America. 2016 Feb 9;113(6):E791–800.

31. Hajishengallis G, Chavakis T, Lambris JD. Current understanding of periodontal disease pathogenesis and targets for host-modulation therapy. Periodontol 2000. 2020 Oct;84(1):14–34.

32. Socransky S s., Haffajee A d., Cugini M a., Smith C, Kent Jr. RL. Microbial complexes in subgingival plaque. Journal of Clinical Periodontology. 1998;25(2):134–44.

33. Griffen AL, Beall CJ, Campbell JH, Firestone ND, Kumar PS, Yang ZK, et al. Distinct and complex bacterial profiles in human periodontitis and health revealed by 16S pyrosequencing: The ISME journal. ISME J. 2012 Jun;6(6):1176–85.

34. Abusleme L, Dupuy AK, Dutzan N, Silva N, Burleson JA, Strausbaugh LD, et al. The subgingival microbiome in health and periodontitis and its relationship with community biomass and inflammation: The ISME journal. ISME J. 2013 May;7(5):1016–25.

35. Haubek D, Ennibi OK, Poulsen K, Vaeth M, Poulsen S, Kilian M. Risk of aggressive periodontitis in adolescent carriers of the JP2 clone of Aggregatibacter (Actinobacillus) actinomycetemcomitans in Morocco: a prospective longitudinal cohort study: Lancet (London, England). Lancet. 2008 Jan 19;371(9608):237–42.

36. Hajishengallis G, Liang S, Payne MA, Hashim A, Jotwani R, Eskan MA, et al. Low-Abundance Biofilm Species Orchestrates Inflammatory Periodontal Disease through the Commensal Microbiota and Complement: Cell Host & Microbe. Cell Host & Microbe. 2011 Nov 17;10(5):497–506.

37. Dutzan N, Konkel JE, Greenwell-Wild T, Moutsopoulos NM. Characterization of the human immune cell network at the gingival barrier: Mucosal immunology. Mucosal Immunol. 2016 Sep;9(5):1163–72.

38. Peterson SN, Meissner T, Su AI, Snesrud E, Ong AC, Schork NJ, et al. Functional expression of dental plaque microbiota: Frontiers in cellular and infection microbiology. Front Cell Infect Microbiol. 2014 Aug 14;4:108.

39. Henne K, Fuchs F, Kruth S, Horz HP, Conrads G. Shifts in Campylobacter species abundance may reflect general microbial community shifts in periodontitis progression: Journal of oral microbiology. J Oral Microbiol. 2014 Nov 19;6:25874.

40. Zhou P, Li X, Qi F. Identification and characterization of a haem biosynthesis locus in Veillonella: Microbiology (Reading, England). Microbiology (Reading). 2016 Oct;162(10):1735–43.

41. Abusleme L, Hoare A, Hong BY, Diaz PI. Microbial signatures of health, gingivitis, and periodontitis: Periodontology 2000. Periodontol 2000. 2021 Jun;86(1):57–78.

42. Ly M, Abeles SR, Boehm TK, Robles-Sikisaka R, Naidu M, Santiago-Rodriguez T, et al. Altered oral viral ecology in association with periodontal disease: MBio. mBio. 2014 May 20;5(3):e01133.

43. Abeles SR, Robles-Sikisaka R, Ly M, Lum AG, Salzman J, Boehm TK, et al. Human oral viruses are personal, persistent and gender-consistent: The ISME journal. ISME J. 2014 Sep;8(9):1753–67.

44. Contreras A, Botero JE, Slots J. Biology and pathogenesis of cytomegalovirus in periodontal disease: Periodontology 2000. Periodontology 2000. 2014 Feb;64(1):40–56.

45. Slots J. Periodontal herpesviruses: prevalence, pathogenicity, systemic risk: Periodontology 2000. Periodontology 2000. 2015 Oct;69(1):28–45.

46. Slots J. Focal infection of periodontal origin: Periodontology 2000. Periodontol 2000. 2019 Feb;79(1):233–5.

47. Zhu C, Li F, Wong MCM, Feng XP, Lu HX, Xu W. Association between Herpesviruses and Chronic Periodontitis: A Meta-Analysis Based on Case-Control Studies: PloS one. PLoS One. 2015 Dec 14;10(12):e0144319.

48. Preshaw PM. Host modulation therapy with anti-inflammatory agents. Periodontol 2000. 2018 Feb;76(1):131–49.

49. Bosshardt DD, Lang NP. The junctional epithelium: from health to disease: Journal of dental research. J Dent Res. 2005 Jan;84(1):9–20.

50. Fujita T, Yoshimoto T, Kajiya M, Ouhara K, Matsuda S, Takemura T, et al. Regulation of defensive function on gingival epithelial cells can prevent periodontal disease: Japanese Dental Science Review. Japanese Dental Science Review. 2018 May;54(2):66–75.

51. Hajishengallis G. The inflammophilic character of the periodontitis-associated microbiota: Molecular oral microbiology. Mol Oral Microbiol. 2014 Dec;29(6):248–57.

52. Rosier BT, Marsh PD, Mira A. Resilience of the Oral Microbiota in Health: Mechanisms That Prevent Dysbiosis: Journal of dental research. J Dent Res. 2018 Apr;97(4):371–80.

53. Dutzan N, Kajikawa T, Abusleme L, Greenwell-Wild T, Zuazo CE, Ikeuchi T, et al. A dysbiotic microbiome triggers T H 17 cells to mediate oral mucosal immunopathology in mice and humans: Science translational medicine. Sci Transl Med. 2018 Oct 17;10(463).

54. Aquino-Martinez R, Khosla S, Farr JN, Monroe DG. Periodontal Disease and Senescent Cells: New Players for an Old Oral Health Problem?: International journal of molecular sciences. Int J Mol Sci. 2020 Oct 9;21(20).

55. Hasturk H, Kantarci A. Activation and resolution of periodontal inflammation and its systemic impact: Periodontology 2000. Periodontology 2000. 2015 Oct;69(1):255–73.

56. Hajishengallis G, Korostoff JM. Revisiting the Page & Schroeder model: the good, the bad and the unknowns in the periodontal host response 40 years later. Periodontol 2000. 2017 Oct;75(1):116–51.

57. Hajishengallis G, Chavakis T. Local and systemic mechanisms linking periodontal disease and inflammatory comorbidities: Nature Reviews Immunology. Nature Reviews Immunology. 2021 Jul 1;21(7):426.

58. Duran-Pinedo AE, Solbiati J, Frias-Lopez J. The effect of the stress hormone cortisol on the metatranscriptome of the oral microbiome: npj Biofilms and Microbiomes. npj Biofilms and Microbiomes. 2018 Oct 18;4(1).

59. Woelber JP, Gärtner M, Breuninger L, Anderson A, König D, Hellwig E, et al. The influence of an anti-inflammatory diet on gingivitis. A randomized controlled trial: Journal of clinical periodontology. J Clin Periodontol. 2019 Apr;46(4):481–90.

60. Woelber JP, Tennert C. Chapter 13: Diet and Periodontal Diseases: Monographs in oral science. Monogr Oral Sci. 2020;28:125–33.

61. Caton JG, Armitage G, Berglundh T, Chapple ILC, Jepsen S, Kornman KS, et al. A new classification scheme for periodontal and peri-implant diseases and conditions – Introduction and key changes from the 1999 classification. Journal of Periodontology. 2018 Jun 3;89:S1–8.

62. Schwach-Abdellaoui K, Vivien-Castioni N, Gurny R. Local delivery of antimicrobial agents for the treatment of periodontal diseases. European Journal of Pharmaceutics and Biopharmaceutics. 2000;

63. Deas DE, Moritz AJ, Sagun Jr. RS, Gruwell SF, Powell CA. Scaling and root planing vs. conservative surgery in the treatment of chronic periodontitis. Periodontology 2000. 2016;71(1):128–39.

64. Baker KA. The role of dental professionals and the patient in plaque control. Periodontol 2000. 1995 Jun;8:108–13.

65. Cobb CM, Sottosanti JS. A re-evaluation of scaling and root planing. Journal of Periodontology. 2021;92(10):1370–8.

66. Do MP, Neut C, Delcourt E, Seixas Certo T, Siepmann J, Siepmann F. In situ forming implants for periodontitis treatment with improved adhesive properties. European Journal of Pharmaceutics and Biopharmaceutics. 2014 Oct;88(2):342–50.

67. Berezow AB, Darveau RP. Microbial shift and periodontitis. Periodontology 2000. 2011;55(1):36–47.

68. Brayer WK, Mellonig JT, Dunlap RM, Marinak KW, Carson RE. Scaling and Root Planing Effectiveness: The Effect of Root Surface Access and Operator Experience. Journal of Periodontology. 1989 Jan 1;60(1):67–72.

69. Sherman PR, Hutchens LH Jr, Jewson LG. The effectiveness of subgingival scaling and root planing. II. Clinical responses related to residual calculus. J Periodontol. 1990 Jan;61(1):9–15.

70. Richardson AC, Chadroff B, Bowers GM. The Apical Location of Calculus Within the Intrabony Defect. Journal of Periodontology. 1990 Feb 1;61(2):118–22.

71. Renvert S, Wikström M, Dahlén G, Slots J, Egelberg J. Effect of root debridement on the elimination of Actinobacillus actinomycetemcomitans and Bacteroides gingivalis from periodontal pockets. J Clin Periodontol. 1990 Jul;17(6):345–50.

72. Renvert S, Wikström M, Dahén G, Slots J, Egelberg J. On the inability of root debridement and periodontal surgery to eliminate Actinobacillus actinomycetemcomitans from periodontal pockets. Journal of Clinical Periodontology. 1990 Jul;17(6):351–5.

73. Szulc M, Zakrzewska A, Zborowski J. Local drug delivery in periodontitis treatment: A review of contemporary literature. Dent Med Probl. 2018 Jul;55(3):333–42.

74. Heitz-Mayfield LJA, Trombelli L, Heitz F, Needleman I, Moles D. A systematic review of the effect of surgical debridement vs. non-surgical debridement for the treatment of chronic periodontitis. Journal of Clinical Periodontology. 2002 Aug 2;29:92–102.

75. Comprehensive Periodontal Therapy: A Statement by the American Academy of Periodontology. Journal of Periodontology. 2011 Jul;82(7):943–9.

76. Bonito AJ, Lux L, Lohr KN. Impact of Local Adjuncts to Scaling and Root Planing in Periodontal Disease Therapy: A Systematic Review. Journal of Periodontology. 2005;76(8):1227–36.

77. Graziani F, Karapetsa D, Alonso B, Herrera D. Nonsurgical and surgical treatment of periodontitis: how many options for one disease? Periodontology 2000. 2017;75(1):152–88.

78. Sgolastra F, Gatto R, Petrucci A, Monaco A. Effectiveness of Systemic Amoxicillin/Metronidazole as Adjunctive Therapy to Scaling and Root Planing in the Treatment of Chronic Periodontitis: A Systematic Review and Meta-Analysis. Journal of Periodontology. 2012 Oct;83(10):1257–69.

79. Walker CB, Karpinia K, Baehni P. Chemotherapeutics: antibiotics and other antimicrobials. Periodontology 2000. 2004 Oct;36(1):146–65.

80. Rams TE, Sautter JD, van Winkelhoff AJ. Emergence of Antibiotic-Resistant Porphyromonas gingivalis in United States Periodontitis Patients. Antibiotics. 2023 Nov 1;12(11).

81. Parnham MJ, Erakovic Haber V, Giamarellos-Bourboulis EJ, Perletti G, Verleden GM, Vos R. Azithromycin: mechanisms of action and their relevance for clinical applications. Pharmacol Ther. 2014 Aug;143(2):225–45.

82. Pajukanta R. In vitro antimicrobial susceptibility of Porphyromonas gingivalis to azithromycin, a novel macrolide. Oral Microbiol Immunol. 1993 Oct;8(5):325–6.

83. Pajukanta R, Asikainen S, Saarela M, Alaluusua S, Jousimies-Somer H. In vitro activity of azithromycin compared with that of erythromycin against Actinobacillus actinomycetemcomitans. Antimicrob Agents Chemother. 1992 Jun;36(6):1241–3.

84. Morales A, Contador R, Bravo J, Carvajal P, Silva N, Strauss FJ, et al. Clinical effects of probiotic or azithromycin as an adjunct to scaling and root planning in the treatment of stage III periodontitis: a pilot randomized controlled clinical trial: BMC Oral Health. BMC Oral Health. 2021 Dec 1;21(1).

85. Brook I, Lewis MAO, Sándor GKB, Jeffcoat M, Samaranayake L p., Vera Rojas J. Clindamycin in dentistry: More than just effective prophylaxis for endocarditis? Oral Surgery, Oral Medicine, Oral Pathology, Oral Radiology & Endodontology. 2005 Nov;100(5):550–8.

86. Walker CB. The acquisition of antibiotic resistance in the periodontal microflora. Periodontol 2000. 1996 Feb;10:79–88.

87. Cacchillo DA, Walters JD. Effect of ciprofloxacin on killing of Actinobacillus actinomycetemcomitans by polymorphonuclear leukocytes. Antimicrob Agents Chemother. 2002 Jun;46(6):1980–4.

88. Sanz M, Herrera D, Kebschull M, Chapple I, Jepsen S, Beglundh T, et al. Treatment of stage I-III periodontitis-The EFP S3 level clinical practice guideline. J Clin Periodontol. 2020 Jul;47 Suppl 22:4–60.

89. Eickholz P, Koch R, Göde M, Nickles K, Kocher T, Lorenz K, et al. Clinical benefits of systemic amoxicillin/metronidazole may depend on periodontitis stage and grade: An exploratory sub-analysis of the ABPARO trial. J Clin Periodontol. 2023 Sep;50(9):1239–52.

90. Sahrmann P, Puhan MA, Attin T, Schmidlin PR. Systematic review on the effect of rinsing with povidone-iodine during nonsurgical periodontal therapy. J Periodontal Res. 2010 Apr;45(2):153–64.

91. El Mobadder M, Nammour S, Grzech-Leśniak Z, Grzech-Leśniak K. Efficacy of the Adjunct Use of Povidone-Iodine or Sodium Hypochlorite with Non-Surgical Management of Periodontitis: A Systematic Review and Meta-Analysis. Journal of Clinical Medicine. 2022 Nov;11(21):6593.

92. Haps S, Slot D, Berchier C, Van der Weijden G. The effect of cetylpyridinium chloride-containing mouth rinses as adjuncts to toothbrushing on plaque and parameters of gingival inflammation: a systematic review. International Journal of Dental Hygiene. 2008 Nov 1;6(4):290.

93. Hossainian N, Slot DE, Afennich F, Van der Weijden GA. The effects of hydrogen peroxide mouthwashes on the prevention of plaque and gingival inflammation: a systematic review. Int J Dent Hyg. 2011 Aug;9(3):171–81.

94. Cummins D. Vehicles: how to deliver the goods: Periodontology 2000. Periodontol 2000. 1997 Oct;15:84–99.

95. Ashfaq R, Sisa B, Kovács A, Berkó S, Szécsényi M, Burián K, et al. Factorial design of in situ gelling two-compartment systems containing chlorhexidine for the treatment of periodontitis. Eur J Pharm Sci. 2023 Dec 1;191:106607.

96. Greene J MFA. Chlorhexidine. In: Salem Press Encyclopedia of Health. Salem Press; 2023.

97. WHO Model List of Essential Medicines - 23rd list, 2023 [Internet]. [cited 2024 Feb 28]. Available from: https://www.who.int/publications-detail-redirect/WHO-MHP-HPS-EML-2023.02

98. Van Strydonck DAC, Slot DE, Van der Velden U, Van der Weijden F. Effect of a chlorhexidine mouthrinse on plaque, gingival inflammation and staining in gingivitis patients: a systematic review. J Clin Periodontol. 2012 Nov;39(11):1042–55.

99. Hajishengallis G, Chavakis T, Lambris JD. Current understanding of periodontal disease pathogenesis and targets for host-modulation therapy. Periodontol 2000. 2020 Oct;84(1):14–34.

100. Reddy MS, Geurs NC, Gunsolley JC. Periodontal host modulation with antiproteinase, anti-inflammatory, and bone-sparing agents. A systematic review. Ann Periodontol. 2003 Dec;8(1):12–37.

101. Salvi GE, Lang NP. Host response modulation in the management of periodontal diseases. Journal of Clinical Periodontology. 2005 Oct 2;32:108–29.

102. FitzGerald GA, Patrono C. The coxibs, selective inhibitors of cyclooxygenase-2: The New England Journal of Medicine. The New England Journal of Medicine. 2001 Aug 9;345(6):433.

103. Roberts FA, Houston LS, Lukehart SA, Mancl LA, Persson GR, Page RC. Periodontitis vaccine decreases local prostaglandin E2 levels in a primate model. Infect Immun. 2004 Feb;72(2):1166–8.

104. Offenbacher S, Heasman PA, Collins JG. Modulation of host PGE2 secretion as a determinant of periodontal disease expression: Journal of periodontology. J Periodontol. 1993 May;64(5 Suppl):432–44.

105. Waite IM, Saxton CA, Young A, Wagg BJ, Corbett M. The periodontal status of subjects receiving non-steroidal anti-inflammatory drugs: Journal of periodontal research. J Periodontal Res. 1981 Jan;16(1):100–8.

106. Howell TH. Blocking periodontal disease progression with anti-inflammatory agents: Journal of periodontology. J Periodontol. 1993 Aug;64(8 Suppl):828–33.

107. Williams RC, Jeffcoat MK, Howell TH, Hall CM, Johnson HG, Wechter WJ, et al. Indomethacin or flurbiprofen treatment of periodontitis in beagles: comparison of effect on bone loss: Journal of periodontal research. J Periodontal Res. 1987 Sep;22(5):403–7.

108. Bezerra MM, De Lima V, Alencar VBM, Vieira IB, Brito GAC, Ribeiro RA, et al. Selective cyclooxygenase-2 inhibition prevents alveolar bone loss in experimental periodontitis in rats. Journal of Periodontology. 2000 Jun;71(6):1009–14.

109. Holzhausen M, Spolidorio DMP, Muscará MN, Hebling J, Spolidorio LC. Protective effects of etoricoxib, a selective inhibitor of cyclooxygenase-2, in experimental periodontitis in rats. J Periodontal Res. 2005 Jun;40(3):208–11.

110. Preshaw PM, Hefti AF, Jepsen S, Etienne D, Walker C, Bradshaw MH. Subantimicrobial dose doxycycline as adjunctive treatment for periodontitis. A review. J Clin Periodontol. 2004 Sep;31(9):697–707.

111. Hanes PJ, Purvis JP. Local anti-infective therapy: pharmacological agents. A systematic review: Annals of periodontology. Ann Periodontol. 2003 Dec;8(1):79–98.

112. Preshaw PM. Host response modulation in periodontics: Periodontology 2000. Periodontology 2000. 2008 Oct 1;48(1):92.

113. Di Paola R, Mazzon E, Muià C, Crisafulli C, Terrana D, Greco S, et al. Effects of etanercept, a tumour necrosis factor-alpha antagonist, in an experimental model of periodontitis in rats: British journal of pharmacology. Br J Pharmacol. 2007 Feb;150(3):286–97.

114. Oates TW, Graves DT, Cochran DL. Clinical, radiographic and biochemical assessment of IL-1/TNF-alpha antagonist inhibition of bone loss in experimental periodontitis: Journal of clinical periodontology. J Clin Periodontol. 2002 Feb;29(2):137–43.

115. Pers JO, Saraux A, Pierre R, Youinou P. Anti-TNF-alpha immunotherapy is associated with increased gingival inflammation without clinical attachment loss in subjects with rheumatoid arthritis: Journal of periodontology. J Periodontol. 2008 Sep;79(9):1645–51.

116. Mayer Y, Balbir-Gurman A, Machtei EE. Anti-Tumor Necrosis Factor-Alpha Therapy and Periodontal Parameters in Patients With Rheumatoid Arthritis: Journal of Periodontology. Journal of Periodontology. 2009 Sep;80(9):1414–20.

117. Cekici A, Kantarci A, Hasturk H, Van Dyke TE. Inflammatory and immune pathways in the pathogenesis of periodontal disease. Periodontology 2000. 2014;64(1):57–80.

118. Do MP, Neut C, Metz H, Delcourt E, Mäder K, Siepmann J, et al. In-situ forming composite implants for periodontitis treatment: How the formulation determines system performance. International Journal of Pharmaceutics. 2015 May 30;486(1):38–51.

119. Position Paper: The Role of Controlled Drug Delivery for Periodontitis. Journal of Periodontology. 2000;71(1):125–40.

120. Amato M, Santonocito S, Polizzi A, Tartaglia GM, Ronsivalle V, Viglianisi G, et al. Local Delivery and Controlled Release Drugs Systems: A New Approach for the Clinical Treatment of Periodontitis Therapy: Pharmaceutics. Pharmaceutics. 2023 Apr;15(4):1312.

121. Wei Y, Deng Y, Ma S, Ran M, Jia Y, Meng J, et al. Local drug delivery systems as therapeutic strategies against periodontitis: A systematic review: Journal of controlled release : official journal of the Controlled Release Society. J Control Release. 2021 May 10;333:269–82.

122. Goodson JM, Haffajee A, Socransky SS. Periodontal therapy by local delivery of tetracycline: Journal of Clinical Periodontology. Journal of Clinical Periodontology. 1979 Apr;6(2):83–92.

123. Litch JM, Encarnacion M, Chen S, Leonard J, Burkoth TL. Use of the polymeric matrix as internal standard for quantitation of in vivo delivery of tetracycline HCl from Actisite® tetracycline fiber during periodontal treatment: Journal of Periodontal Research. Journal of Periodontal Research. 1996 Nov;31(8):540–4.

124. Vandekerckhove BN, Quirynen M, van Steenberghe D. The use of tetracycline-containing controlled-release fibers in the treatment of refractory periodontitis: Journal of periodontology. J Periodontol. 1997 Apr;68(4):353–61.

125. Larsen T. In Vitro Release of Doxycycline From Bioabsorbable Materials and Acrylic Strips: Journal of Periodontology. Journal of Periodontology. 1990 Jan 1;61(1):30–4.

126. Bromberg LE, Buxton DK, Friden PM. Novel periodontal drug delivery system for treatment of periodontitis: Journal of controlled release : official journal of the Controlled Release Society. J Control Release. 2001 Apr 28;71(3):251–9.

127. Tabary N, Chai F, Blanchemain N, Neut C, Pauchet L, Bertini S, et al. A chlorhexidine-loaded biodegradable cellulosic device for periodontal pockets treatment: Acta Biomaterialia. Acta Biomaterialia. 2014 Jan;10(1):318–29.

128. Paolantonio M, D'Ercole S, Pilloni A, D'Archivio D, Lisanti L, Graziani F, et al. Clinical, Microbiologic, and Biochemical Effects of Subgingival Administration of a Xanthan-Based Chlorhexidine Gel in the Treatment of Periodontitis: A Randomized Multicenter Trial. Journal of Periodontology. 2009 Sep;80(9):1479–92.

129. Kempe S, Mäder K. In situ forming implants — an attractive formulation principle for parenteral depot formulations. Journal of Controlled Release. 2012 Jul 20;161(2):668–79.

130. Persson GR, Salvi GE, Heitz-Mayfield LJA, Lang NP. Antimicrobial therapy using a local drug delivery system (Arestin®) in the treatment of peri-implantitis. I: microbiological outcomes: Clinical Oral Implants Research. Clinical Oral Implants Research. 2006 Aug;17(4):386–93.

131. Kong LX, Peng Z, Li SD, Bartold PM. Nanotechnology and its role in the management of periodontal diseases: Periodontology 2000. Periodontology 2000. 2006 Feb 1;40(1):184.

132. Zazo H, Colino CI, Lanao JM. Current applications of nanoparticles in infectious diseases: Journal of Controlled Release. Journal of Controlled Release. 2016 Feb 28;224:86–102.

133. Hu F, Zhou Z, Xu Q, Fan C, Wang L, Ren H, et al. A novel pH-responsive quaternary ammonium chitosan-liposome nanoparticles for periodontal treatment: International journal of biological macromolecules. Int J Biol Macromol. 2019 May 15;129:1113–9.

134. Allen TM, Cullis PR. Liposomal drug delivery systems: From concept to clinical applications: Advanced Drug Delivery Reviews. Advanced Drug Delivery Reviews. 2013 Jan;65(1):36–48.

135. Agossa K, Lizambard M, Rongthong T, Delcourt-Debruyne E, Siepmann J, Siepmann F. Physical key properties of antibiotic-free, PLGA/HPMC-based in-situ forming implants for local periodontitis treatment. International Journal of Pharmaceutics. 2017 Apr 15;521(1):282–93.

136. Packhaeuser CB, Schnieders J, Oster CG, Kissel T. In situ forming parenteral drug delivery systems: an overview. European Journal of Pharmaceutics and Biopharmaceutics. 2004;

137. Thakur RRS, McMillan HL, Jones DS. Solvent induced phase inversion-based in situ forming controlled release drug delivery implants. Journal of Controlled Release. 2014 Feb 28;176:8–23.

138. Wang X, Burgess DJ. Drug release from in situ forming implants and advances in release testing. Advanced Drug Delivery Reviews. 2021 Nov 1;178:113912.

139. Shore ND, Guerrero S, Gambús G, Parente A. A New Sustained-release, 3-Month Leuprolide Acetate Formulation Achieves and Maintains Castrate Concentrations of Testosterone in Patients With Prostate Cancer. Clinical Therapeutics. 2019;41(3).

140. Sartor O. Eligard: leuprolide acetate in a novel sustained-release delivery system: Urology. Urology. 2003 Feb;61(2 Suppl 1):25–31.

141. Sublocade: The Once-Monthly Buprenorphine Injectable: Journal of addictions nursing. J Addict Nurs. 2018 Jun 4;29(2):139–40.

142. Krogmann A, Peters L, von Hardenberg L, Bödeker K, Nöhles VB, Correll CU. Keeping up with the therapeutic advances in schizophrenia: a review of novel and emerging pharmacological entities: CNS spectrums. CNS Spectr. 2019 Aug;24(S1):38–69.

143. Dunn R, Tipton A, Harkrader R, Rogers J. Intragingival Delivery Systems for Treatment of Periodontal Disease [Internet]. 1992 [cited 2024 Mar 20]. Available from: https://patentscope.wipo.int/search/en/detail.jsf?docId=WO1992000718

144. Juvekar S, Kathpalia H. Solvent removal precipitation based in situ forming implant for controlled drug delivery in periodontitis. Journal of Controlled Release. 2017 Apr 10;251:75–81.

145. Agossa K. Implants formés in-situ pour le traitement des poches parodontales : évaluation in-vitro et in-vivo [Internet] [These de doctorat]. Université de Lille (2018-2021); 2018 [cited 2024 Mar 19]. Available from: https://theses.fr/2018LILUS037

146. Nair LS, Laurencin CT. Biodegradable polymers as biomaterials: Progress in Polymer Science. Progress in Polymer Science. 2007 Aug;32(8/9):762–98.

147. Ibrahim TM, El-Megrab NA, El-Nahas HM. An overview of PLGA in-situ forming implants based on solvent exchange technique: effect of formulation components and characterization. Pharmaceutical Development and Technology. 2021 Aug 9;26(7):709–28.

148. Dunn RL, English JP, Cowsar DR, Vanderbilt DP. Biodegradable in-situ forming implants and methods of producing the same [Internet]. US4938763A, 1990 [cited 2024 Jan 10]. Available from: https://patents.google.com/patent/US4938763A/en

149. Do MP. Implants se formant in situ pour le traitement des parodontites [Internet] [These de doctorat]. Lille 2; 2014 [cited 2024 Jan 10]. Available from: https://www.theses.fr/2014LIL2S019

150. Parent M, Nouvel C, Koerber M, Sapin A, Maincent P, Boudier A. PLGA in situ implants formed by phase inversion: Critical physicochemical parameters to modulate drug release. Journal of Controlled Release. 2013 Nov 28;172(1):292–304.

151. Wang L, Wang A, Zhao X, Liu X, Wang D, Sun F, et al. Design of a long-term antipsychotic in situ forming implant and its release control method and mechanism. International Journal of Pharmaceutics. 2012 May 10;427(2):284–92.

152. Wang L, Kleiner L, Venkatraman S. Structure formation in injectable poly(lactide–co-glycolide) depots: Journal of Controlled Release. Journal of Controlled Release. 2003 Jul 31;90(3):345.

153. Camargo JA, Sapin A, Nouvel C, Daloz D, Leonard M, Bonneaux F, et al. Injectable PLA-based in situ forming implants for controlled release of Ivermectin a BCS Class II drug: solvent selection based on physico-chemical characterization: Drug development and industrial pharmacy. Drug Dev Ind Pharm. 2013 Jan;39(1):146–55.

154. Kempe S, Mäder K. In situ forming implants — an attractive formulation principle for parenteral depot formulations. Journal of Controlled Release. 2012;

155. Germán L, Cuevas JM, Cobos R, Pérez-Alvarez L, Vilas-Vilela JL. Green alternative cosolvents to N-methyl-2-pyrrolidone in water polyurethane dispersions. RSC Adv. 2021 May 24;11(31):19070–5.

156. European Chemicals Agency. How to comply with REACH Restriction 71, guideline for users of NMP (1-methyl-2-pyrrolidone). [Internet]. LU: Publications Office; 2019 [cited 2024 Jul 30]. Available from: https://data.europa.eu/doi/10.2823/69566

157. Khera N, Ghayor C, Pavlova E, Atanassova N, Weber FE. Exposure to the bromodomain inhibitor N-methyl pyrrolidone blocks spermatogenesis in a hormonal and non-hormonal fashion. Toxicol Appl Pharmacol. 2021 Jul 15;423:115568.

158. European Commission. Directorate General for Health and Consumers. Opinion on N-Methyl-2-pyrrolidone (NMP). [Internet]. LU: Publications Office; 2011 [cited 2024 Aug 13]. Available from: https://data.europa.eu/doi/10.2772/31663

159. PubChem. Hazardous Substances Data Bank (HSDB) : 5022 [Internet]. [cited 2024 Aug 6]. Available from: https://pubchem.ncbi.nlm.nih.gov/source/hsdb/5022

160. Flick B, Talsness CE, Jäckh R, Buesen R, Klug S. Embryotoxic potential of N-methyl-pyrrolidone (NMP) and three of its metabolites using the rat whole embryo culture system. Toxicology and Applied Pharmacology. 2009 Jun 1;237(2):154–67.

161. Jungbauer FH, Coenraads PJ, Kardaun SH. Toxic hygroscopic contact reaction to N-methyl-2-pyrrolidone. Contact Dermatitis. 2001 Nov;45(5):303–4.

162. Akesson B, Paulsson K. Experimental exposure of male volunteers to N-methyl-2-pyrrolidone (NMP): acute effects and pharmacokinetics of NMP in plasma and urine. Occup Environ Med. 1997 Apr;54(4):236–40.

163. Q3C — Tables and List Guidance for Industry.

164. Pagán OR, Rowlands AL, Urban KR. Toxicity and behavioral effects of dimethylsulfoxide in planaria. Neuroscience Letters. 2006 Oct 30;407(3):274–8.

165. Awan M, Erro E, Forster-Brown E, Brookshaw T, Chandel S, Chalmers SA, et al. Dimethyl sulfoxide for cryopreservation of alginate encapsulated liver cell spheroids in bioartificial liver support; assessments of cryoprotectant toxicity tolerance and dilution strategies. Cryobiology. 2022 Jun 1;106:79–83.

166. Marren K. Dimethyl sulfoxide: an effective penetration enhancer for topical administration of NSAIDs. Phys Sportsmed. 2011 Sep;39(3):75–82.

167. Schroeder T, Fenk R, Saure C, Czibere A, Bruns I, Zohren F, et al. The Mexican Way: a feasible approach to avoid DMSO toxicity. Bone Marrow Transplantation: Official journal of the European Society for Blood and Marrow Transplantation. 2011 Mar 1;46(3):469–71.

168. PubChem. Dimethyl Sulfoxide [Internet]. [cited 2024 Aug 6]. Available from: https://pubchem.ncbi.nlm.nih.gov/compound/679

169. Registration Dossier - ECHA [Internet]. [cited 2024 Aug 14]. Available from: https://echa.europa.eu/pt/registration-dossier/-/registered-dossier/15007/7/3/2

170. Stubbs S, Yousaf S, Khan I. A review on the synthesis of bio-based surfactants using green chemistry principles. DARU Journal of Pharmaceutical Sciences. 2022 Dec 1;30(2):407–26.

171. US EPA O. Basics of Green Chemistry [Internet]. 2013 [cited 2024 Aug 5]. Available from: https://www.epa.gov/greenchemistry/basics-green-chemistry

172. American Chemical Society [Internet]. [cited 2024 Aug 5]. What Is Green Chemistry? Available from: https://www.acs.org/greenchemistry/what-is-green-chemistry.html

173. Newell C. Green chemistry. In: Salem Press Encyclopedia of Science. Salem Press; 2023.

174. Makadia HK, Siegel SJ. Poly Lactic-co-Glycolic Acid (PLGA) as Biodegradable Controlled Drug Delivery Carrier. Polymers (20734360). 2011 Sep;3(3):1377–97.

175. Rocha CV, Gonçalves V, da Silva MC, Bañobre-López M, Gallo J. PLGA-Based Composites for Various Biomedical Applications. International Journal of Molecular Sciences. 2022 Feb 15;23(4):2034.

176. Schloegl W. Porosity and mechanically optimized PLGA based in situ hardening systems. European Journal of Pharmaceutics and Biopharmaceutics. 2012;

177. Butreddy A, Gaddam RP, Kommineni N, Dudhipala N, Voshavar C. PLGA/PLA-Based Long-Acting Injectable Depot Microspheres in Clinical Use: Production and Characterization Overview for Protein/Peptide Delivery. International Journal of Molecular Sciences. 2021 Jan;22(16):8884.

178. Singh A, Van den Mooter G. Spray drying formulation of amorphous solid dispersions. Advanced Drug Delivery Reviews. 2016 May 1;100:27.

179. Dudognon E, Correia NT, Danède F, Descamps M. Solid-Solid Transformation in Racemic Ibuprofen. Pharm Res. 2013 Jan 1;30(1):81–9.

180. Mazaleuskaya LL, Theken KN, Gong L, Thorn CF, FitzGerald GA, Altman RB, et al. PharmGKB summary: ibuprofen pathways. Pharmacogenetics and Genomics. 2015 Feb;25(2):96.

181. Brás AR, Noronha JP, Antunes AMM, Cardoso MM, Schönhals A, Affouard F, et al. Molecular Motions in Amorphous Ibuprofen As Studied by Broadband Dielectric Spectroscopy. J Phys Chem B. 2008 Sep 4;112(35):11087–99.

182. Dudognon E, Danède F, Descamps M, Correia NT. Evidence for a new crystalline phase of racemic Ibuprofen. Pharm Res. 2008 Dec;25(12):2853–8.

183. Cattaneo D, MCormick LJ, Cordes DB, Slawin AMZ, Morris RE. Crystal structure resolution of two different chlorhexidine salts. Journal of Molecular Structure. 2016 Oct 5;1121:70–3.

184. Poppolo Deus F, Ouanounou A. Chlorhexidine in Dentistry: Pharmacology, Uses, and Adverse Effects. International Dental Journal. 2022 Jun 1;72(3):269–77.

185. Elisei E, Willart JF, Danède F, Siepmann J, Siepmann F, Descamps M. Crystalline Polymorphism Emerging From a Milling-Induced Amorphous Form: The Case of Chlorhexidine Dihydrochloride. JPharmSci. 2018 Jan 1;107(1):121–6.

186. Marsac PJ, Shamblin SL, Taylor LS. Theoretical and Practical Approaches for Prediction of Drug–Polymer Miscibility and Solubility. Pharm Res. 2006 Oct 1;23(10):2417–26.

187. Knopp MM. A Promising New Method to Estimate Drug-Polymer Solubility at Room Temperature. Journal of Pharmaceutical Sciences. 2016;

188. Rask MB. Comparison of two DSC-based methods to predict drug-polymer solubility. International Journal of Pharmaceutics. 2018;

189. Knopp MM, Tajber L, Tian Y, Olesen NE, Jones DS, Kozyra A, et al. Comparative Study of Different Methods for the Prediction of Drug–Polymer Solubility. Mol Pharmaceutics. 2015 Sep 8;12(9):3408–19.

190. Latreche M. Interest of molecular/crystalline dispersions for the determination of solubility curves of drugs into polymers. International Journal of Pharmaceutics. 2019;

191. Tao J, Sun Y, Zhang GGZ, Yu L. Solubility of Small-Molecule Crystals in Polymers: d-Mannitol in PVP, Indomethacin in PVP/VA, and Nifedipine in PVP/VA. Pharm Res. 2009 Apr 1;26(4):855–64.

192. Mahieu A, Willart JF, Dudognon E, Danède F, Descamps M. A New Protocol To Determine the Solubility of Drugs into Polymer Matrixes. Mol Pharmaceutics. 2013 Feb 4;10(2):560–6.

193. Sun Y. Solubilities of Crystalline Drugs in Polymers: An Improved Analytical Method and Comparison of Solubilities of Indomethacin and Nifedipine in PVP, PVP/VA, and PVAc. JOURNAL OF PHARMACEUTICAL SCIENCES. 2010;99(9).

194. Amharar Y. Solubility of crystalline organic compounds in high and low molecular weight amorphous matrices above and below the glass transition by zero enthalpy extrapolation. International Journal of Pharmaceutics. 2014;

195. Coquerel PG. Maîtrise de la stabilité physique des alliages moléculaires amorphes pour optimiser l'efficacité des médicaments. 2019;

196. Dupont A. Cinétiques de transformations de produits pharmaceutiques sous broyage [Internet] [These de doctorat]. Université de Lille (2022-....); 2022 [cited 2023 Dec 3]. Available from: https://www.theses.fr/2022ULILR020

197. Descamps M, Willart JF, Dudognon E, Caron V. Transformation of Pharmaceutical Compounds upon Milling and Comilling: The Role of Tg. JPharmSci. 2007 May 1;96(5):1398–407.

198. Ngono Mebenga F. Investigations from experiments and simulations of amorphous forms of lactulose obtained by different routes [Internet] [These de doctorat]. Lille 1; 2017 [cited 2023 Dec 3]. Available from: https://www.theses.fr/2017LIL10213

199. Descamps M, Aumelas A, Desprez S, Willart J f. The amorphous state of pharmaceuticals obtained or transformed by milling: Sub-Tg features and rejuvenation: Journal of Non-Crystalline Solids. Journal of Non-Crystalline Solids. 2015 Jan;407:72–80.

200. Jameel BM, Huynh A, Chadha A, Pandey S, Duncan J, Chandler M, et al. Computer-based formulation design and optimization using Hansen solubility parameters to enhance the delivery of ibuprofen through the skin. International Journal of Pharmaceutics. 2019 Oct 5;569:118549.

201. Jalan I, Lundin L, van Stam J. Using Solubility Parameters to Model More Environmentally Friendly Solvent Blends for Organic Solar Cell Active Layers. Materials. 2019 Jan;12(23):3889.

202. Novaes FJM, de Faria DC, Ferraz FZ, de Aquino Neto FR. Hansen Solubility Parameters Applied to the Extraction of Phytochemicals. Plants. 2023 Jan;12(16):3008.

203. Madsen CG, Skov A, Baldursdottir S, Rades T, Jorgensen L, Medlicott NJ. Simple measurements for prediction of drug release from polymer matrices – Solubility parameters and intrinsic viscosity. European Journal of Pharmaceutics and Biopharmaceutics. 2015 May 1;92:1–7.

204. Hansen CM. Hansen Solubility Parameters: A User's Handbook, Second Edition. 2nd ed. Boca Raton: CRC Press; 2007. 544 p.

205. Cascant MM, Breil C, Garrigues S, de la Guardia M, Fabiano-Tixier AS, Chemat F. A green analytical chemistry approach for lipid extraction: computation methods in the selection of green solvents as alternative to hexane. Anal Bioanal Chem. 2017 May 1;409(14):3527–39.

206. Otárola-Sepúlveda J, Cea-Klapp E, Aravena P, Ormazábal-Latorre S, Canales RI, Garrido JM, et al. Assessment of Hansen solubility parameters in deep eutectic solvents for solubility predictions. Journal of Molecular Liquids. 2023 Oct 15;388:122669.

207. van der Tol JJB, Vantomme G, Meijer EW. Solvent-Induced Pathway Complexity of Supramolecular Polymerization Unveiled Using the Hansen Solubility Parameters. J Am Chem Soc. 2023 Aug 16;145(32):17987–94.

208. Salem A, Hagymási A, Vörös-Horváth B, Šafarik T, Balić T, Szabó P, et al. Solvent dependent 4-aminosalicylic acid-sulfamethazine co-crystal polymorph control. European Journal of Pharmaceutical Sciences. 2021 Jan 1;156:105599.

209. Abbott S. An integrated approach to optimizing skin delivery of cosmetic and pharmaceutical actives. Int J Cosmet Sci. 2012 Jun;34(3):217–22.

210. HSP Basics | Hansen Solubility Parameters [Internet]. [cited 2024 Jan 30]. Available from: https://www.hansen-solubility.com/HSP-science/basics.php

211. Grune C, Zens C, Czapka A, Scheuer K, Thamm J, Hoeppener S, et al. Sustainable preparation of anti-inflammatory atorvastatin PLGA nanoparticles: International Journal of Pharmaceutics. International Journal of Pharmaceutics. 2021 Apr 15;599:N.PAG-N.PAG.

212. Kempe S, Metz H, Pereira PGC, Mäder K. Non-invasive in vivo evaluation of in situ forming PLGA implants by benchtop magnetic resonance imaging (BT-MRI) and EPR spectroscopy. European Journal of Pharmaceutics and Biopharmaceutics. 2010 Jan 1;74(1):102–8.

213. Kranz H, Bodmeier R. A novel in situ forming drug delivery system for controlled parenteral drug delivery. International Journal of Pharmaceutics. 2007 Mar 6;332(1):107–14.

214. Parent M, Clarot I, Gibot S, Derive M, Maincent P, Leroy P, et al. One-week in vivo sustained release of a peptide formulated into in situ forming implants. International Journal of Pharmaceutics. 2017 Apr 15;521(1):357–60.

215. Molinier C, Picot-Groz M, Malval O, Le Lamer-Déchamps S, Richard J, Lopez-Noriega A, et al. Impact of octreotide counterion nature on the long-term stability and release kinetics from an in situ forming depot technology. Journal of Controlled Release. 2021 Aug 10;336:457–68.

216. Kranz H, Bodmeier R. Structure formation and characterization of injectable drug loaded biodegradable devices: In situ implants versus in situ microparticles. European Journal of Pharmaceutical Sciences. 2008 Jul 3;34(2):164–72.

217. Schoenhammer K, Boisclair J, Schuetz H, Petersen H, Goepferich A. Biocompatibility of an Injectable In Situ Forming Depot for Peptide Delivery. JPharmSci. 2010 Oct 1;99(10):4390–9.

218. Ibrahim TM, Eissa RG, El-Megrab NA, El-Nahas HM. Morphological characterization of optimized risperidone-loaded in-situ gel forming implants with pharmacokinetic and behavioral assessments in rats. Journal of Drug Delivery Science and Technology. 2021 Feb 1;61:102195.

219. Li Z, Mu H, Weng Larsen S, Jensen H, Østergaard J. An in vitro gel-based system for characterizing and predicting the long-term performance of PLGA in situ forming implants. International Journal of Pharmaceutics. 2021 Nov 20;609:121183.

220. Lin Q, Shan X, Li X, Luo Z, Yu X, Liu H, et al. Solvent exchange-motivated and tunable in situ forming implants sustaining triamcinolone acetonide release for arthritis treatment. International Journal of Pharmaceutics. 2023 Oct 15;645:123383.

221. Suh MS, Kastellorizios M, Tipnis N, Zou Y, Wang Y, Choi S, et al. Effect of implant formation on drug release kinetics of in situ forming implants. International Journal of Pharmaceutics. 2021 Jan 5;592:120105.

222. Wang X, Bao Q, Wang R, Kwok O, Maurus K, Wang Y, et al. In situ forming risperidone implants: Effect of PLGA attributes on product performance. Journal of Controlled Release. 2023 Sep 1;361:777–91.

223. Wang X, Bao Q, Suh MS, Kastellorizios M, Wang R, Burgess DJ. Novel adapter method for in vitro release testing of in situ forming implants. International Journal of Pharmaceutics. 2022 Jun 10;621:121777.

224. Wang X, Bao Q, Wang R, Li T, Wang Y, Qin B, et al. In vivo characterization of Perseris and compositionally equivalent formulations. International Journal of Pharmaceutics. 2023 Jul 25;642:123170.

225. Fredenberg S, Wahlgren M, Reslow M, Axelsson A. The mechanisms of drug release in poly(lactic-co-glycolic acid)-based drug delivery systems -- A review. International Journal of Pharmaceutics. 2011 Aug 30;415(1–2):34.

226. Ding AG, Schwendeman SP. Acidic Microclimate pH Distribution in PLGA Microspheres Monitored by Confocal Laser Scanning Microscopy. Pharm Res. 2008 Sep 1;25(9):2041–52.

227. Kempe S, Metz H, Mäder K. Do in situ forming PLG/NMP implants behave similar in vitro and in vivo? A non-invasive and quantitative EPR investigation on the mechanisms of the implant formation process. Journal of Controlled Release. 2008 Jan 1;130(3):220–5.

228. Siepmann J, Elkharraz K, Siepmann F, Klose D. How Autocatalysis Accelerates Drug Release from PLGA-Based Microparticles: A Quantitative Treatment. Biomacromolecules. 2005 Jul 1;6(4):2312–9.

229. Ford Versypt AN, Pack DW, Braatz RD. Mathematical modeling of drug delivery from autocatalytically degradable PLGA microspheres — A review. Journal of Controlled Release. 2013 Jan 10;165(1):29–37.

230. Siepmann J, Siepmann F. Sink conditions do not guarantee the absence of saturation effects. Int J Pharm. 2020 Mar 15;577:119009.

231. Bode C, Kranz H, Fivez A, Siepmann F, Siepmann J. Often neglected: PLGA/PLA swelling orchestrates drug release: HME implants. Journal of Controlled Release. 2019 Jul 28;306:97–107.

232. Blasi P, Schoubben A, Giovagnoli S, Perioli L, Ricci M, Rossi C. Ketoprofen poly(lactide-co-glycolide) physical interaction. AAPS PharmSciTech. 2007 Jun 1;8(2):E78–85.

233. Brunner A, Mäder K, Göpferich A. pH and Osmotic Pressure Inside Biodegradable Microspheres During Erosion1. Pharm Res. 1999 Jun 1;16(6):847–53.

234. Bode C, Kranz H, Kruszka A, Siepmann F, Siepmann J. In-situ forming PLGA implants: How additives affect swelling and drug release. Journal of Drug Delivery Science and Technology. 2019 Oct;53:101180.

235. Anusavice KJ, Zhang NZ, Shen C. Controlled release of chlorhexidine from UDMA-TEGDMA resin. J Dent Res. 2006 Oct;85(10):950–4.

236. Velasco D, Danoux ChB, Redondo J a., Elvira C, San Román J, Wray P s., et al. pH-sensitive polymer hydrogels derived from morpholine to prevent the crystallization of ibuprofen. Journal of Controlled Release. 2011 Jan 1;149(2):140–5.

237. Garnett JA, Simpson PJ, Taylor J, Benjamin SV, Tagliaferri C, Cota E, et al. Structural insight into the role of Streptococcus parasanguinis Fap1 within oral biofilm formation. Biochem Biophys Res Commun. 2012 Jan 6;417(1):421–6.

Résumé

La parodontite est une maladie inflammatoire chronique très répandue caractérisée par une dysbiose du microbiome buccal. Il est intéressant de noter qu'elle est considérée comme la 6ème maladie la plus répandue dans le monde. Le traitement de la parodontite vise à retrouver la santé parodontale, à éviter la progression de la maladie et sa réapparition et enfin à préserver le bien-être et la fonction dentaire. De plus, la parodontite étant caractérisée par une dysbiose bactérienne et une inflammation, il est de la plus haute importance de gérer et de contrôler ces paramètres. Pour ce faire, la première ligne de traitement correspond à l'élimination mécanique du biofilm bactérien. Cependant, cette thérapie pourrait être combinée à un système local d'administration de médicaments, capable de contrôler la libération d'agents antiseptiques et anti-inflammatoires. Les implants se formant *in situ* (ISFI) à base d'acide poly(lactique-co-glycolique) (PLGA) offrent un potentiel intéressant pour le traitement de la parodontite. Un polymère biocompatible et biodégradable non miscible à l'eau est dissous dans un solvant organique soluble dans l'eau. Le médicament sélectionné est ajouté postérieurement, formant une solution ou une dispersion injectable. Après injection au site d'action, le solvant miscible à l'eau se dissipe dans les tissus environnants en même temps que les fluides aqueux pénètrent dans la formulation. En conséquence, le polymère précipite, piégeant le médicament et formant un implant solide *in situ*. Cependant, à ce jour, le N-méthylpyrrolidone (NMP) est le solvant le plus couramment utilisé en raison de sa préséance pharmaceutique dans les produits parentéraux approuvés ainsi que de sa grande capacité de solvatation. Toutefois, le NMP soulève des problèmes de toxicité lorsqu'il est administré par voie parentérale. Le but de cette étude est d'identifier des systèmes de solvants alternatifs moins toxiques. Pour ce faire, les paramètres de solubilité de Hansen ont été utilisés comme une technique de sélection et trois solvants prometteurs ont été proposés : le poly(éthylène glycol) 400 (PEG 400), le citrate de triéthyle (TEC) et l'éthanol. Enfin, des mélanges tertiaires de ces composés ont été utilisés pour préparer des formulations liquides contenant du PLGA, de l'ibuprofène (comme médicament anti-inflammatoire) et/ou de chlorhexidine (comme agent antiseptique). Enfin, la formation d'implants et la cinétique de libération du médicament ont été surveillées lors de l'exposition à un tampon phosphate pH 6,8 à 37 °C. De plus, les changements dynamiques de la masse des implants et du pH du milieu ont été évalués ainsi que les propriétés mécaniques et antibactériennes des implants. Il est important de noter que les mélanges PEG 400:TEC:éthanol 85:10:5 et 60:30:10 ont fourni de bonnes propriétés mécaniques et ont permis la formation d'implants. Les systèmes résultants ont contrôlé la libération d'ibuprofène et de chlorhexidine pendant plusieurs semaines et ont assuré une activité antimicrobienne efficace.

Mots clés : implant se formant in-situ, PLGA, parodontite, chlorhexidine, ibuprofène

Abstract

Periodontitis is a highly prevalent chronic inflammatory disease characterized by the dysbiosis of the oral microbiome. It is interesting to note that it is considered the 6th most prevalent disease globally. The treatment of periodontitis attempts to regain periodontal health, avoid the disease's progression and its reappearance and lastly, preserve the dentition well-being, and function. Additionally, being periodontitis characterized by a bacterial dysbiosis and inflammation, it is of foremost importance to manage and control these parameters. To do so, the first line of treatment corresponds to the mechanical removal of the bacterial biofilm and calculus (known as scaling and root planing). However, this therapy could be combined with a local drug delivery system, able to control the release of both antiseptics and anti-inflammatory agents. Poly(lactic-co-glycolic acid) (PLGA)-based *in-situ* forming implants (ISFIs) offer an interesting potential for the treatment of periodontitis. A water-immiscible biocompatible and biodegradable polymer is dissolved in a water-soluble organic solvent. The selected drug is posteriorly added, forming an injectable solution or dispersion. After subcutaneous injection in the site of action, the water-miscible solvent dissipates into the surrounding tissues at the same time as aqueous fluids penetrate into the injected formulation. As a result, the polymer precipitates entrapping the drug and forming a solid implant *in-situ*. However, up to date, N-methyl pyrrolidone (NMP) is the most commonly employed solvent due to its pharmaceutical precedence in approved parenteral products as well as its large solvating ability. Nevertheless, NMP raises toxicity concerns, when administered parenterally. The aim of this study is to identify less toxic alternative solvent systems to NMP. To do so, Hansen Solubility Parameters were employed as a screening technique and three promising solvents were proposed: poly(ethylene glycol) 400 (PEG 400), triethyl citrate (TEC) and ethanol. Lastly, tertiary blends of these compounds were employed to prepare liquid formulations containing PLGA, ibuprofen (as an anti-inflammatory drug) and/or chlorhexidine dihydrochloride (as an antiseptic agent). Finally, implant formation and drug release kinetics were monitored upon exposure to phosphate buffer pH 6.8 at 37 °C. Additionally, dynamic changes in the implants' wet mass and the pH of the release medium were assessed as well as the implants' mechanical and antibacterial properties. Importantly, 85:10:5 and 60:30:10 PEG 400:TEC:ethanol blends provided good mechanical properties and allowed for implant formation. The resulting systems were able to control ibuprofen and chlorhexidine dihydrochloride release over several weeks and assured efficient antimicrobial activity.

Keywords: *in-situ* forming implant; PLGA; periodontitis; solvent; chlorhexidine; ibuprofen